TELEVISION DEFLECTION SYSTEMS

by

A. BOEKHORST and J. STOLK

In preparation.

ca. 240 pages 6 x 9 ins 145 ill.

A general account is first given of the picture tube and its auxiliary components, including focusing and ion trap magnets; and of the principal causes of faults. After a short analysis of a deflection unit for 110° deflection, which has been developed in the Mullard Research Laboratory at Salford, the greater part of the book is devoted to the theory and design of line-deflection and frame-deflection circuits.

INDUSTRIAL ELECTRONICS HANDBOOK

by

R. KRETZMANN

3rd enlarged edition

310 pages 6 x 9 ins 326 ill.

This authoritative technical manual is distinguished from other books in the field in that it is largely devoted to a detailed descriptive study of successful modern devices of many types, with numerous circuit diagrams and photographs.
It will thus appeal to the engineer who is already responsible for the maintenance of such plants and wants to extend his mastery of the detail and his knowledge of other devices using electronic principles.

PHILIPS TECHNICAL LIBRARY

ELECTRONIC VALVES · BOOK XV

MAGNETRONS

BY

K. HINKEL

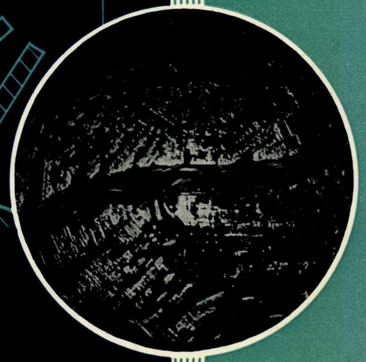

PHILIPS TECHNICAL LIBRARY

The uses of high frequency energy have been very greatly extended in the last twenty years, and both frequencies and power have constantly increased.
The classical transmitting valve — triode or tetrode — is not always capable of delivering the required output at such very high frequencies, and a new family of tubes are being more and more widely used. Of these "transit-time" tubes, the magnetron was one of the first to be employed commercially on a large scale.
It is used as a source of high frequency energy in pulsed radar, linear accelerators, diathermy equipment and so on.
Microwaves are also being used to an increasing extent for heating purposes in industry and in such devices as the "radar oven".
The book is meant as an introduction for technologists and students to the applications of microwaves in general and magnetrons in particular; especially to the physical background and properties of this kind of tube.

ELECTRONIC VALVES XV

MAGNETRONS

MAGNETRONS

Distributed in Great Britain and Eire by:
CLEAVER-HUME PRESS LTD.
31, Wright's Lane, Kensington — London W. 8

MAGNETRONS

BY

K. HINKEL

1961

PHILIPS TECHNICAL LIBRARY

Translated by G. du Cloux, Wallington (England)

Publisher's note:

The book will be published in the English, Spanish, German and French languages

This book contains 104 pages, 55 illustrations and 6 photographs on art paper hors texte

U.D.C. nr. 621.385.16

Printed in the Netherlands

First edition 1961

FOREWORD

The uses to which high frequency energy are put have been very greatly extended in the last twenty years; the frequencies and power used in the new applications have been constantly increased.

The classical transmitting valve, i.e. the triode or tetrode is not always capable of delivering the required output at such very high frequencies and a new family of tubes has appeared on the scene (klystrons, travelling wave tubes, magnetrons, backward-wave oscillators, amplitrons and so on) which are being more and more widely used. Of these "transit-time" tubes the magnetron was one of the first to be employed commercially on a large scale.

It is hoped that this little book will prove useful as an introduction to the problems arising in the applications of magnetrons in particular and microwaves in general, and more especially as an aid to a better understanding of the physical background of this kind of tube.

November 1960 K. HINKEL

TABLE OF CONTENTS

I. INTRODUCTION

The multicavity magnetron has now been in use for more than 15 years. It is used as a source of high frequency energy in pulsed radar, linear accelerators, diathermy equipment, industrial heating and so on.

In many cases the magnetron is preferred to other types of tube such as the klystron, because of its low cost, simple operation and relatively low internal resistance.

Interest in the magnetron has fallen off in recent years, however, particularly among designers of new radar equipment, the main reason for this being the fact that there is a limit to the extent to which magnetrons can be electronically tuned.

On the other hand the demand for these tubes for use in civil radar installations and for various industrial purposes has steadily increased; developments in the design of magnetrons for the millimetric wave range have resulted in the appearance on the market of a precision radar unit for navigational purposes, known as the "ship-shape" radar because the shape of the vessel is recognisable on the screen. Microwaves are also being used to an increasing extent for heating purposes in industry, and mention should also be made of the "radar oven" in which food can be cooked in a few minutes.

Experience has shown that there are many who have only a very vague idea of magnetrons and microwaves, but who are nevertheless directly concerned with their applications; and it is probable that there will be many more such persons in the near future.

The object of this book is to enlighten these persons as to the properties of magnetrons, as well as their physical background; students of electronics and microwave technology will also find in it a valuable source of information.

1.1 General description of the magnetron

A magnetron is a piece of equipment that is capable of converting electrical energy in the form of direct current into high frequency electrical energy of a certain wavelength. Dependent on the design of the magnetron, this wavelength will be approximately between 1 metre and 1 millimetre. At the longer wavelengths, the efficiency of the conversion is about 80%, but this drops steeply to only some 2 or 3 per cent at 1 mm. The attainable *pulsed* power output is several megawatts in a band of approximately 10 cm to 100 cm; at 3 cm the present limit is 1 MW whilst, in the region of 1 mm, it

is not possible to obtain more than a few hundred watts. Magnetrons intended for continuous operation do not develop more than a few kilowatts (Figs. 1 and 2).

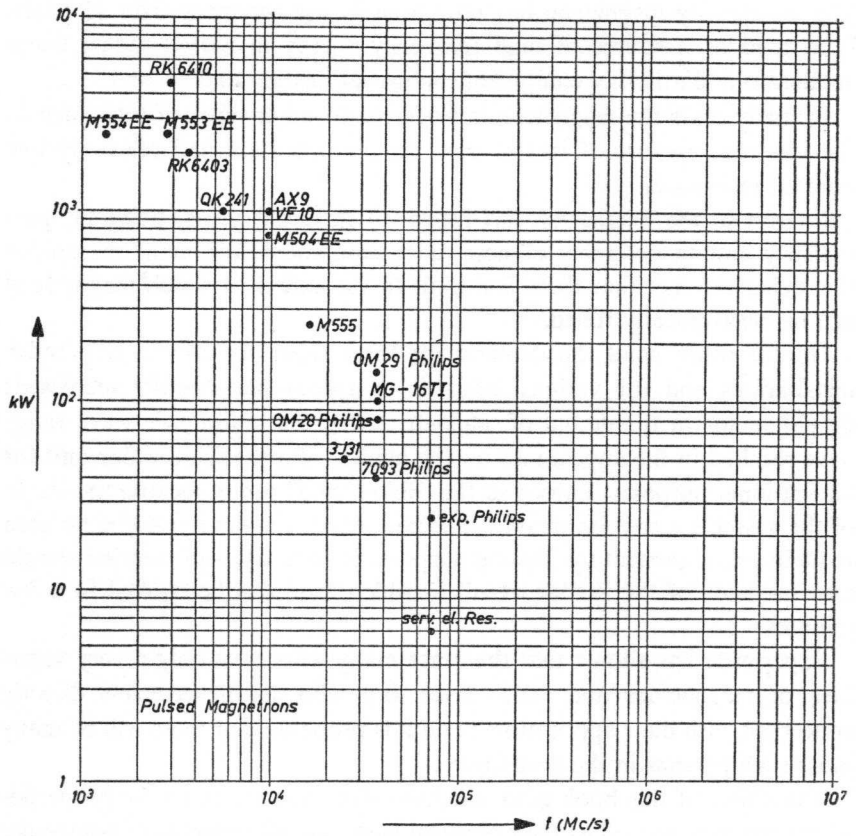

Fig. 1. The pulsed power obtainable from a magnetron as a function of frequency.

The magnetron is in effect a diode, the input electrodes being a cathode and an anode. Usually the high frequency energy is taken from it by means of either a coaxial connection or a waveguide, but sometimes special radiators are incorporated in the magnetron for directing the high frequency energy. In order to function in the manner described, the magnetron must have within it a certain magnetic field, and there are two ways of achieving this. The magnet can either be attached to the tube to form a complete unit, in which case we speak of a "packaged" magnetron (Fig. 3) or the magnet may be separate, that is, mounted in the equipment in which the magnetron

is to operate; in this case we refer to an "unpackaged" magnetron. The latter type is generally used for high output power ratings and for the longer wavelengths, as the great weight of the magnet would otherwise render the assembly unmanageable (Fig. 4).

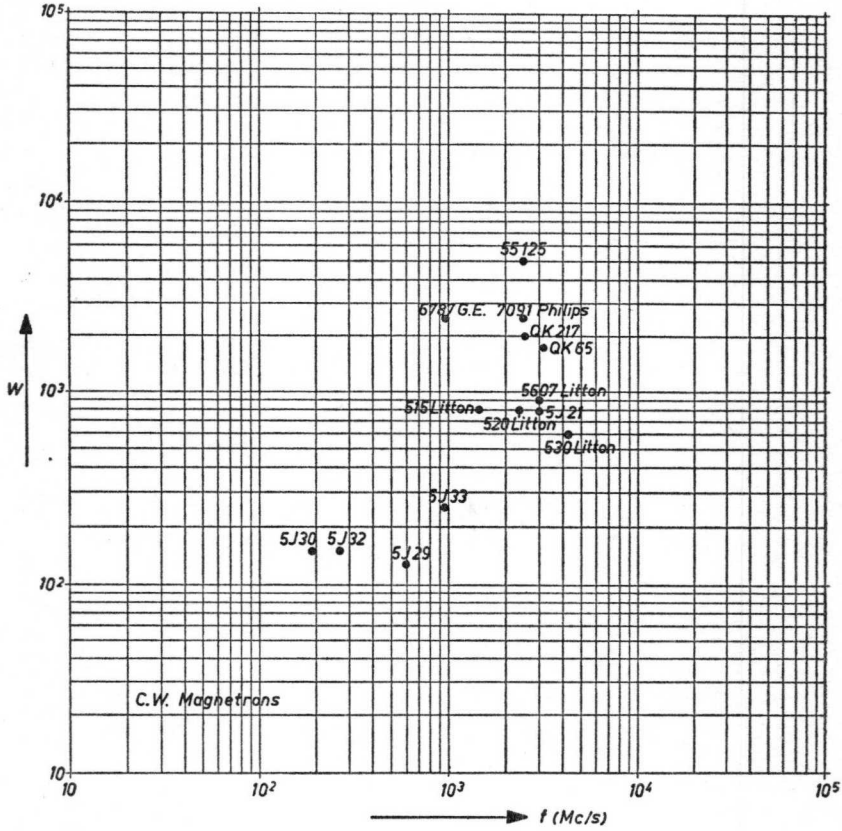

Fig. 2. The output of some "continuous wave" magnetrons plotted against frequency.

In a certain sense the magnetron has the same characteristics as a complete radio frequency transmitter; it is not necessary to connect to a magnetron the inductors and capacitors usually required to obtain the desired frequency; these are already contained in the magnetron. All that is necessary is to apply electric power to the input and to connect the load to the output side. This is the great advantage from the point of view of the user, that he need not concern himself with frequency adjustments or transformation of the load.

Before discussing the components of a magnetron in greater detail let us first consider the manner in which the conversion of direct current to high frequency alternating current takes place in the magnetron. It is essential to understand this in order to appreciate the functions of the various components.

II. THE ELECTRICAL MECHANISM

2.1 Principle of the magnetron

We have seen then that, stated briefly, magnetrons are capable of converting direct current to alternating current of a certain frequency; hence the magnetron contains the means of determining the frequency, i.e. self inductances and capacitances. These are contained in the anode, and this combination is connected to the output of the magnetron by means of a loop in the case of coaxial coupling, or a slot for coupling to a waveguide (Fig. 5). In this way, a high frequency voltage is made available at the output side of the magnetron when the oscillatory circuits in the anode are brought into oscillation.

In practice, neither the oscillatory circuit nor the coupling system are entirely free from losses, which means that the available power is not all effectively utilised.

If W_o denotes the power passed to the load and W_c represents W_o plus the losses in the circuit and coupling system, the circuit efficiency η_c can be expressed as:

$$\eta_c = \frac{W_o}{W_c} \tag{1}$$

Practical values of η_c lie between 50 and 95% for various types of magnetron.

Let us now see how the oscillatory circuit in the tube is brought into a state of oscillation. In this process the electrons emitted by the cathode act as the intermediary. They draw energy from the source of direct current and pass some of it to the oscillatory circuit to cause this to oscillate; the rest of the energy which the electrons still retain is dissipated as heat at the anode.

It is thus possible to speak of the electronic efficiency, η_e, which is the ratio of the power W_c delivered to the circuit in the anode as electromagnetic field energy, to the power W_i taken from the source, at the input:

$$\eta_e = \frac{W_c}{W_i} \tag{2}$$

It is possible to measure the value of η_e indirectly for every magnetron.

The amount of power taken from and delivered to an electric field by electrons calls for some explanation. Let us consider a capacitor with a voltage V applied to the electrodes; between the plates there is an electron of mass m and charge e (Fig. 6).

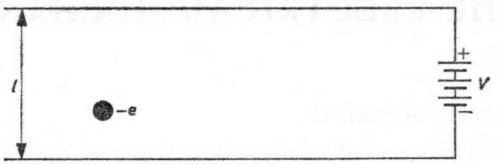

Fig. 6. An electron of mass m and charge e between the plates of a capacitor, under the influence of an electric field.

Let l denote the spacing of the electrodes. The electron in the electric field between the electrodes will then be subjected to a force K, so that:

$$K = e\frac{V}{l} \tag{3}$$

Under the influence of this force the electron moves towards the positive plate (equivalent to the anode of the magnetron), and, when it has travelled the whole distance from plate to plate the battery will have imparted an amount of energy eV to the electron (owing to the flow of current). This energy is converted wholly to kinetic energy in the electron, hence:

$$e \cdot V = \frac{m \cdot v_o^2}{2} \tag{4}$$

where v_o denotes the velocity of the electron after the passage of current (see also 12).

In this example the electron derives energy from the electric field; let us now consider the case where the electron imparts energy to the electric field. To do this we shall imagine the positive plate to have a hole in it (Fig. 7) and suppose that an electron is shot through the capacitor from the positive plate towards the negative plate.

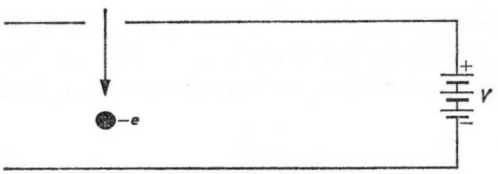

Fig. 7. An electron injected into a capacitor and decelerated by the electric field.

When the electron arrives in the space between the electrodes at a velocity of v_1, its kinetic energy will be $\frac{mv_1^2}{2}$. In its passage from one side to the

other it is slowed down by the electric field and, the direction of the motion being from + to —, the counteracting force will be from — to + .

On completion of the journey the velocity of the electron will have dropped to v_2. A current $e \cdot V$ will have flowed through the battery, but in the opposite direction from that in the first example, and this current must therefore have the effect of charging the battery. When the electron reaches the negatively charged electrode of the capacitor, at a velocity of v_2, its kinetic energy $\frac{mv_2^2}{2}$ will be converted to heat in the plate. The difference, $\frac{m}{2}(v_1^2 - v_2^2)$, in the kinetic energies on entering the capacitor and on striking the electrode at the other side is delivered up to the electric field.

Hence, $\frac{m}{2}(v_1^2 - v_2^2) = e \cdot V$,

where $e \cdot V$ is the amount of energy imparted to the field.

The electronic efficiency of this process is:

$$\eta_e = \frac{e \cdot V}{\frac{m}{2} \cdot v_1^2} = \frac{v_1^2 - v_2^2}{v_1^2} = 1 - \frac{v_2^2}{v_1^2}. \tag{5}$$

It is seen that η_e can be unity if, at the end of its passage through the field, the electron comes to a standstill ($v_2 = 0$).

We may therefore say that when an electron passes through an electric field from — to +, it absorbs energy which then appears as kinetic energy in the electron itself. On the other hand if an electron passes through the field from + to —, it is retarded and the loss in kinetic energy is taken up by the field as electrical energy.

The action of a magnetron can thus be visualised as follows. Electrons from the cathode (— ve plate) move towards the anode (+ ve plate). On their way they are diverted through the oscillatory circuits at the anode, to ensure that they are retarded by the R.F. field of these circuits, and so impart energy to the field. This energy is taken from the output side of the magnetron by way of a coupling loop or a slot.

The overall efficiency η_t of a magnetron can now be written as:

$$\eta_t = \frac{W_o}{W_i} = \frac{W_o}{W_c} \cdot \frac{W_c}{W_i} = \eta_c \cdot \eta_e \tag{6}$$

So far nothing has been said of the manner in which the electrons, on their way from the cathode to the anode, are made to pass through the oscillatory circuits in such a way that they are retarded by the electric field

and so made to yield energy. This is achieved by means of a magnetic field, the lines of force of which lie parallel to the axis of the cathode.

In order to understand this fully let us now for a moment consider the movements of the electrons in electric and magnetic fields.

2.2 The movements of charges in electric and magnetic fields

As a full treatment of this subject would be beyond the scope of this book we refer the reader to textbooks of physics and electrotechnology. Here we shall mention enough to explain the behaviour of electrons in a magnetron.

We have already seen that an electrically-charged particle (charge e) in an electric field, the strength of which is E, encounters a force K, so that

$$K = e \cdot E \tag{7}*$$

The direction of the force is parallel to that of the electric lines of force. If the charge is positive, the force will be in the direction from + to — in the field; the force operates in the opposite direction on a negative charge.

Under the influence of this force K the movement of the charge is accelerated, the acceleration a being expressed as:

$$a = \frac{k}{m} = \frac{eE}{m} \tag{8}$$

where m is the mass of the charged particle.

If the force K operates on the particle for a time $\mathrm{d}t$, the velocity v will undergo a change $\mathrm{d}v$:

$$\mathrm{d}v = a \cdot \mathrm{d}t \tag{9}$$

The kinetic energy $W_o = \frac{mv^2}{2}$ then changes to the extent of:

$$\mathrm{d}\,(Wv) = m \cdot v \cdot \mathrm{d}v \tag{10}$$

Now $v = \frac{\mathrm{d}s}{\mathrm{d}t}$, where s is the distance travelled by the particle. Equation (10) together with (9) thus becomes

$$\mathrm{d}\,(W_v) = m \frac{\mathrm{d}s}{\mathrm{d}t} \cdot a \cdot \mathrm{d}t = K \cdot \mathrm{d}s = e \cdot E \cdot \mathrm{d}s \tag{11}$$

---

* The Lorentz force is disregarded here; this is permissible when considering the phenomena taking place in a magnetron. See W. Kleen, Mikrowellen Elektronik I, pp. 4 & 5.

The total kinetic energy is found to be:

$$W_v = \int \mathrm{d}\,(W_v) = \int e \cdot E \cdot \mathrm{d}s = e \cdot V \qquad (12)$$

whereby $\int E \cdot \mathrm{d}s = V$ is the voltage to which the particle has been subjected. Equation (12) thus gives the amount of the kinetic energy of a charged particle converted to field energy, and vice versa.

From equation (12) we can also calculate the velocity of the charged particle after it has been subjected to the voltage V, assuming zero initial velocity:

$$v = \sqrt{\frac{2 \cdot e \cdot V}{m}}. \qquad (13)$$

Substituting the values of m and e for an electron we obtain:

$$v = 5.9 \cdot 10^7 \sqrt{V}\ \mathrm{cm\ sec^{-1}} \text{ with } V \text{ in volts} \qquad (14)$$

Let us now see what the effect is of a magnetic field on the electrically-charged particles.

In general, the direction of motion of such a particle will contain a component parallel to a line of force of the magnetic field at the point where the particle happens to be, and also a component perpendicular to the magnetic field (see Fig. 8). By thus dividing the direction of motion of the electrons into its components it is a simple matter to define the effect of the magnetic field.

On the basis of the fundamental equations used in electrodynamics it may be said that:

1. The motion of electrically-charged particles moving through a magnetic field in a direction parallel to the lines of force is unaffected by the field.

2. An electrically-charged particle, the motion of which is normal to a line of force in a magnetic field will encounter a force at that point.

The direction of this force is normal both to the magnetic field and to the direction of motion of the particle. The magnitude of the force is proportional to the charge, to the velocity of the particle and to the magnetic field strength.

In other words the direction of the force acting on a particle in a magnetic field always lies in a plane normal to the magnetic line of force at that particular point.

Expressed mathematically this is as follows:

$$K = e \cdot v \cdot B \cdot \sin\,(\sphericalangle\, v \cdot B) \qquad (15)$$

where B is the magnetic field strength and $(\sphericalangle\, v \cdot B)$ the angle between the

direction of travel of the particle and the direction of the magnetic field, as shown diagrammatically in Fig. 8.

The direction of the particle and that of the magnetic field lie in the plane of the drawing; the angle between the two is φ.

The particle possesses a component v_p of the velocity v, which is in a direction parallel to the magnetic field:

$$v_p = v \cdot \cos. \varphi$$

This component has no effect on the particle.

There is also another component, v_t, normal to the direction of the magnetic field:

$$v_t = v \cdot \sin \varphi$$

as a result of which the particle encounters a force in accordance with (15):

$$K = B \cdot e \cdot v \cdot \sin \varphi$$

The direction of this force is normal to the plane of the drawing, dependent on the sign of the charge e*.

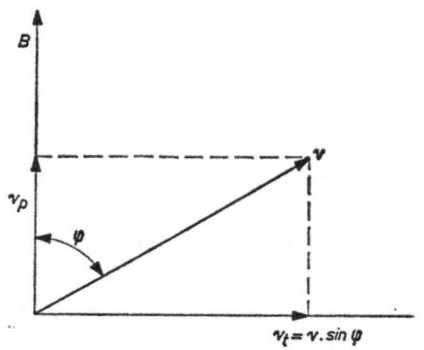

Fig. 8. Movement of a charged particle in a magnetic field. v_p is the component of the velocity parallel to the field and v_t the component normal to it.

Thus it is seen that the force acting on an electrically-charged particle moving through a magnetic field is always normal to the direction of motion of the particle.

Now that we have seen what forces electric and magnetic fields exert on electrically-charged particles we shall proceed to an investigation of the path followed by such particles under certain conditions.

---

* See Physic van Westphal, pp. 349–1947.

2.3 The "cyclotron" motion

Let us now see what movements an electrically-charged particle performs when it is injected with a velocity v into a uniform magnetic field of strength denoted by B.

We shall assume that the direction of v is normal to the direction of B, and that the path of the particle under the above conditions is circular. To prove that it will be circular, we ascertain the force acting on the particle as it travels along such a path. (Fig. 9).

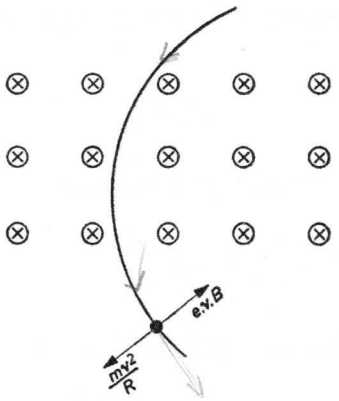

Fig. 9. Circular path of a particle in a magnetic field B. m is the mass of the particle e its charge, v its velocity and R the radius of the path.

The particle is subjected to a centrifugal force K_m, so that

$$K_m = \frac{mv^2}{R} \tag{16}$$

where m is the mass and v the velocity of the particle, and R the radius of the path. It will be possible for the particle to describe this path if the centrifugal force K_m is equal to the force K_B exerted on the particle by the magnetic field, that is, when

$$\frac{mv^2}{R} = e \cdot v \cdot B \tag{17}$$

Thus the radius of the path is found to be

$$R = \frac{m \cdot v}{e \cdot B} \tag{18}$$

In our example, the magnetic field is uniform, so that B and v are constant

at any point along the path; therefore R is also constant, which means that the path is a closed one and circular.

Having seen that the particle does describe a circular path under the above conditions we can now find out how many times it completes the circuit per unit of time. Let us call this the "revolution frequency". It can be computed quite simply.

The distance involved in one revolution is

$$s = 2\pi R \tag{19}$$

The velocity of the particle is v. To travel round the path s once, the time required, T_0, is:

$$T_0 = \frac{s}{v}. \tag{20}$$

Taking (20), (19) and (18) together we then have:

$$T_0 = 2\pi \frac{m}{eB} \tag{21}$$

Hence the revolution frequency may be written as:

$$f_0 = \frac{1}{T_o} = \frac{1}{2\pi} \cdot \frac{eB}{m}. \tag{22}$$

Now equation (22) reveals a remarkable fact, namely that the revolution frequency f_0 of the particle does not depend on its velocity within the magnetic field. Apart from the characteristics of the particle (e, m), f_0 is determined only by the field strength B.

This is most important and is, in fact, one of the things that has made possible the evolution of the cyclotron, which is a kind of particle accelerator.* The quantity

$$2\pi f_0 = w_c = \frac{eB}{m} \tag{23}$$

is known as the "cyclotron frequency". It is seen from equation (23) that this cyclotron frequency is 2π times the revolution frequency.

Fig. 10 shows the graph of equation (22) as applied to the electron.

---

* In the cyclotron the process that takes place in the magnetron is to some extent reversed; here energy is taken from a high frequency electric field and is converted to kinetic energy in electrically-charged particles.

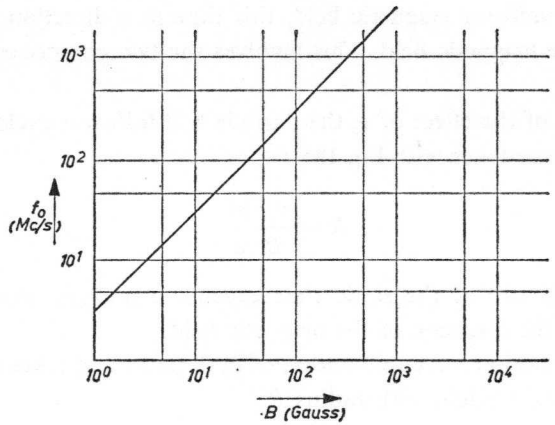

Fig. 10. Revolution frequency f_0 plotted against the magnetic field strength B.

The vertical axis represents the revolution frequency in Mc/s and the horizontal axis the magnetic field strength in gauss.

For practical purposes equation (22) is sometimes used in a slightly modified form. If we regard f_0 as the frequency of an electrical oscillation, its wavelength λ_c in free space will be:

$$\lambda_c = \frac{c}{f_0} \tag{24}$$

where c is the speed of light in free space.

Combining (22) and (24) we then obtain:

$$\frac{c}{\lambda_c} = \frac{e \cdot B}{2\pi \cdot m}, \qquad \text{or}$$

$$B \cdot \lambda_c = \frac{2 \cdot \pi \cdot c \cdot m}{e} = \text{constant} \tag{25}$$

which means that the product of the wavelength of the cyclotron motion and the magnetic field strength is constant.

We can now calculate the value of the constant in (25) for the electron:

$$B \cdot \lambda_c = 10.7 \ [K\Gamma \cdot \text{cm}] \tag{26}$$

where B is expressed in kilogauss and λ_c in cm. Equation (26) is easy to remember and is therefore often used in practical calculations for magnetron circuits.

Lastly, let us for a moment consider the path of an electrically-charged

particle in a uniform magnetic field, this time in a direction which is not normal to the magnetic field. This involves the two components v_p and v_t. (see page 10).

As a result of the effect of v_t the particle will follow a cyclotron path of radius R in accordance with Eq. 18:

$$R = \frac{v_t \cdot m}{B \cdot e}$$

The particle will at the same time execute a uniform movement at a velocity v_p in the direction of the magnetic field.

The actual motion is a combination of both paths and takes the form of a spiral of constant pitch, with radius R.

The pitch may be expressed as:

$$h = v_p \cdot T_0 = 2\pi \frac{m \cdot v_p}{e \cdot B}$$

from which we obtain:

$$\frac{h}{R} = 2\pi \cdot \frac{v_p}{v_t}$$

This kind of motion of electrically-charged particles along a line of force is not very important when dealing with magnetrons, but it plays a significant part in such applications as magnetic focusing.

2.4 Movement of a particle in crossed electric and magnetic fields

We shall now consider the movement of an electrically-charged particle when it is simultaneously subjected to a magnetic and an electric field.

In so doing we shall assume the magnetic field to be uniform, and the electric field to have components only in a plane normal to the direction of the magnetic field. These limitations are such as to meet conditions which prevail in a magnetron.

For convenience let us imagine a capacitor having a voltage V across

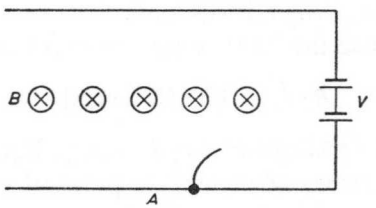

Fig. 11. Path of a charged particle in electric and magnetic fields. The initial velocity is zero.

its electrodes and a magnetic field of strength B between them. (Fig. 11). The direction of the magnetic field is normal to the plane of the drawing.

To ascertain the path of an electrically-charged particle let us assume that the particle commences at the capacitor electrode A, at zero velocity. At that moment it will be subjected only to a force due to the electrical field. It now commences to move at right angles from the electrode. As the velocity increases, the effect of the magnetic field comes into play and the particle is deflected in its path. As long as the particle is moving towards the other electrode its velocity will increase and this means that the force exerted by the magnetic field on the particle also increases. At a certain point in the path of the particle this magnetic force exceeds the force exerted by the electric field and the particle is then deflected back towards the electrode from which it originated, ultimately arriving there with zero velocity. Let us assume that the path described by the particle under such conditions is cycloidal. A cycloid is the figure described by a point on a circle when the latter is rolled along a plane (Fig. 12).

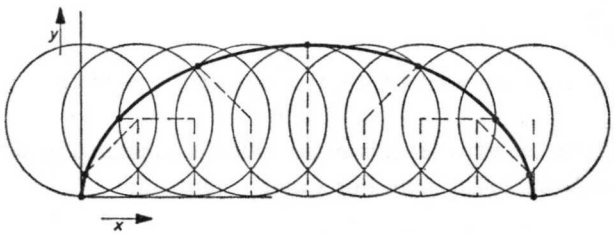

Fig. 12. Cycloidal path of an electrically-charged particle in intersecting electric and magnetic fields. The initial velocity is zero.

To uphold these assumptions we shall first determine the path of the particle by analysis.

Let the vertical axis of a system of co-ordinates be denoted by Y and the horizontal axis by X; then,

$$y = R(1 - \cos\varphi)$$
$$x = R(\varphi - \sin\varphi)$$

where φ is the angle through which the hypothetical circle has turned; R is the radius of the circle.

With constant angular velocity: $\varphi = \omega \cdot t$
where t is the time. A cycloidal path is thus described by parameters:

$$y = R(1 - \cos\omega t) \tag{27}$$
$$x = R(\omega t - \sin\omega t) \tag{28}$$

The particle in tracing its path must comply with the energy law, i.e. that its kinetic energy W_v must be equal to the energy W_E absorbed from the electrical field. According to Eq. (12):

$$W_v = e \cdot V$$

In our case $V = E \cdot y$, so

$$W_v = \frac{mv^2}{2} = e \cdot E \cdot y \tag{29}$$

For the velocity v we use the general formula

$$v = \frac{ds}{dt} = \sqrt{\frac{dx^2 + dy^2}{dt}} = \sqrt{\dot{x}^2 + \dot{y}^2}$$

hence (29) becomes

$$\dot{x}^2 + \dot{y}^2 = 2 \cdot \frac{E \cdot e}{m} \cdot y \tag{30}$$

with $\dot{x} = \frac{dx}{dt}$, $\dot{y} = \frac{dy}{dt}$.

Because of the energy law, then, the path of the particle must conform to Eq. (30).

We shall now see whether this path, which is expressed in terms of (27) and (28), conforms to Eq. (30). For $\dot{x}$ and $\dot{y}$ we write:

$$\dot{y} = R \cdot \omega \cdot \sin \omega t \tag{31}$$

$$\dot{x} = R \cdot \omega \, (1 - \cos \omega t) \tag{32}$$

With Eq. (30) this gives

$$2R^2\omega^2 \, (1 - \cos \omega t) = \frac{2eE}{m} \cdot R \cdot (1 - \cos \omega t) \text{ or}$$

$$eE = m \cdot R \cdot \omega^2 \tag{33}$$

Eq. (33) shows that the path of the particle will conform to the law of energy only if e, E, m, R and ω satisfy this equation. As the time does not appear in this equation, the law of energy is met at every point along the path. The second requirement to be imposed on the path is that the sum of all the forces acting on the particle at every point along the path shall be zero. These forces are as follows; by the electric field a force $K_E = e \cdot E$ in the direction of the y axis; by the magnetic field $K_E = e \cdot v \cdot B$ normal to the direction of the path; the force of inertia $K_m = m \cdot \frac{dv}{dt}$ in the direction

opposed to that of the motion and, finally, the centrifugal force $K_{RK} = m \cdot \frac{v^2}{R_k}$ normal to the path; R_k is the radius of the path.

It will be sufficient to see in how far the path satisfies this requirement at one point only, namely at the highest point of the path, where $\omega t = \pi$.

The velocity at that point is:

$$v = \sqrt{\dot{x}^2 + \dot{y}^2} = R\omega \sqrt{2\,(1 - \cos \omega t)} = 2R\omega \tag{34}$$

In general, the following applies to the radius R_k of the path:

$$R_k = \frac{\left[1 + \left(\frac{\mathrm{d}y}{\mathrm{d}x}\right)^2\right]^{\frac{3}{2}}}{\frac{\mathrm{d}^2 y}{\mathrm{d}x^2}} = \frac{(\dot{x}^2 + \dot{y}^2)}{\ddot{y}\dot{x} - \dot{y}\ddot{x}}. \tag{35}$$

Inserting the values for the path:

$$R_k = 2R \sqrt{2\,(1 - \cos \omega t)} \tag{36}$$

and $\omega t = \pi$ for the top of the path:

$$R_k = 4R \tag{37}$$

At that point the path is parallel to the x axis, so we write for the forces involved (Fig. 13):

$$eE + m \cdot \frac{v^2}{R_k} = e \cdot v \cdot B \tag{38}$$

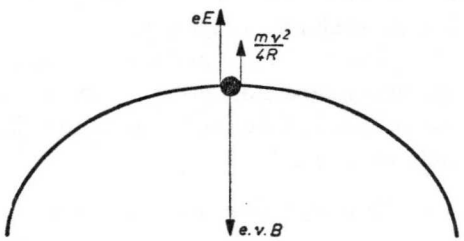

Fig. 13. Cycloidal path of an electrically-charged particle. The forces acting on the particle at the highest point of the path are in accordance with Eq. (38).

Combining (33), (34) and (37) with (38) we then have:

$$\omega = \frac{eB}{m}, \tag{39}$$

which shows that the sum of all the forces acting on the particle is zero

only when the angular velocity for the cycloidal motion is equal to (39). It is also seen that the right hand term of (39) is the same as (23), which means that:

$$\omega = \omega_c \tag{33}$$

and, with

$$R = \frac{E}{B^2} \cdot \frac{m}{e} \tag{41}$$

Thus it is proved that, under the conditions described, the path of the particle is cycloidal.

The cyclotron frequency is the same as the angular frequency of the rolling circle. The speed v_x at which the centre point of the circle travels along the x axis is obtained by (33) and (34):

$$v_x = R \cdot \omega_c = \frac{E}{B}. \tag{42}$$

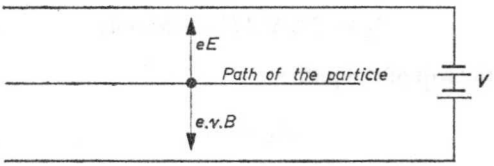

Fig. 14. Forces acting on an electrically-charged particle travelling in a straight path within intersecting electric and magnetic fields.

Thus it may be said that the particle makes a movement at constant velocity along the x axis and simultaneously a rotary movement, the angular frequency of which is the cyclotron frequency.

Let us now ascretain the conditions under which an electrically charged particle will travel through a capacitor, along a path parallel to the capacitor electrodes. The magnetic field in the capacitor is again uniform, (see Fig. 14).

The particle is subjected to the following forces:

$$K_E = e \,.\, E \text{ and } K_B = e \cdot v \cdot B.$$

The required condition is

$$K_E = K_B \text{ or } e \cdot E = e \cdot v \cdot B \tag{43}$$

We find that the velocity is:

$$v = \frac{E}{B} \tag{44}$$

A charged particle passing at this velocity through the capacitor along

a path parallel to the electrodes will be able to contine travelling and will not bend towards either of the electrodes.

Now, if we vary the velocity of the particle by an amount Δv (e.g. accelerate it), it will not be able to maintain a straight path, but will be deflected towards one of the electrodes of the capacitor. Under these conditions the following again applies (see (38)):

$$eE + m \cdot \frac{v^2}{R_k} = e \cdot v \cdot B$$

In this equation, $R_k > 0$ would indicate that a negatively charged particle is deflected towards the negative electrode. $R_k < 0$ would show that it is moving towards the other electrode.

We shall now calculate the radius of curvature R_k for the case where the velocity v differs from (44). It follows from (38) that:

$$R_k = \frac{m \cdot v^2}{e \cdot v \cdot B - eE} \tag{45}$$

With $v = \frac{E}{B} + \Delta v$ and $|\Delta v| \ll \left|\frac{E}{B}\right|$ we obtain

$$R_k \cdot \Delta v = \frac{mE^2}{eB^3} > 0 \tag{46}$$

Equation (46) shows that the product $R_k \cdot \Delta v$ is always positive, so that, if the velocity is increased ($\Delta v > 0$), R_k is positive. If the velocity is reduced ($\Delta v < 0$), R_k will be negative. Applying (46) to an electron, we may conclude that if the electron is travelling along a path parallel to the capacitor electrodes, and is accelerated, it will be deflected towards the negatively charged electrode and, conversely, if it is decelerated, it will move towards the positive electrode.

This phenomenon is very important from the point of view of the principle on which magnetrons operate and we shall refer to it again later.

So far we have dealt only with the movements of a charged particle in a parallel plane capacitor; we shall now examine the path of the particle in a cylindrical or wound type of capacitor (Fig. 15).

The electrical field strength in this type of capacitor is represented by:

$$E = \frac{1}{R} \cdot \frac{V_0}{\ln \frac{R_2}{R_1}} \tag{47}$$

where V_0 is the voltage between the inner and outer electrodes. For the voltage across the inner electrodes at a point R from the axis we write:

$$V = \int_{R_1}^{R} E \mathrm{d}R = \frac{V_0}{\log \frac{R_2}{R_1}} \cdot \log \frac{R}{R_1} \tag{48}$$

Denoting the path of the particle in polar co-ordinates:

$$R = R(t) \tag{49}$$

$$\varphi = \varphi(t) \tag{50}$$

we again have Equation (12) $= \frac{mv^2}{2} = eV$

The following applies to v^2:

$$v^2 = \left(\frac{\mathrm{d}s}{\mathrm{d}t}\right)^2 = R^2 \dot{\varphi}^2 + \dot{R}^2 \tag{51}$$

where $\dot{\varphi}$ and $\dot{R}$ denote the derivatives with respect to time. Equations (49) and (50) must now satisfy the differential equation:

$$\frac{m}{2}(R^2 \dot{\varphi}^2 + \dot{R}^2) = e \cdot V_0 \frac{\log \frac{R}{R_1}}{\log \frac{R_2}{R_1}}. \tag{52}$$

Equation (52) may be interpreted for the path of a particle in a cylindrical capacitor in the same way as (30) for the plane capacitor.

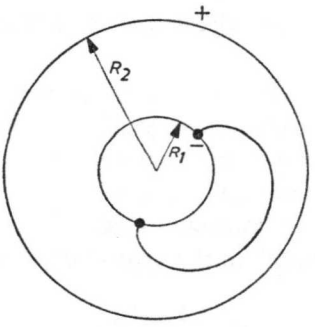

Fig. 15. Path of an electrically-charged particle under the influence of electric and magnetic fields in a cylindrical capacitor. The direction of the magnetic field is normal to the plane of the paper. R_1 and R_2 are the radii of the inner and outer electrodes respectively.

It would take us too far afield to work out Equation (52) here, but it will be found that the path described is much like the cycloid shown in Fig. 15.

Again we see that on leaving the inner electrode the particle first makes an excursion towards the outer electrode and finally returns to the inner one.

Now that we have noted the path of an electrically-charged particle in intersecting electric and magnetic fields we may pass to the subject of the cut-off parabola.

2.5 The cut-off parabola

We have seen above that under certain conditions in a capacitor, electrically charged particles follow a path such that they return to the electrode from which they started out. In effect this means that no current flows through the capacitor; in a certain sense a magnetic field plays the part of a control grid, i.e. the current is cut off by the magnetic field. The more the magnetic field is reduced the closer the paths of the particles will approach the opposite electrode of the capacitor; ultimately there will be a certain combination of magnetic field and voltage at which the particles just touch the opposite electrode and a current will flow through the capacitor.

Let us now see in the case of the plane capacitor what the conditions will have to be for the charged particles just to reach the opposite electrode.

From the previous chapter we have seen that the radius R of the cycloidal path is:

$$R = \frac{E}{B^2} \cdot \frac{m}{e} \tag{41}$$

The particle moves a maximum distance $d = 2 \cdot R$ from the electrode from which it departs, during which interval it passes through a potential:

$$V = 2RE = d \cdot E$$

We may therefore write:

$$2R^2 = \frac{V}{B^2} \cdot \frac{m}{e}$$

or,

$$d^2 = 2 \cdot \frac{m}{e} \cdot \frac{V}{B^2} \tag{54}$$

Solution of (54) with respect to V gives:

$$V = \frac{d^2 \cdot e \cdot B^2}{2 \cdot m} \tag{55}$$

which shows the relationship between the particle magnitudes (e, m), the capacitor (d) and V or B when the particles are just able to pass through the capacitor. The particles then reach the electrode tangentially.

Inserting the values for the electron in Eq. (55):

$$V = 8.8 \cdot 10^{-2} \cdot d^2 \cdot B^2 \tag{56}$$

with V in volts, B in gauss and d in cm.

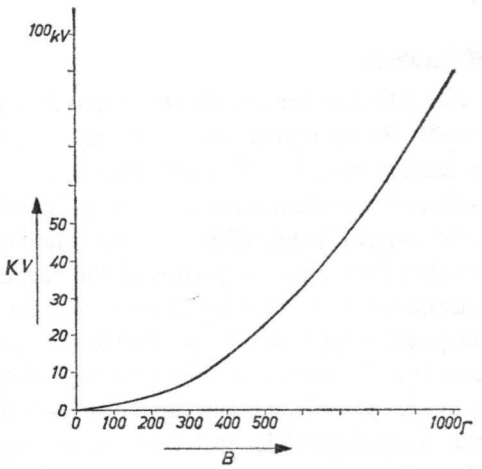

Fig. 16. Cut-off parabola plotted in accordance with Eq. 56.

This is shown plotted in Fig. 16 for the case where $d = 1$ cm.

A very similar relationship applies also to the cylindrical type of capacitor; in its ultimate form this is:

$$V = \frac{e}{m} \cdot \frac{R_A^2}{8} \cdot \left[1 - \left(\frac{R_C}{R_A}\right)^2\right]^2 \cdot B^2 \tag{57}$$

This equation was derived in the first instance by Hall, after whom it has been named. In it R_A is the radius of the outer electrode, R_C the radius of the inner electrode.

Inserting $R_C = R_A - d$ in Eq. (57) and taking $R_A \to \infty$ Eq. (57) becomes Eq. (55).

Substituting the values for the electron in (57) we have:

$$V = 2.2 \cdot 10^{-2} \cdot R_A^2 \cdot \left[1 - \left(\frac{R_C}{R_A}\right)^2\right]^2 \cdot B^2 \tag{58}$$

with V in volts, B in gauss, R_A and R_C in cm.

When (57) is plotted with B on the horizontal axis and V on the vertical axis Eq. (57) reveals a parabola. This is known as the cut-off parabola, because it gives the values of B and V at which the capacitor just ceases to pass current. Points above the parabola represent combinations of V and B at which current will flow, whereas points below it give those values at which no current can pass (Fig. 16).

Let us now see what the angular velocity of the charged particles will be on reaching the anode.

The particles will have passed through a potential V (57). According to (13), then, the velocity v is:

$$v = \sqrt{\frac{2eV}{m}} = \frac{e}{2m} \cdot R_A \left[1 - \left(\frac{R_C}{R_A}\right)^2\right] \cdot B$$

The angular velocity is given by:

$$\omega = \frac{v}{R_A} = \frac{e}{2m} \cdot \left[1 - \left(\frac{R_C}{R_A}\right)^2\right] \cdot B \tag{58a}$$

which gives us for every point in the cut-off parabola the angular velocity of the charged particle at the moment of reaching the anode. It is seen that ω is proportional to the magnetic field strength.

Sufficient has now been said to give the reader some idea of the movements of electrically-charged particles in crossed electric and magnetic fields. We now therefore pass on to a discussion of the high frequency electric field within the space between the cathode and the anode.

III. THE CIRCUIT

3.1 The anode as a delay line

It has been shown (p 6) that when an electron is decelerated by an electric field it delivers energy to the field. Now, in order to generate high frequency oscillations in this manner, matters must be so arranged that the electric field of these high frequency oscillations is present in the space where the electrons are free to move, that is, between cathode and anode, this space being known as the interaction space; only in this way can the electrons interact with the field.

We must also see that the electrons deliver energy to the field for as long as possible (preferably for several cycles of the high frequency oscillations) i.e. that they are decelerated or delayed by the field. Expressed otherwise, it may be said that the electrons must remain in phase with the high frequency electric field. This condition will obtain if the velocity at which the electrons travel through the interaction space is equal to the phase velocity of the high frequency field.

It is known that, under certain conditions, the phase velocity of an electric field along a straight conductor is equal to the speed of light. If the high frequency electric field in a magnetron were propagated along a straight conductor, the velocity of the electrons would thus have to be equal to the speed of light in order to remain in phase with the field, but it is not possible to accelerate electrons to this extent.

In the magnetron, then, the phase velocity of the high frequency field must be delayed to enable the electrons to keep abreast of it.

To do this we guide the electric field along a conductor which has the property of delaying the phase velocity of the high frequency field and which is known as a delay line or circuit. A few remarks will now be devoted to such delay circuits.

Most magnetrons have a cylindrical anode with a concentric cathode, which implies an annular, closed delay circuit. The fact that this circuit is closed has several important consequences for the characteristics of the magnetron itself, but we shall return to this subject later.

3.2 General considerations concerning non-homogeneous delay circuits

In the following we shall consider certain properties of delay circuits of periodic structure; for a detailed review reference may be made to existing literature.

Fig. 17a is a diagram of a non-homogeneous delay circuit; it can be

regarded as being built up from four elements, which can be approximated by the equivalent circuit shown below.

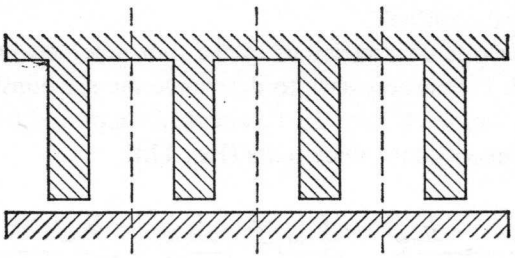

Fig. 17a. Straight periodic delay circuit of 4 elements.

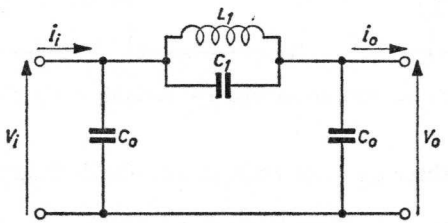

Fig. 17b. Equivalent circuit diagram of an element as in Fig. 17a.

i and V are respectively the current and voltage measured at the input and output.

It is true of course that an equivalent circuit diagram such as that in Fig. 17b only represents an approximation of the real characteristics of the actual circuit, but the value of such an approximation lies in the fact that, on the one hand, it facilitates a qualitative understanding of the properties of the approximated structure and, on the other hand, it enables us to study the effects of modifications to the delay circuit, as will presently be shown by an example.

The circuit in Fig. 17b can also be presented in a more general form (Fig. 17c).

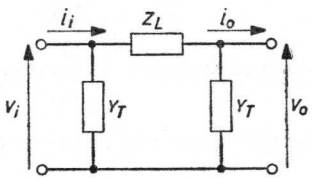

Fig. 17c. The general form of a four-pole network, as in Fig. 17b.

The single element in the circuit is here represented as a four-terminal network; at the two left-hand terminals a voltage V_i and a current i_i will be measured, in the directions shown. A voltage V_o with current i_o appear at the right-hand terminals.

To calculate those characteristics of the four-pole network in which we are interested it is first necessary to determine the relationship between V_i and i_i as a function of V_o and i_o. To simplify the procedure we can divide the four-pole network into three parts (Fig. 17d).

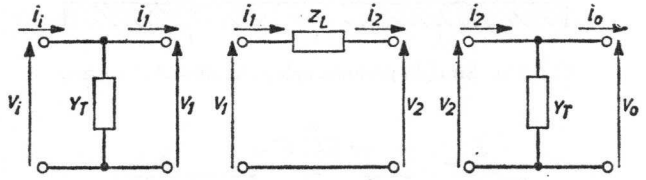

Fig. 17d. Four-pole network as in Fig. 17c divided into 3 elementary networks.

The following three equations can at once be derived from this diagram:

$$V_i = V_1 \text{ (59a)} \qquad V_1 = V_2 + Z_L \cdot i_2 \text{ (59b)} \qquad V_2 = V_0 \text{ (59c)}$$

$$i_i = Y_T V_1 + i_1 \text{ (60a)} \qquad i_1 = i_2 \text{ (60b)} \qquad i_2 = Y_T V_0 + i_0 \text{ (60c)}$$

Combining (59a) and (60a) with (59b) and (60b) we have:

$$\left.\begin{aligned} V_i &= V_2 + Z_L \cdot i_2 \\ i_i &= Y_T V_2 + (1 + Z_L Y_T) i_2 \end{aligned}\right\} \text{ with and (59c) and (60c):}$$

$$V_i = (1 + Z_L Y_T)\, V_0 + Z_L \cdot i_0 \tag{61}$$

$$i_i = Y_T\,(2 + Z_L Y_T)\, V_0 + (1 + Z_L Y_T)\, i_o \tag{62}$$

Thus (61) and (62) show the dependence of the current and voltage at the input of the four-pole network upon the current and voltage at the output.

We shall now show that an angle φ and an impedance Z_0 can be found, such that:

$$1 + Z_L Y_T = \cos\varphi \tag{63}$$

$$Z_L = j\, Z_0 \sin\varphi \tag{64}$$

$$Y_T\,(2 + Z_L Y_T) = j \cdot \frac{1}{Z_0} \sin\varphi \tag{65}$$

The question is whether the value of φ in (63 or (65) will satisfy the well-known equation:

$$\cos^2\varphi + \sin^2\varphi = 1$$

It is found that

$$\cos^2 \varphi = (1 + Z_L Y_T)^2 = 1 + 2Z_L Y_T + Z_L^2 Y_T^2 \tag{67}$$

From (64) and (65):

$$\sin^2 \varphi = -Z_L Y_T (2 + Z_L Y_T) = -2Z_L Y_T - Z_L^2 Y_T^2 \tag{68}$$

and from (67) and (68):

$$\cos^2 \varphi + \sin^2 \varphi = 1$$

For Z_0, Eq. (64) and (65) give us:

$$Z_0^2 = \frac{Z_L}{Y_T (2 + Z_L Y_T)} = \frac{1}{Y_T (2Y_L + Y_T)} \text{ with } Y_L = \frac{1}{Z_L} \tag{66}$$

Having shown the validity of (63), (64) and (65) we may now write (61) and (62) in the following form:

$$V_i = V_0 \cos \varphi + jZ_0 i_0 \sin \varphi \tag{69}$$

$$i_i = V_0 \cdot j \cdot \frac{1}{Z_0} \sin \varphi + i_0 \cos \varphi \tag{70}$$

with

$$\cos \varphi = 1 + Z_L Y_T \tag{63}$$

and

$$\frac{1}{Z_0^2} = Y_T (2Y_L + Y_T) \tag{66}$$

Let us now see how an impedance Z_2 at the output (right hand) side of the four-pole network can be referred to the input side.

From (69) and (70) we obtain by division:

$$\frac{V_i}{i_i} = Z_1 = Z_0 \cdot \frac{Z_2 \cos \varphi + jZ_0 \sin \varphi}{jZ_2 \sin \varphi + Z_0 \cos \varphi} \text{ (71) with } Z_2 = \frac{V_0}{i_0} \tag{71}$$

It appears, then, that Eq. (71) is identical with the following:

$$Z_1 = Z_0 \cdot \frac{Z_2 \cdot \cos \frac{2\pi}{\lambda g} \cdot l + jZ_0 \sin \frac{2\pi}{\lambda g} \cdot l}{jZ_2 \sin \frac{2\pi}{\lambda g} \cdot l + Z_0 \cos \frac{2\pi}{\lambda g} \cdot l} \tag{72}$$

which shows the manner in which the impedance Z_2 at the output of an ordinary line, having a characteristic impedance of Z_0, a length l, and at a frequency with wavelength λg on the line, is transformed to the input.

Z_1 is therefore the impedance that exists at the input terminals of our line if an impedance Z_2 is connected to the output.

From the identity of Eq. (71) and (72) with $\varphi = \frac{2\pi}{\lambda g} \cdot l$ (73) it follows that the four-pole network in Fig. 17c at a certain frequency behaves as an ordinary line of length l, wavelength λ_g and characteristic impedance Z_0. There is this difference between the four-pole network and the line, however, that the characteristic impedance of the four-pole network is dependent on frequency and that of the line is not. It follows, then, that at different frequencies four-pole networks can be replaced by lines of different length and characteristic impedance.

This fact, that an element in a delay circuit can be replaced by an ordinary transmission line, at any rate for a certain range of frequencies, considerably simplifies our study of the electrical conditions in a delay circuit.

If we now terminate the four-pole network in Fig. 17c with its characteristic impedance Z_0, the input impedance, according to Eq. (71) will be:

$$Z_1 = Z_0 \text{ with } Z_2 = Z_0$$

Hence the impedance at the input is the same as at the output.

This being so, the voltage and current at the input are (from (69) and (70)):

$$V_i = V_0 (\cos \varphi + j \sin \varphi) = V_0 e^{i\varphi} \tag{74}$$

$$i_i = i_0 \ (\cos \varphi + j \sin \varphi) = i_0 e^{i\varphi} \tag{75}$$

The amplitudes are the same; only the phase is displaced to the extent of φ.

If we denote the physical length of our four-pole network by L and the phase difference in the voltage as between the input and output by φ (see 74) we can speak of a phase velocity v_p, in accordance with:

$$v_p = \frac{L}{\varphi} \cdot 2\pi \cdot f = L \cdot \frac{\omega}{\varphi} \tag{77}$$

where f is the frequency at which the phase difference φ occurs:
Now $f \cdot \lambda = c$, so:

$$v_p = \frac{L}{\lambda} \cdot \frac{2\pi c}{\varphi} \text{ or } \frac{c}{v_p} = \frac{\varphi}{2\pi} \cdot \frac{\lambda}{L} \tag{76a}$$

The value of $\frac{c}{v_p}$ in Eq. (76) indicates how much less the phase velocity of the wave on the delay line is than the speed of light c.

According to Eq. (63), φ is a function of λ, and we can therefore calculate the value of $\frac{c}{v_p}$ as a function of λ for any given four-pole network.

By plotting $\frac{c}{v_p}$ on the vertical axis of a system of coördinates with $\frac{\lambda}{L}$ on the horizontal axis the properties of the four-pole network with respect to the phase velocity can be shown (see Fig. 18a). The resultant curve is called a dispersion curve. According to Eq. (76a) the curves for φ = constant are, in effect, straight lines passing through the origin.

Besides the phase velocity v_p it is also necessary to consider the group velocity v_g, by which is meant the velocity at which energy is propagated through the four-pole network. The group and phase velocities in a transmission line, for example, are both equal to the speed of light and are independent of the frequency. If there is any dispersion in the line, however, that is if the phase velocity is dependent on frequency, then $v_p \neq v_g$. Textbooks on physics tell us that v_p bears the following relationship to v_g:

$$\frac{1}{v_g} = \frac{\mathrm{d}}{\mathrm{d}\omega}\left(\frac{\varphi}{L}\right) = \frac{1}{L} \cdot \frac{\mathrm{d}\varphi}{\mathrm{d}\omega} \tag{78}$$

where φ represents the phase difference in the four-pole network and L its physical length.

Taking the case of four-pole networks in general it is conceivable that:

$$\frac{\mathrm{d}\varphi}{\mathrm{d}\omega} > 0 \quad \text{or} \quad \frac{\mathrm{d}\varphi}{\mathrm{d}\omega} < 0$$

If $\frac{\mathrm{d}\varphi}{\mathrm{d}\omega} > 0$ the group velocity has the same direction as the phase velocity, in which case the energy and the phase of the electromagnetic wave travel in the same direction through the four-pole network. We then speak of a forward wave. Where $\frac{\mathrm{d}\varphi}{\mathrm{d}\omega} < 0$ the group velocity has the opposite direction to the phase velocity and we have what is called a backward wave.

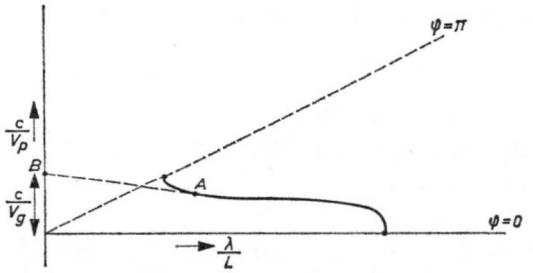

Fig. 18a. Dispersion curve of a delay line. The phase and energy of the fundamental wave proceed in the same direction.

The group velocity v_g can be found at once from Fig. 18a for any value of $\frac{\lambda}{L}$. If the tangent to the curve is drawn at point A to the $\frac{c}{v_p}$ axis (point B), the distance from the origin to point B will be equal to $\frac{c}{v_g}$. When the tangent intersects the $\frac{\lambda}{L}$ axis between the point of contact A and the point of intersection B, we have a backward wave (Fig. 18b); but if there is no point of intersection with the $\frac{\lambda}{L}$ axis, the wave is forward (Fig. 18a).

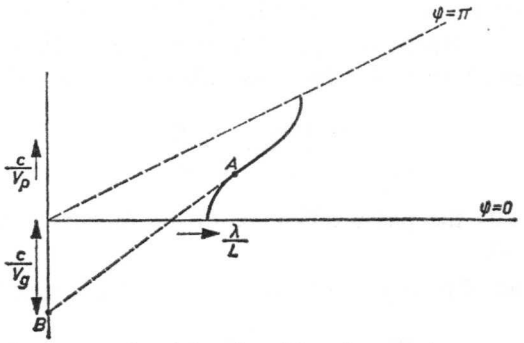

Fig. 18b. Dispersion curve of a delay line. The phase and energy of the fundamental wave proceed in opposite directions.

In the above we have referred to the phase difference φ that occurs when a wave is propagated through the four-pole network, and by this is meant the measurable phase difference of the wave as between the input and output. It is conceivable that a wave having such a measurable difference in phase (φ) is in actual fact rotated to the extent of $\varphi + 2\pi$ on its way through the network; moreover, as measurements cannot be effected within the four-pole network itself, it is even possible that, where there is measurable phase difference φ, the phase really varies about the value:

$$\varphi + m \cdot 2\pi \qquad m = 0, \pm 1, \pm 2, \pm \ldots \tag{79}$$

on the way through the four-pole network.

Again denoting the length of the four-pole network by L, and the phase velocity by v_p, such waves may be written as:

$$v_p = L \cdot \frac{\omega}{\varphi + m \cdot 2\pi} \quad \text{and} \quad \frac{c}{v_p} = \left(\frac{\varphi}{2\pi} + m\right) \cdot \frac{\lambda}{L} \tag{76b}$$

from which it is seen that the waves pass through the network at different

phase velocities. The wave in respect of which $m = 0$ will have the greatest phase velocity; the higher the value of m the less the phase velocity.

The group velocity v_g of the energy transported by the waves is obtained from:

$$\frac{1}{v_p} = \frac{\mathrm{d}}{\mathrm{d}\omega}\left(\frac{\varphi + m \cdot 2\pi}{L}\right) = \frac{1}{L} \cdot \frac{\mathrm{d}\varphi}{\mathrm{d}\omega} \tag{80}$$

so v_g is the same for all the waves.

It is seen, then, that at *one particular frequency* an infinite series of waves can pass through our four-pole network; the group velocity of all these component waves is the same, but the phase velocity differs in each case. That component for which $m = 0$ is usually refered to as the fundamental wave; the phase velocity is greater than that of all the other components. Waves for which $m \neq 0$ are known as spatial harmonics, but the word harmonic can be misleading as there is no question of different *frequencies*; the phenomenon occurs only at *one* definite frequency.

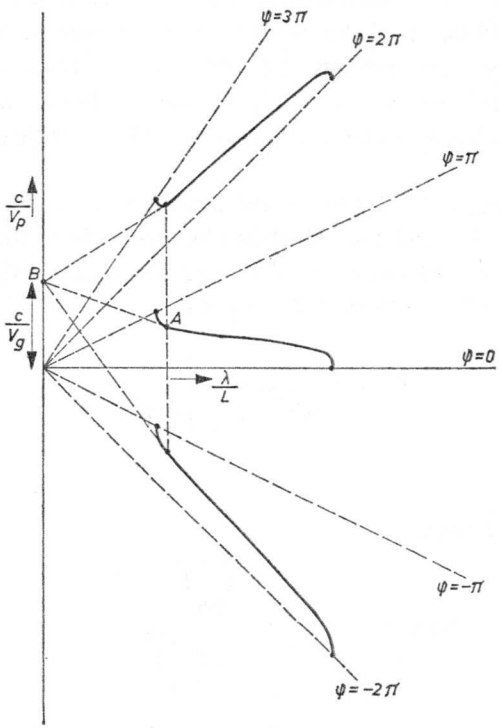

Fig. 19. Dispersion curve of a delay line. The figure shows the fundamental wave and the components $m = +1$ and $m = -1$. (See also Eq. 76b).

Such component waves can also be included in the diagram showing $\frac{c}{v_p}$ as a function of $\frac{\lambda}{L}$. If the curve of the fundamental is known, the lines for the component waves can be derived from it in accordance with Eq. (76b) (Fig. 19). It will be seen that the component waves fall into two groups, viz. one of forward waves and one of backward waves. Thus any non-uniform delay line may transmit both forward and backward waves.

The amplitude ratios of all these component waves are determined by the geometrical form of the delay line or four-pole network. If the electric field in the direction of propagation of the wave were sinusoidal, only the fundamental wave would be produced, but, as the field in the region of the vanes in the line departs very considerably from the sinusoidal, component waves must necessarily occur. Near the straight section of the line the departure from the sinusoidal is not so pronounced and the field of the component waves accordingly not so strong. In general it can be said that the field strength of the component waves penetrates less deeply into the space between the vanes and straight conductor according as m increases.

Lastly, it should be noted that no isolated component wave can occur in the line; if energy is injected into the field of one of the component waves this energy is distributed among all the components in such a way that their amplitudes are related to one another in accordance with the geometrical form of the line.

Having now determined certain characteristics of a fourpole network as shown in Fig. 17b and 17c, which are important from the point of view of our investigation, let us now finally compute $\varphi_1 Z_0$ as a function of ω.

It follows from Fig. 17b that $Y_T = j\omega C_0$

$$Z_L = j\frac{\omega}{\omega_1^2 C_1} \cdot \frac{1}{1 - \left(\frac{\omega}{\omega_1}\right)^2}$$

where $\omega_1^2 = L_1 C_1$

With Eq. (63) and (66):

$$\cos\varphi = 1 - \frac{C_0}{C_1} \cdot \frac{\left(\frac{\omega}{\omega_1}\right)^2}{1 - \left(\frac{\omega}{\omega_1}\right)^2} \tag{81}$$

$$\frac{1}{Z_0^2 \omega_1^2 C_0^2} = 2 \cdot \frac{C_1}{C_0}\left[1 - \left(\frac{\omega}{\omega_1}\right)^2\right] - \left(\frac{\omega}{\omega_1}\right)^2 \tag{82}$$

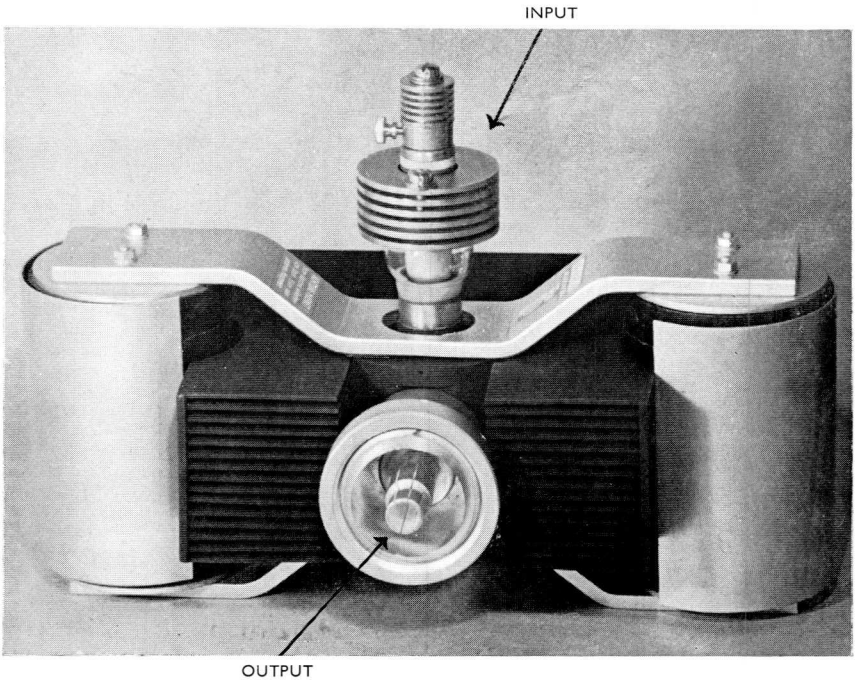

Fig. 3. Packaged magnetron, Philips type 7091. This tube delivers 2 kW continuous wave at 2450 Mc/s.

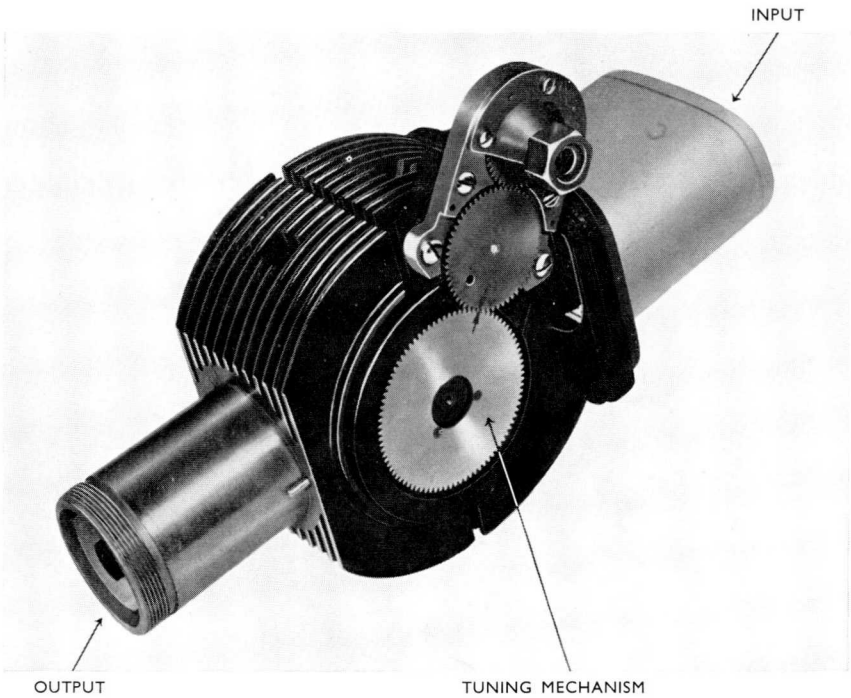

Fig. 4. Unpackaged magnetron, Philips type 5J 26. This is a tunable magnetron for pulsed operation delivering 500 kW. Frequency variable from 1220 to 1350 Mc/s.

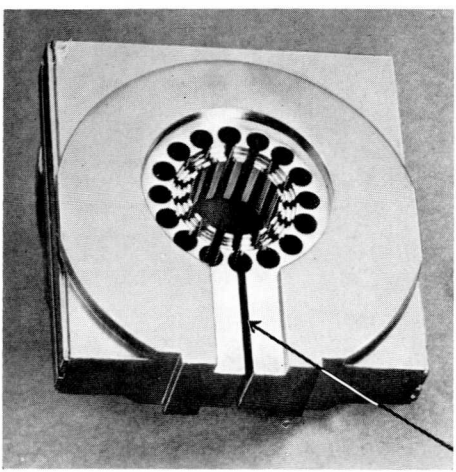

Fig. 5. The anode of a magnetron, showing the components which determine the frequency and the output coupling slot.

Equation (81) shows that $|\cos\varphi|$ is $\leqslant 1$ only in the range of frequencies:

$$0 \leqslant \left(\frac{\omega}{\omega_1}\right)^2 \leqslant \frac{2C_1}{2C_1 + C_0}.$$

At these frequencies Z_0 is real.

At frequencies $\left(\frac{\omega}{\omega_1}\right)^2 \leqslant \cdot \frac{2C_1}{2C_1 + C_0}$, $|\cos\varphi| > 1$.

The physical meaning of this is that, in the range $0 \leqslant \left(\frac{\omega}{\omega_1}\right)^2 \leqslant \frac{2C_1}{2C_1 + C_0}$, electric waves can travel through fourpole networks without attenuation; they undergo only a shift in phase. With $\left(\frac{\omega}{\omega_1}\right)^2 > \frac{2C_1}{2C_1 + C_0}$ the voltage at

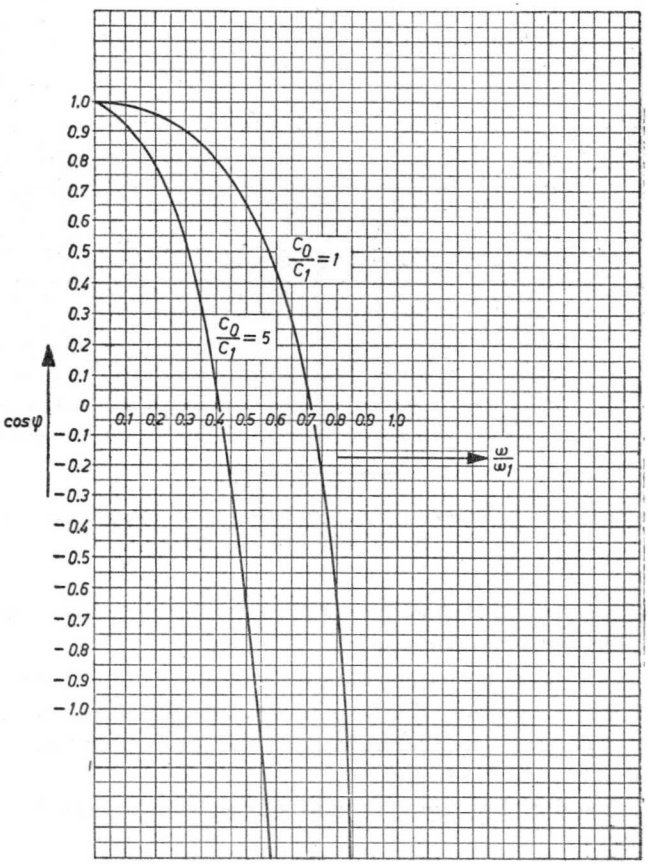

Fig. 20. Phase difference cos φ per element of a delay line as shown in Figs. 17a and 17b as a function of ω/ω_1 with C_0/C_1 as parameter.

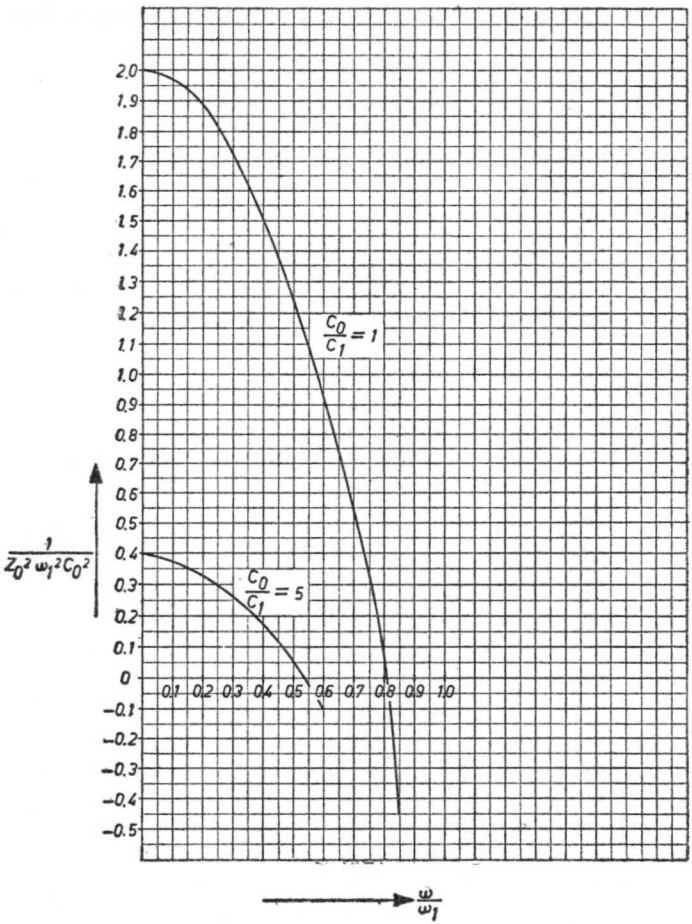

Fig. 21. Characteristic impedance Z_0 plotted against ω/ω_1 for the delay line shown in Figs. 17a and 17b with C_0/C_1 as parameter.

the output is less than that at the input and, moreover, the characteristic impedance then becomes complex.

The fact that waves are propagated without attenuation within a certain range applies in general to all delay circuits. Actually there is a number of such pass bands, but only that containing the lowest frequency is of any importance in magnetron techniques.

In Figs. 20 and 21 Equation (81) and (82) are shown plotted at different values of $\frac{C_0}{C_1}$.

At this point we pass on to a study of closed annular delay circuits.

3.3 The closed ring-shaped delay circuit

Let us imagine a straight delay circuit comprising N identical elements, terminated with its characteristic impedance. If we apply to the input a voltage V at a frequency f in the pass-band we know that waves will be propagated in the circuit whereby the phase difference per element of the circuit is:

$$\varphi + 2m\pi \qquad m = 0, \pm 1, \pm 2, \pm \ldots$$

The various values of m relate to the component waves. At the output, then, there will be a total phase difference ψ in accordance with:

$$\psi = N \cdot (\varphi + 2m\pi) \tag{83}$$

It is seen from Eq. (63) that φ is a function of the frequency f; hence ψ is also a function of the frequency:

$$\psi = N \cdot \varphi(f) = \psi(f) \tag{84}$$

If f is taken throughout the pass-band, φ varies between zero and π. With $m = 0$, Eq. (83) thus gives:

$$0 \leqslant \psi(f)_0 \leqslant \frac{N}{2} \cdot 2\pi \tag{85}$$

from which it is seen that there are several discrete frequencies f_n at which the phases at the input and output of the line are the same. These frequencies f_n can be ascertained from the following equation:

$$N \cdot \varphi(f_n) = n \cdot 2\pi \qquad n = 0, 1, 2, \ldots \frac{N}{2} \tag{86}$$

$$\varphi(f_n) = \frac{n}{N} \cdot 2\pi \qquad n = 0, 1, 2, \ldots \frac{N}{2} \tag{87}$$

At all frequencies at which $f \neq f_n$ the input and output voltages are not in phase. Also, at the frequencies f_n from Eq. (86) not only the fundamental wave, whereby $m = 0$, yields the same phase at input and output, but all the component waves do so as well. For, from Eq. (87) in respect of the phase difference of the component wave per element of the line:

$$\varphi(f_n) = \frac{n}{N} \cdot 2\pi + m \cdot 2\pi = \frac{2\pi}{N}(n + mN)$$

$$m = 0, \pm 1, \pm 2, \pm \ldots \tag{87a}$$

Hence the phase difference at the end of the line comprising N elements is:

$$\psi(f_n) = N \cdot \varphi(f_n) = n \cdot 2\pi + m \cdot N \cdot 2\pi = (n + mN)\, 2\pi \tag{88}$$

Now, since

$$\gamma = n + mN \tag{89}$$

is a whole number, $\psi(f_n)$ is a multiple of 2π.

If we now imagine the input terminals of the line connected to the output terminals we shall have a closed ring-shaped delay line (see Fig. 22), through which only the frequencies f_n in Eq. (87) and all their component waves will be able to travel. For, in respect of these frequencies, there is no phase difference as between the input and output of the original line; the fact that the input is now connected to the output makes no difference — other frequencies at which $f \neq f_n$ will not be able to develop in the closed circuit.

The result of joining the ends of the delay line is that it is now capable of oscillations at a number of discrete frequencies f_i in accordance with Eq. (87).

This can be explained by so connecting the delay line in Fig. 17a. It follows from Eq. (87) that:

$$\varphi(f_i) = \frac{n}{4} \cdot 2\pi \qquad 0 \leqslant n \leqslant 2$$

hence

$$\varphi_{n=0} = 0; \quad \varphi_{n=1} = \frac{\pi}{2}; \quad \varphi_{n=2} = \pi \quad \text{and from Eq. (81)}$$

$$f_{n=0} = 0; \quad f_{n=1} = f_1 \cdot \sqrt{\frac{C_1}{C_0 + C_1}} \quad f_{n=2} = f_1 \cdot \sqrt{2\frac{C_1}{2C_1 + C_0}}.$$

When referring to the various resonances of the closed delay line we usually mean the values of n in Eq. (82). Thus we speak of the "2nd mode" when we mean the resonance occurring at frequency $f_{n=2}$. In practice, one exception is made, namely in relation to the resonance at $n = \frac{N}{2}$, which is known as the "π-mode", since in this case the phase shift occasioned by one element in the line at this frequency is equal to π radians; from Eq. (87) it follows that for $n = \frac{N}{2}$ the angle $\varphi = \pi$.

We have now seen, then, that a number of discrete frequencies can be attributed to a closed delay line, so that we may speak of a certain "mode spectrum". The position occupied by the various resonant frequencies within the entire range is determined solely by Eqs. (63) and (87), which implies that the number of elements and the geometrical form of the line are the deciding factors.

We are now confronted with the curious fact that a system comprising N elements has only $\frac{N}{2} + 1$ resonant frequencies.

A system of this kind might otherwise be expected to have N resonances and in fact, this is so; the resonances whereby $n = 1, 2, \ldots \frac{N}{2} - 1$ occur in the form of doublets, but we shall refer to this again later. Only those resonances for which $n = 0$ and $n = \frac{N}{2}$ do not occur in the doublet form.

In all, then, there are $2\left(\frac{N}{2} - 1\right) + 2 = N$ different possibilities of resonance, as anticipated.

Under the conditions as described (the form of the delay line) two doublet frequencies are in each case the same.

To illustrate the above it may be useful to calculate the values of γ for a closed delay circuit comprising 8 elements. The 5 possible resonances $\left(\frac{N}{2} + 1\right)$ will be denoted by 0, 1, 2, 3 and 4; each fundamental wave contains an infinite number of spatial harmonics designated as γ:

$$\gamma = n + m \cdot N$$

The following values can thus be attributed to the 0 mode:

$$\gamma_0 = 0, \pm 8, \pm 16, \pm 32 \text{ etc.}$$

The first mode gives:

$$\gamma_1 = 1, +9, -7, +17, -15, \ldots\ldots$$

The second mode:

$$\gamma_2 = 2, +10, -6, +18, -14, \ldots\ldots$$

and the 3rd and 4th modes give respectively:

$$\gamma_3 = 3, +11, -5, +19, -13, \ldots\ldots$$
$$\gamma_4 = 4, +12, -4, +20, -12, \ldots\ldots$$

It is seen that each natural quantity occurs in one of the series.

3.4 The phase velocity in the closed delay circuit

As starting point we shall assume a closed delay circuit of N elements; in Fig. 22, $N = 8$.

It has been shown in the previous chapter that a line of this kind will be capable of oscillating at a number of discrete frequencies. Let f_i be one such frequency. We shall now ascertain the phase velocity at which the waves will be propagated along the line at this frequency.

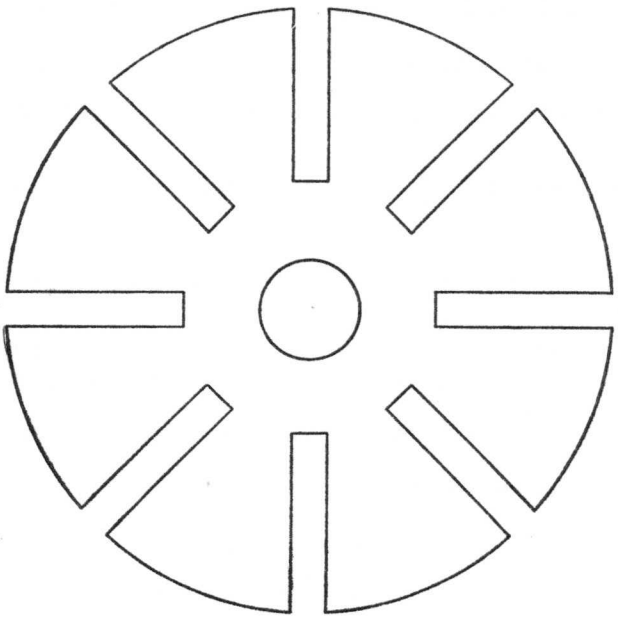

Fig. 22. Closed ring-shaped delay line of 8 elements.

We know that, at this frequency f_i, there will be an infinite series of values for γ to indicate the phase shift φ_i per element in the line. According to (87a):

$$\varphi_i = 2\pi \cdot \left(\frac{n}{N} + m\right) = \frac{2\pi}{N} \cdot \gamma_i \tag{87a}$$

Now the time T required for a variation in phase of 2π to take place is the period of oscillation of the frequency f_i:

$$T = \frac{1}{f_i}$$

To compute the phase angle φ_i from Eq. (87a) we thus require a time t:

$$t = \frac{T}{2\pi} \cdot \varphi_i = \frac{T}{N} \cdot \gamma_i$$

By the time the wave has passed an element in the line it will have travelled a distance $S = \frac{2\pi}{N} \cdot R_A$ (R_A = radius of anode) at a phase velocity v_i; hence

$$v_i = \frac{S}{t} = \frac{2\pi R_A}{T \cdot \gamma_i} = 2\pi \cdot c \cdot R_A \cdot \frac{1}{\lambda_i \cdot \gamma_i} \tag{91}$$

where c = speed of light and λ_i = wavelength of the frequency f_i in air.

The angular phase velocity ω can now be derived from the phase velocity v_i:

$$\omega = \frac{v_i}{R_A} = 2\pi \cdot c \cdot \frac{1}{\lambda_i \cdot \gamma_i} \tag{92}$$

From this it follows that with a given resonant frequency of the line (that is, a given value of λ_i) the various spacial harmonics progress at different angular frequencies. The most rapid of these is the fundamental wave, for the value of γ_i is the lowest.

The fact that each resonant frequency means an infinite number of discrete values of the angular frequency ω of the phase introduces certain complications in the working of magnetrons.

IV. CONDITIONS FOR OSCILLATION

4.1 Electrons synchronised with the r.f. electric field

On *p* 24 it was shown that it is essential in the operation of a magnetron for the electrons to be in phase with the r.f. electric field. We shall now ascertain the conditions under which this is fulfilled.

Equation (58a) shows that for every point (V, B) on the cut-off parabola (57), the angular velocity ω of the electrons, at the moment of reaching the anode is:

$$\omega = \frac{e}{2m} \cdot \left[1 - \left(\frac{R_C}{R_A}\right)^2\right] \cdot B \tag{58a}$$

The angular phase velocity ω of an r.f. field of wavelength λ in free space was found to be:

$$\omega = \frac{2\pi c}{\lambda_i \cdot \gamma_i} \tag{92}$$

Apparently, then, there is a point V^*, B^* on the cut-off parabola whereby the electrons, at the point in their path which is as close as possible to the anode, are synchronised with the field:

$$\frac{2\pi c}{\lambda_i \cdot \gamma_i} = \frac{e}{2m} \cdot \left[1 - \left(\frac{R_C}{R_A}\right)^2\right] \cdot B^*$$

or

$$B^* = 4\pi c \cdot \frac{m}{e} \cdot \frac{1}{\lambda_i \cdot \gamma_i \left[1 - \left(\frac{R_C}{R_A}\right)^2\right]}. \tag{93}$$

Inserting the speed of light and the values relative to the electron we then have:

$$B^* = \frac{21.4}{\lambda_i \cdot \gamma_i \left[1 - \left(\frac{R_C}{R_A}\right)^2\right]} \cdot 10^3 \quad \text{(gauss)} \tag{94}$$

B^* is the lowest value of the magnetic field at which synchronism with the electric field (defined by λ_i and γ_i) is possible and this is known as the "characteristic magnetic field".

From Eq. (57) the appropriate value V^* is found to be:

$$V^* = 2 \cdot \frac{m}{e} \cdot (\pi c)^2 \left(\frac{R_A}{\lambda_i \gamma_i}\right)^2 \tag{95}$$

With the electron values this becomes:

$$V^* = 1.01 \cdot 10^7 \left(\frac{R_A}{\lambda_i \gamma_i}\right)^2 \text{ (volts)} \tag{96}$$

and V^* is called the characteristic voltage of the magnetron at wavelength λ_i with γ_i indicating the mode.

The combination (V^*, B^*) contains the lowest values of V and B at which synchronism between the electrons and the field (defined by λ_i and γ_i) can exist.

From Eqs. (94) and (96) it is seen that the characteristic quantities B^* and V^*, apart from certain dimensions of the magnetron (R_C and R_A), are dependent only on the product $\lambda_i \cdot \gamma_i$. It is therefore possible for various modes of a magnetron to yield the same, or practically the same, value of the product $\lambda\gamma$. For example, if the π-mode of a particular magnetron gives the same value of this product $\lambda\gamma$ as any other mode, it may be expected that the working of this magnetron will not be stable, seeing that the fields of both modes are synchronised with the electrons.

So-called missing lines will then occur in the r.f. spectrum owing to the fact that at any given moment no energy will be delivered in the π-mode.

An example may make this clear. The wavelength of the π-mode in a 16-cavity magnetron is 3.2 cm, that of the 7th mode (the π-mode is the eighth) being 2.85 cm.

The values of γ_8 for the π-mode are:

$$\gamma_8 = n + m \cdot N = \pm 8, \pm 24, \pm 40, \text{ etc.}$$

and those of the 7th mode:

$$\gamma_7 = 7, +23, -9, +39, -25, \text{ etc.}$$

Hence for the fundamental wave of the π-mode we have:

$$\lambda_\pi \cdot \gamma_8 = 3.2 \cdot 8 = 25.6$$

whilst the first spatial harmonic of the 7th mode is

$$\lambda_7 \cdot \gamma_7 = 2.85 \cdot 9 = 25.65$$

The two products are thus practically the same and the magnetron

would not function properly. A modification to the geometrical form of the delay line would improve matters; if the wavelength of the 7th mode were reduced slightly whilst retaining that of the π-mode, the product would be sufficiently different for the magnetron to work effectively.

So far we have investigated only the synchronisation of electrons with the electric field in respect of values of V and B on the cut-off parabola.

It is quite as important, however, to know the condition under which synchronisation will occur for values of V and B which are greater than the characteristic values. The solution to this problem cannot be given here but the result will suffice. With a wave whose characteristic values are V^* and B^* the electrons and the electric field will be synchronised so long as the voltage V and the magnetic field B satisfy the equation:

$$V = V^* \left(2\frac{B}{B^*} - 1\right) \tag{97}$$

Equation (97) shows the manner in which the anode voltage of a magnetron depends on the magnetic field. The relationship between V and B is linear and Eq. (97) will therefore appear in the V-B diagram as a straight line. At the same time Eq. (97) represents the tangent to the cut-off parabola at the point (V^*B^*), and we shall now give the proof of this.

According to Eq. (57) the cut-off parabola may be written as:

$$V = \alpha \cdot B^2 \text{ where } \alpha = \frac{e}{m} \cdot \frac{R_A^2}{8} \cdot \left[1 - \left(\frac{R_C}{R_A}\right)^2\right]^2$$

The slope of the tangent is given by

$$\tan \beta = \frac{\mathrm{d}V}{\mathrm{d}B} = 2\alpha B$$

and with Eq. (93), $\tan \beta$ at the point B^x is:

$$\tan \beta = 2\alpha B_x = \pi c R_A^2 \cdot \left[1 - \left(\frac{R_C}{R_A}\right)^2\right] \cdot \frac{1}{\lambda_i \gamma_i} \tag{98}$$

$\frac{\mathrm{d}V}{\mathrm{d}B}$ for the straight line to Eq. (97) is (with (94) and (95)):

$$\frac{\mathrm{d}V}{\mathrm{d}B} = 2 \cdot \frac{V^*}{B^*} = \pi c R_A^2 \left[1 - \left(\frac{R_C}{R_A}\right)^2\right] \frac{1}{\lambda_i \gamma_i} \tag{99}$$

Equations (98) and (99) mean that the slope of the tangent to the cut-off parabola at point (V^*B^*) is the same as that of the straight line according to (97). But (V^*B^*) is also a point in Eq. (97), so (97) must be the tangent to the cut-off parabola at V^*B^*.

The practical application of Eq. (97) can now be explained with the aid of an example. Assuming a magnetron with $N = 16$ cavities, anode radius $R_A = 0.437$ cm., cathode radius $R_C = 0.277$ cm., and a wavelength of the π-mode of 3.2 cm., what is the relationship between the anode voltage V and the magnetic field B? This is calculated from Eq. (97) and is then plotted graphically.

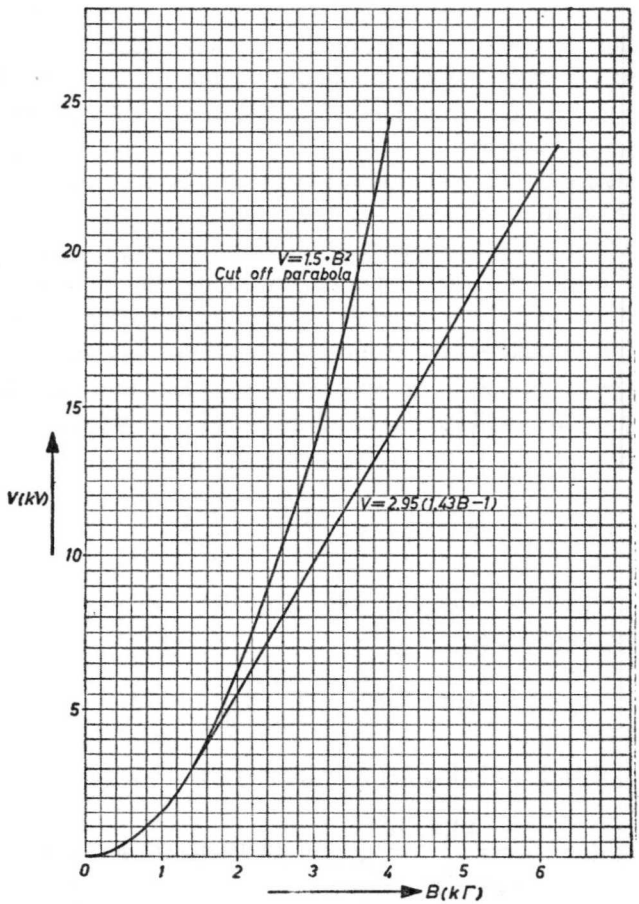

Fig. 23. Cut-off parabola and Eq. 101 for the π mode: Philips magnetron type 6972. The electrons and the r.f. electric field are synchronised.

From Eq. (96): $V^* = 2.95$ kV; B^* from Eq. (94) $= 1.4$ k Γ.
With Eq. (97) then:

$$V = 2.95\,(1.43B - 1)\ (V \text{ in kV};\ B \text{ in k}\,\Gamma) \tag{101}$$

The cut-off parabola and Eq. (101) are shown plotted in Fig. 23.

To return for a moment to the significance of the spatial harmonics occurring in the oscillations of a magnetron. We have seen that every mode of oscillation, with the exception of the fundamental wave, contains an infinite number of spacial harmonics (p 31), these being designated by a number given by $\gamma = n + m \cdot N$ where n is the mode number, m a random natural number and N the number of elements in the delay line. According to Eq. (92) spatial harmonics of given mode are propagated at different angular velocities. Now, if the line oscillates at a frequency f in the n^{th}-mode, all the spatial harmonics of this mode will occur simultaneously. This is due to the fact that the electromagnetic field has to expand along the line with all its angles and corners.

If the electrons are synchronised with one of the spatial harmonics, energy is delivered to the field of that harmonic.

As an outcome of the geometry of the delay line this energy is uniformly distributed among all the harmonics, including the fundamental wave. It is therefore possible to generate a mode by synchronism between the electrons and the field of one of the spatial harmonics. If the anode voltage V, the magnetic field B in the space between anode and cathode, and the wavelength λ of the oscillation are known, we can calculate the value γ of the driven spatial harmonic. According to Eq. (97) and (57):

$$B^* = B \cdot \left(1 - \sqrt{1 - \frac{V}{\alpha B^2}}\right) \tag{102}$$

where V is the anode voltage in volts and B is the magnetic field in gauss.
According to (58) α is:

$$\alpha = 2.2 \cdot 10^{-2} \cdot R_A{}^2 \left[1 - \left(\frac{R_C}{R_A}\right)^2\right]^2 \text{ with } R \text{ in cm.}$$

With Eq. (94) the solution for B^* with respect to γ is:

$$\gamma = \frac{21.4 \cdot 10^3}{\lambda \cdot B^* \cdot \left[1 - \left(\frac{R_C}{R_A}\right)^2\right]} \quad (\lambda \text{ in cm.},\ B^* \text{ in gauss}) \tag{103}$$

Thus, with the aid of Eq. (102) and (103) it is possible to ascertain with

which spatial harmonic the electrons interact at an anode voltage V, with magnetic field B and the wavelength λ of the oscillation generated.

To conclude this chapter some formulae are given by means of which the effect of small variations in R_A, R_C and B on the anode voltage V can be calculated. From (97):

$$dV = \left(\frac{2B}{B^*} - 1\right) dV^* + 2\frac{V^*}{B^*} dB - 2\frac{V^*B}{B^{*2}} dB^* \tag{104}$$

and further, in accordance with (93) and (95):

$$dV^* = \left(\frac{2}{R_A} dR_A - \frac{2}{\lambda} d\lambda\right) V^* \tag{105}$$

and

$$dB^* = \left[\frac{2R_C}{R_A^2 - R_C^2} dR_C - 2\left(\frac{R_C}{R_A}\right)^2 \cdot \frac{1}{R_A\left[1 - \left(\frac{R_C}{R_A}\right)^2\right]} dR_A - \frac{1}{\lambda} d\lambda\right] \cdot B^* \tag{106}$$

Using Eq. (104), (105) and (106) the effect of tolerances on R_A, R_C, B and λ on the anode voltage can be computed.

4.2 Elimination of unfavourably-phased electrons

In the previous chapters we have been concerned only with the condition under which the electrons can be synchronised with the electric field. Synchronisation, however, is not in itself sufficient to result in oscillation. The whole surface of the cathode emits electrons continuously and there are therefore just as many electrons delivering energy to the electric field as there are electrons absorbing energy from it. In order to deliver to the field more energy than is withdrawn from it we must see that those electrons which absorb energy from the field are eliminated as quickly as possible from the space between the anode and cathode.

This elimination of unwanted electrons in magnetrons is effected in the following manner. Electrons which on leaving the cathode take energy from the r.f. field move at a higher velocity than is necessary for synchronisation. Now, on p 19 it was seen that in such cases the electron travels back to the cathode; the energy absorbed by it from the r.f. field is then dissipated as heat at the cathode because of this bombardment. In general, the power returned to the cathode by such bombardment represents a few per cent of the input power. Hence, many magnetrons, when in the oscillating condition, require a lower heating voltage to maintain a particular cathode temperature than if they were not oscillating.

The collisions between the returning electrons and the cathode cause a large number of secondary electrons to be liberated, and, in the case of the pulsed type of magnetron, in particular, this is very advantageous. Otherwise, the cathode would not be capable of delivering the required peak current on the basis of thermal electrons only.

The proportion of secondary electrons to the total emission current is not exactly known, but it is certain that some 50% or more is provided by secondary electrons.

On this basis it is possible to form a qualitative idea of the distribution of electrons in the space between the cathode and the anode. In the immediate neighbourhood of the cathode the r.f. field has little or no effect; the cathode is surrounded by a circle of electrons which rotate round it.

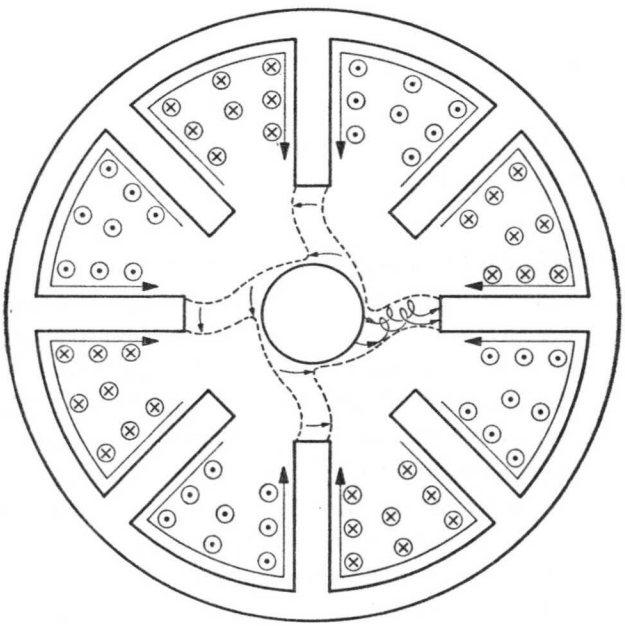

Fig. 24. Schematic diagram of the rotating "wheel" formed by the electrons in a magnetron oscillating in the π mode.

In the space between cathode and anode the elimination of unwanted electrons occurs and the remaining electrons appear to be distributed in the manner of spokes of a wheel. The space beyond these "spokes" will be only sparsely populated with electrons. Fig. 24 illustrates this condition diagrammatically as applied to the π-mode.*) The r.f. electric field has a focusing

* The "spoked" ring of electrons rotates at the angular velocity of the field.

effect on the "spokes" in that it tends to hold the electrons together. According as the current is increased, however, the repulsion of the electrons in the "spokes" may exceed the focusing effect because of the increased density of the charge, in which case oscillation ceases.

4.3 Unwanted modes of oscillation

We have seen (p 36) that a magnetron having a delay circuit of N elements can oscillate at $\frac{N}{2} + 1$ different frequencies, but it is, of course, not desirable that a magnetron should generate more than one frequency. In general, oscillation in the π-mode is preferred as this ensures the greatest electronic efficiency, and every precaution must therefore be taken that all other modes of oscillation are suppressed. This is dealt with in the next chapter, but it should be added here that there is no known method of complete suppression of all unwanted modes of oscillation. A percentage of some 0.001% of pulses missing the π-mode is attainable and such pulses are accordingly called "missing pulses" or "missing lines".

In practical forms of the magnetron there is besides the delay circuit an output coupling for the r.f. energy, which has certain effects on the mode of oscillation of the magnetron.

It has already been shown (p 27) that one element of the delay line will have the following characteristics:

$$V_i = V_0 \cos \varphi + jZ_0 i_0 \sin \varphi \tag{69}$$

$$i_i = j \frac{V_0}{Z_0} \sin \varphi + i_0 \cos \varphi \tag{70}$$

With two such elements coupled together Eqs. (69) and (70) give us:

$$V_i = V_0 \cos 2\varphi + Z_0 i_0 \sin 2\varphi \tag{107}$$

$$i_i = \mathrm{j} \cdot \frac{1}{Z_0} V_0 \sin 2\varphi + i_0 \cos 2\varphi \tag{108}$$

If a number of elements are coupled in succession the voltage V_i and current i_i at the beginning of the line will bear the following relationship to the voltage V_0 and current i_i at the end:

$$V_i = V_0 \cos N\varphi + \mathrm{j}\, Z_0 i_0 \sin N\varphi \tag{109}$$

$$i_i = \mathrm{j} \cdot \frac{1}{Z_0} V_0 \sin N\varphi + i_0 \cos N\varphi \tag{110}$$

On closing the circuit by connecting the ends of the line together $V_i = V_0$ and $i_i = i_0$, hence:

$$0 = V_0(\cos N\varphi - 1) + \mathrm{j}Z_0 i_0 \sin N\varphi \tag{111}$$

$$0 = \mathrm{j}\cdot\frac{1}{Z_0} V_0 \sin N\varphi + i_0(\cos N\varphi - 1) \tag{112}$$

In the case of $V_0 \neq 0$ and $i_0 \neq 0$ we obtain the following solutions for φ_i:

$$(\cos N\varphi_i - 1) + \sin^2 N\varphi_i = 0 \tag{113}$$

or

$$\cos N\varphi_i = 1 \tag{114}$$

or

$$\varphi_i = \frac{n}{N}\cdot 2\pi \quad 0 \leqslant n \leqslant \frac{N}{2}\cdot \tag{115}$$

Now Eq. (115) is the same as (87) and tells us nothing new, but we have so far not taken into account the coupling of the output load to the magnetron. We shall assume that a load $\mathrm{j}Y_L$ is connected across the terminals of the final element in the line (Fig. 25). $\mathrm{j}Y_L$ then represents a certain asymmetry in the otherwise symmetrical line.

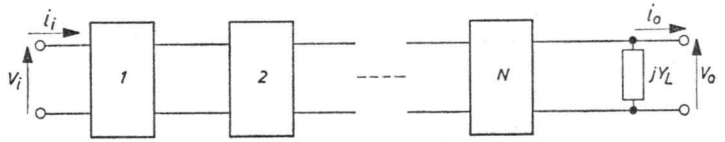

Fig. 25. Equivalent circuit diagram of a straight delay line terminated with an admittance φ_L.

V_i and i_i are now found to be (see also Fig. 17d):

$$V_i = V_0(\cos N\varphi - Z_0 Y_L \sin N\varphi) + \mathrm{j}Z_0 i_0 \sin N\varphi \tag{116}$$

$$i_i = \mathrm{j}\cdot\frac{V_0}{Z_0}(\sin N\varphi + Z_0 Y_L \cos N\varphi) + i_0 \cos N\varphi \tag{117}$$

If we now close the circuit (input to output), V_i must again equal V_0 and the angles φ_i must comply with the following:

$$0 = V_0(\cos N\varphi - Z_0 Y_L \sin N\varphi - 1) + \mathrm{j}Z_0 i_0 \sin N\varphi \tag{118}$$

$$0 = \mathrm{j}\cdot\frac{V_0}{Z_0}(\sin N\varphi + Y_L Z_0 \cos N\varphi) + i_0(\cos N\varphi - 1) \tag{119}$$

These equations have two possible solutions. If we admit $V_0 = 0$, $i_0 \neq 0$,

Fig. 30b. Magnetronanode for $\lambda = 8{,}6$ mm.

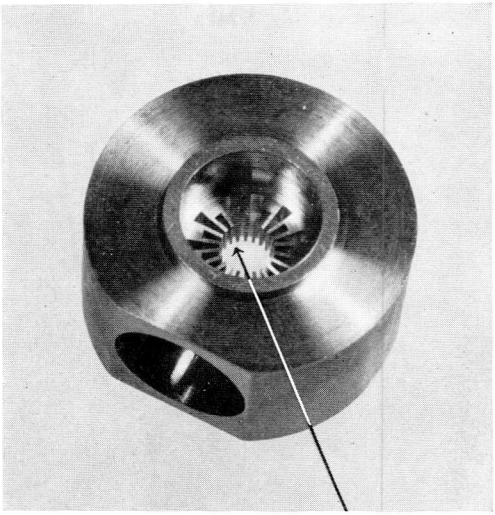

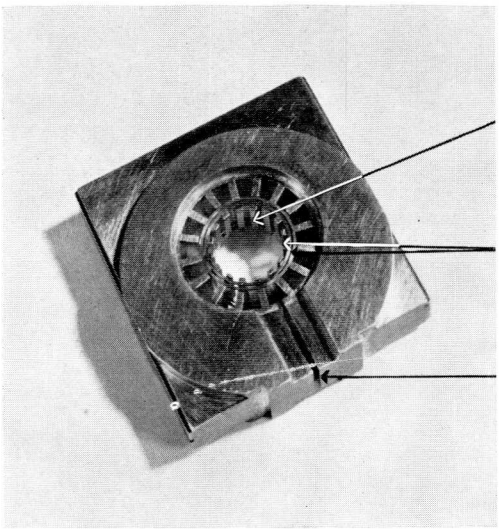

Fig. 37. Delay line with four strap rings and coupling-out slot.

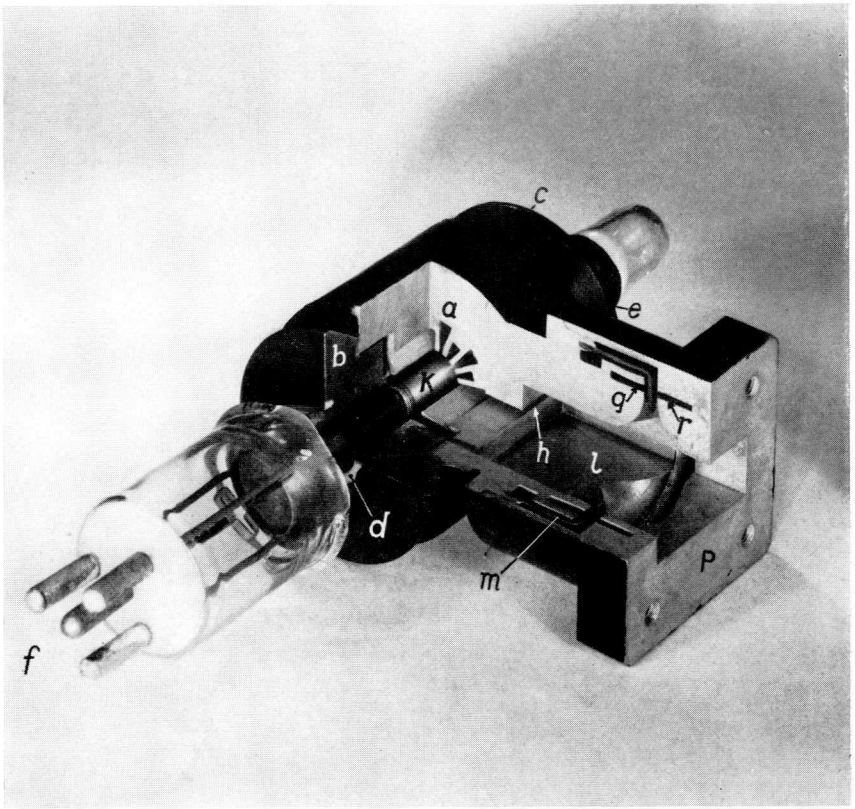

Cutaway view of 32 mm magnetron showing the following components: *a.* anode block; *b.* and *c.* iron end pieces, serving as pole pieces; *d.* and *e.* fernico rings for hard-glass seals; *k.* cathode; *f.* connections for cathode and filament; *h.* transformer slot in copper disc; *l.* output waveguide; *m.* fernico cap with hole for glass output window; *p.* brass connection flange; *q.* and *r* slots functioning as RF chokes.

phase angles φ_i for modes of oscillation are obtained which will not couple with the load jY_L. No current then flows through jY_L, seeing that $V_0 = 0$. Then

$$0 = jZ_0 i_0 \sin N\varphi \tag{118a}$$

$$0 = i_0 (\cos N\varphi_i - 1) \tag{119a}$$

with $i_0 \neq 0$.

Both expressions yield the same solution:

$$\varphi_i = \frac{n}{N} 2\pi \qquad 0 \leqslant n \leqslant \frac{N}{2} \tag{120a}$$

The phase angles φ_i in Eq. 120a thus produce modes of oscillation which will not couple with the load.

The second solution, φ_i^* with $V_0 \neq 0$ and $i_0 \neq 0$ is obtained by writing (118) and (119) in the form:

$$\varphi_i^* = -\frac{2}{N} \text{arc tan} \frac{Z_0 Y_L}{N} + \frac{n}{N} 2\pi \qquad n = 0, \ldots \frac{N}{2} \text{ or}$$

$$\varphi_i^* = -\frac{2}{N} \text{arc tan} \frac{Z_0 Y_L}{2} + \varphi_i \tag{120b}$$

Each mode number n from (120a) and (120b) can thus correspond to two modes of oscillation of slightly different frequencies, which implies that each mode occurs in the form of a doublet, one component of which couples with the load jY_L and one of which does not. It will now be shown that there are wot exceptions to this. The 0-mode and the π-mode do not give doublets; both will at all times couple with the load. If we assume that $V_0 = 0$ for a certain element in the line, the voltage V_i at the input of that element will be in accordance with Eq. (69):

$$V_i = jZ_0 i_0 \sin \varphi$$

Now, in the 0-mode $\varphi = 0$ and in the π-mode $\varphi = \pi$, so in both cases:

$$V_i = 0, \text{ where } i_0 \neq 0.$$

This means that the voltage is zero throughout the delay line, i.e. that no oscillation takes place.

All this has a very important effect on our delay line, namely that the introduction of asymmetry in the line (the load represents asymmetry) results in modes of oscillation that will not couple with that asymmetry. Where there is a load as only asymmetry, then, certain modes of oscillation

are not damped and these must have an adverse effect on the behaviour of a magnetron oscillating in the (necessarily damped) π-mode.

It can be demonstrated, however, that if a second source of asymmetry is included in the delay line at a certain distance from the first, the two modes of oscillation of certain doublets will in every case couple with the two asymmetries.

In this way the two modes of the most troublesome doublet of the mode $n = N - 1$ (adjacent to the π-mode) can always be coupled out and so also damped. A suitable point for introducing the second asymmetry is at a distance equal to $\frac{N}{8}$ elements from the output coupling.

Thus the introduction of asymmetry at certain points results in the damping of various modes of oscillation. Similar considerations to those mentioned above can be applied to different values of N and optimum positions for the introduction of asymmetry can be devised, but suffice it to say that even in symmetrically constructed lines there is always some asymmetry due to physical tolerances. Such asymmetry is distributed statistically, with the result that both components of the unwanted mode are more or less coupled out. It is for this reason that it has been possible to make good magnetrons with the "symmetrical" delay lines so far employed.

Another possible method of suppressing unwanted modes of oscillation would consist in what is known as selective damping; the introduction into the magnetron block of materials with high losses has the effect of damping to a large extent such unwanted modes of oscillation. At the same time, the π-mode itself must not be affected by such high-loss materials, which means that these materials must be introduced at points where the unwanted modes have an associated electric field, but where the π-mode has no such field. In most practical forms of delay line this is not feasible, for which reason this method is of little importance. Certain forms of delay circuits have been suggested, however, in which selective damping might be successfully employed.

Having dealt briefly with the effect of the delay line on the occurrence of unwanted modes of oscillation we shall now mention one or two other important points, and, in the first place, the modulator which is used for supplying the necessary voltage pulses to the magnetron. Experience has shown that the modulator should have a low internal impedance to ensure effective working of the magnetron in the π-mode, the reason being that in this case the voltage on the magnetron does not rise to any extent when little or no current is taken by the magnetron. If the anode voltage in respect of an unwanted mode of oscillation is sufficiently separated from that of the

π-mode the interfering voltage does not develop and the unwanted mode is not excited. It is found that when a magnetron is operated with a modulator of low R_i a pulse having a much steeper wave-front can be used than if R_i were high.

The emissive properties of the cathode of the magnetron itself are also important; in general, good primary emission promotes effective working in the π-mode, although cases are known where magnetrons with very poor primary emission have also worked well in this mode.

Another factor affecting the stability of operation in the π-mode is the ratio R_C/R_A, for which an optimum value exists; it appears that the electronic efficiency drops with increasing values of R_C/R_A.

Lastly, it may be said that a certain irregularity in the diameter of the cathode improves the starting propertiels of the magnetron. Fig. 26 shows one possible design. It is quite feasible that the cloud of electrons rotating round the cathode also has a protuberance which initiates synchronisation with the r.f. field and so brings the rest of the electrons into the wheel-like pattern mentioned above.

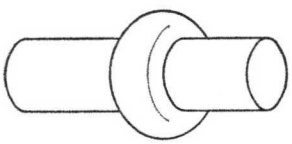

Fig. 26. Cylindrical cathode with ridge to ensure better excitation of the π-mode.

One very essential feature of effective π-mode operation is the spectrum of the modes. The spectrum may be regarded as satisfactory so long as the value of $\gamma\lambda$, which according to Eq. (92) is related to the angular velocity of the electric field, is higher for the π-mode than for the neighbouring mode and its first spatial harmonic. The requisite, then, is:

$$\frac{N}{2} \cdot \lambda_\pi > \left(\frac{N}{2} + 1\right) \cdot \lambda_{\frac{N}{2}-1} \tag{121}$$

or

$$\frac{\lambda_\pi}{\lambda_{\frac{N}{2}-1}} > 1 + \frac{2}{N} \tag{122}$$

If (122) is met, the anode voltage required for producing the mode the number of which is $\frac{N}{2} - 1$ is higher than that needed for the π-mode. (See also Eq. (94), (96), and (97)).

Only if the magnetron for some reason does not commence oscillation in the π-mode can the voltage rise, thus making synchronisation in the $\frac{N}{2} - 1$ mode possible.

V. EXAMPLES OF PRACTICAL DELAY LINES AND CATHODES

5.1 The most common delay lines in magnetrons

a) The unstrapped delay line

In the preceding section the condition for the separation of the π-mode from the adjacent mode is given as:

$$\frac{\lambda_\pi}{\lambda_{\frac{N}{2}-1}} > 1 + \frac{2}{N} \tag{122}$$

and in the following paragraphs we shall compute the mode spectra of a number of delay lines and check their usefulness against Eq. (122).

In relation to the line shown in Fig. 17a on p 25 we have already obtained the formula for cos φ in respect of this line (Eq. 81, p 32).

$$\cos\varphi = 1 - \frac{C_0}{C_1} \cdot \frac{\left(\frac{\omega}{\omega_1}\right)^2}{1 - \left(\frac{\omega}{\omega_1}\right)^2} \tag{81}$$

Further, Eq. (87) on p 35 gives us the means of ascertaining the mode frequencies. From (87) and (81) we can now find the frequency ω_n of the n mode:

$$\omega_n = \omega_1 \sqrt{\frac{1}{1 + \frac{C_0}{C_1} \cdot \frac{1}{1 - \cos\frac{n}{N} \cdot 2\pi}}} \tag{123}$$

and Fig. 27 shows the mode spectrum of a delay line of 12 elements in accordance with Eq. (123). Here $\frac{C_0}{C_1}$ is taken to be unity.

To calculate $\frac{\lambda_\pi}{\lambda_{\frac{N}{2}-1}}$ we may write the general formula:

$$\frac{\lambda_\pi}{\lambda_{\frac{N}{2}-1}} = \frac{\omega_{\frac{N}{2}-1}}{\omega_\pi}$$

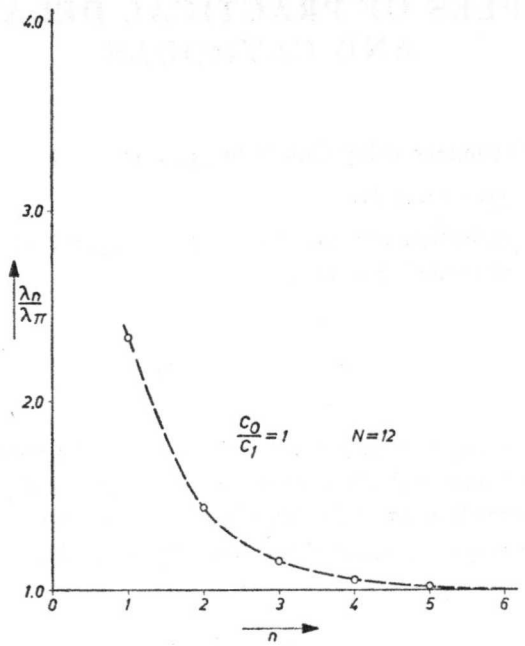

Fig. 27. Mode spectrum of an unstrapped delay line as shown in Fig. 17b. λ_π is the wavelength of the π-mode, λ_n the wavelength of the n mode. For C_0 and C_1 see Fig. 17b.

and Eq. (123) then gives us:

$$\frac{\lambda_\pi}{\lambda_{\frac{N}{2}-1}} \simeq 1 - \frac{\pi^2}{4} \cdot \frac{C_0}{C_1} \cdot \frac{1}{N^2} \tag{124}$$

It is seen that separation of the modes depends on $\frac{C_0}{C_1}$ and, also, that $\frac{\lambda_\pi}{\lambda_{\frac{N}{2}-1}}$ for our line is in every case less than unity. This means that the line is unsuitable for use in a magnetron. Eq. (124) also shows that with higher values of N the wavelength of the π-mode approaches more closely to the adjacent mode. For a delay line of 16 elements the separation is only about 1% for $\frac{C_0}{C_1} = 1$.

It should be noted, however, that the characteristics of the line in Fig. 17a are represented qualitatively by the equivalent circuit in Fig. 17b only in the band of frequencies where $0 \leqslant \omega \leqslant \omega_1$. To investigate the behaviour of the line above ω_1 the cavity resonator in the line line must be depicted rather

differently; Z_L cannot be represented as consisting of L_1 and C_1; instead we must employ a short-circuited transmission line of length L and characteristic impedance ξ_1.

Thus we obtain: $Z_L = \mathrm{j}\xi_1 \tan \omega \dfrac{L}{c}$ and, with $\omega_1 = \dfrac{\pi}{2}\dfrac{c}{L}$:

$$Z_L = \mathrm{j}\xi_1 \tan \frac{\pi}{2}\frac{\omega}{\omega_1} \tag{125}$$

$\cos \varphi$ of a single element is obtained from Eq. (63):

$$\cos \varphi = 1 - \xi_1 \omega C_0 \tan \frac{\pi}{2}\frac{\omega}{\omega_1}$$

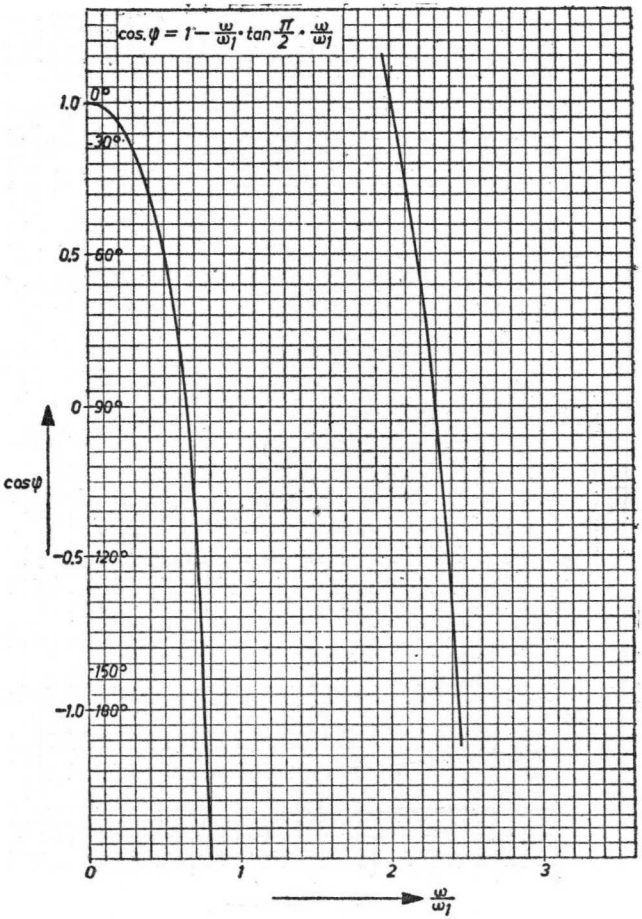

Fig. 28. Phase difference φ of an element in an unstrapped delay line plotted against ω/ω_1 (see also p 33).

and, with

$$\omega_1 C_0 = \frac{1}{\xi_0}$$

$$\cos\varphi = 1 - \frac{\omega}{\omega_1} \cdot \frac{\xi_1}{\xi_0} \cdot \tan\frac{\pi}{2} \cdot \frac{\omega}{\omega_1} \tag{126}$$

This is shown graphically in Fig. 28 for $\frac{\xi_1}{\xi_0} = 1$, from which it is seen that in the zone of $0 \leqslant \omega \leqslant \omega_1$, the curves in Figs. 20 and 28 are qualitatively the same. In Fig. 28, it appears, however, that for $\frac{\omega}{\omega_1} > 1$ there are also

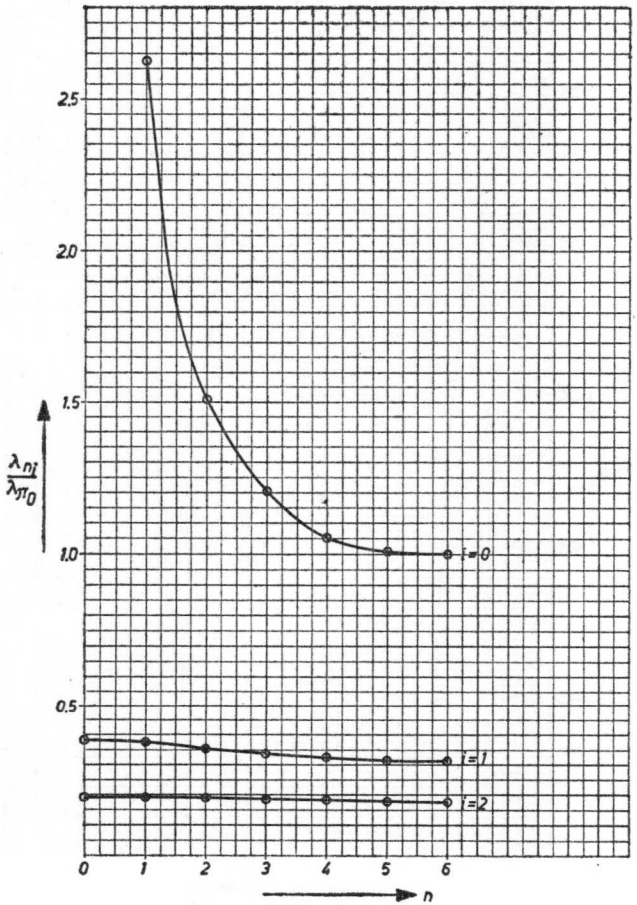

Fig. 29. Mode spectrum of an unstrapped 12-cavity magnetron: i indicates the order of the resonance, n the mode.

zones where $|\cos \varphi| < 1$ i.e. where waves are propagated along the line. Equation (87), in the form $\varphi = \varphi(f)$ then gives no unequivocal solution for f with a certain value of $\varphi = \varphi_n$:

$$\varphi_n = \varphi(f_{ni}) \qquad k = 0, 1 \ldots \infty \tag{127}$$

The frequencies f_{ni}, where $i > 1$ are called resonances of the order of i; they occur because a short-circuited transmission line is capable of resonating at an infinite number of frequencies. In practical applications of the magnetron, however, such forms of oscillation have no significance.

By means of Fig. 28 we can now ascertain the mode spectrum of a delay line comprising 12 elements; from Fig. 29 it is seen that resonances up to the 2nd order have been included. Fig. 29 agrees qualitatively with Fig. 27.

b) The "rising-sun" structure.

If we now modify the delay line in Fig. 17b by enlarging every other element (Fig. 30) we have what is known as the rising-sun structure. The dotted lines in Fig. 30 indicate that each element of the line thus obtained can be regarded

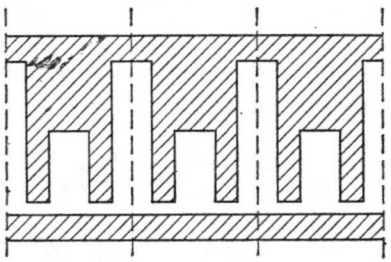

Fig. 30a. Rising sun structure.

as consisting of a small cavity resonator, flanked on each side by half a large resonator. The equivalent circuit of an element of this type is shown in Fig. 31, from which it is apparent that this figure is derived from Fig. 17c by adding an impedance Z_{LL} on the left and right hand sides.

Here the relationship between V_i and i_i, V_0 and i_0 is given by:

$$V_i = V_0 \cos \psi + \mathrm{j} Z_0 i_0 \sin \psi \tag{128}$$

$$i_i = V_0 \cdot \frac{j}{Z_0} \sin \psi + i_0 \cos \psi \tag{129}$$

so that

$$\cos \psi = (1 + Z_L Y_T)(1 + Z_{LL} Y_T) + Z_{LL} Y_T \tag{130}$$

If we write:

$$\cos \varphi_1 = 1 + \frac{Z_L Y_T}{2} \tag{131}$$

$$\cos \varphi_2 = 1 + Z_{LL} Y_T \tag{132}$$

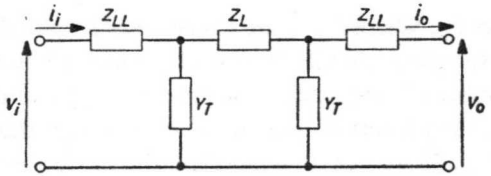

Fig. 31. Equivalent circuit diagram of a large and small rising sun cavity.

Eq. (130) can be put in the form:

$$\cos^2 \frac{\psi}{2} = \cos \varphi_1 \cos \varphi_2 \tag{133}$$

The significance of $\cos \varphi_1$ and $\cos \varphi_2$ can be seen from the following. According to Eq. (63): $\cos \varphi_1 = 1 + \frac{Z_L Y_T}{2}$ is the phase shift between the input and output voltage of a four-pole network terminated with its characteristic impedance, as shown below.

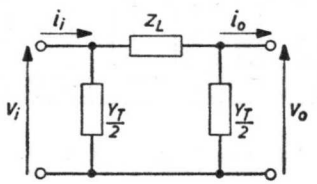

Fig. 32. Equivalent circuit diagram of a small rising-sun cavity.

Further, $\cos \varphi_2 = 1 + Z_{LL} Y_T$ gives the phase shift of the following four-pole network.

$$Z_L \rightarrow 2 Z_{LL}$$

$$\frac{Y_T}{2} \rightarrow \frac{Y_T}{2}$$

Thus $\cos \varphi_2$ and $\cos \varphi_1$ represent respectively the characteristics of the large and small cavity resonators in our delay line in conjunction with $\frac{Y_T}{2}$. It follows from (133) that where $\varphi_1 = \varphi_2$, $\psi = 2 \varphi_1$. This must be so for,

where $\varphi_1 = \varphi_2$, we have 2 identical cavity resonators in series, so that the angle ψ as measured across the 2 elements must be twice φ_1.

To ascertain the mode spectrum, $\frac{\psi}{2}$ in Eq. (133) is replaced by: $\frac{\psi}{2} = \frac{n}{N} \cdot 2\pi$ where N is the number of cavity resonators; the mode spectrum is then given by:

$$\cos^2 \frac{n}{N} \cdot 2\pi = \cos \varphi_1 \cdot \cos \varphi_2 \qquad n = 0,1, \ldots \frac{N}{2} \tag{134}$$

Real solutions of this are possible only if $\cos \varphi_1$ and $\cos \varphi_2$ are both either positive or negative. To calculate the mode spectrum we must also know φ_1 and φ_2 as a function of the frequency and for this purpose we shall assume that:

$$Z_L = \mathrm{j} \cdot \xi_1 \cdot \tan \frac{\pi}{2} \cdot \frac{\omega}{\omega_1} \tag{135}$$

$$Z_{LL} = \mathrm{j} \cdot \frac{\xi_2}{2} \cdot \tan \frac{\pi}{2} \cdot \frac{\omega}{\omega_2} \tag{136}$$

$$Y_T = \mathrm{j}\omega C_0 \tag{137}$$

Eq. (135) tells us that the centre cavity resonator in Figs. 30 and 31 is to be regarded as a short-circuited transmission line of characteristic impedance ξ_1 with ω_1 as its lowest resonant frequency.

Similarly, Eq. (136) shows that the second cavity resonator will be regarded as a short-circuited transmission line with a lowest resonant frequency of ω_2 and characteristic impedance of ξ_2. We regard Y_T as a capacitance C_0 (between the cathode and the vane.)

To determine the mode spectrum as a function of $\frac{\omega_1}{\omega_2}$ (as a function of the "detuning" of the large cavities with respect to the small ones) we may write Eq. (135) to (137) as:

$$Z_L = \mathrm{j}\xi_1 \tan \frac{\pi}{2} \cdot \frac{\omega}{\omega_1} \tag{138}$$

$$Z_{LL} = \mathrm{j} \cdot \frac{\xi_2}{2} \tan \frac{\pi}{2} \cdot \frac{\omega}{\omega_1} \cdot \alpha \quad \text{with } \alpha = \frac{\omega_1}{\omega_2} \tag{139}$$

$$Y_T = \mathrm{j} \cdot \frac{\omega}{\omega_1} \cdot \omega_1 C_0 = \mathrm{j} \cdot \frac{\omega}{\omega_1} \cdot \frac{1}{\xi} \quad \text{with } \xi_0 = \frac{1}{\omega_1 C_0} \tag{140}$$

Making use of (131) and (132) we then obtain:

$$\cos\varphi_1 = 1 - \frac{1}{2}\cdot\frac{\omega}{\omega_1}\cdot\frac{\xi_1}{\xi_0}\tan\frac{\pi}{2}\cdot\frac{\omega}{\omega_1} \tag{141}$$

$$\cos\varphi_2 = 1 - \frac{1}{2}\cdot\frac{\omega}{\omega_1}\cdot\frac{\xi_2}{\xi_0}\tan\frac{\pi}{2}\cdot\frac{\omega}{\omega_1}\cdot\alpha \tag{142}$$

Fig. 33 shows $\cos\frac{\psi}{2}$ plotted against $\frac{\omega}{\omega_1}$ for $\alpha = 3$ and $\frac{\xi_1}{\xi_0} = \frac{\xi_2}{\xi_0} = 0.2$.

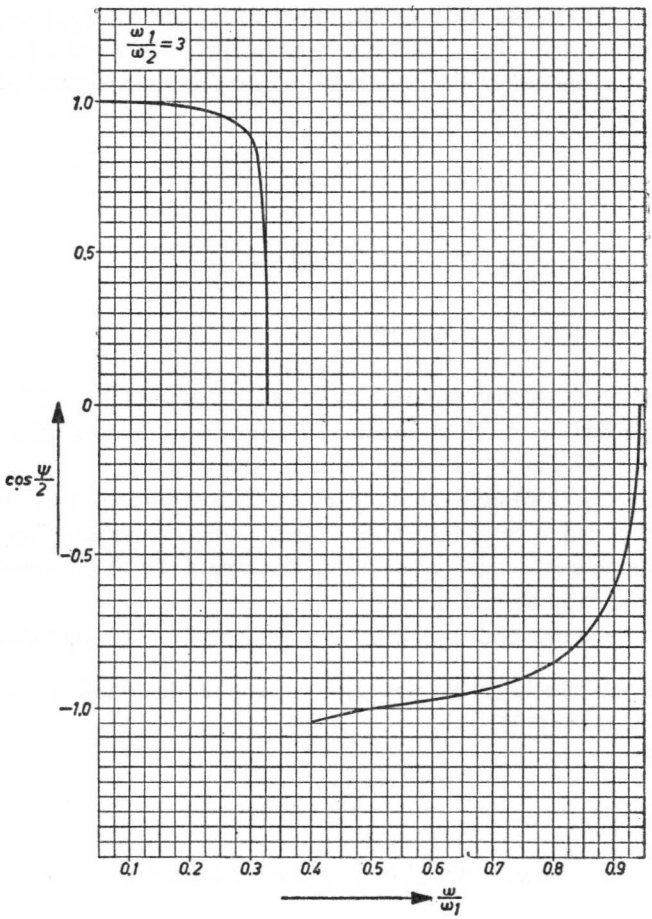

Fig. 33. Phase difference $\cos\frac{\psi}{2}$ plotted against $\frac{\omega}{\omega_1}$ for $\frac{\omega_1}{\omega_2} = 3$.

From this the mode spectrum can be derived by determining $\frac{\omega_n}{\omega_1}$, with $\psi_n = 2 \cdot \frac{n}{N} \cdot 2\pi$.

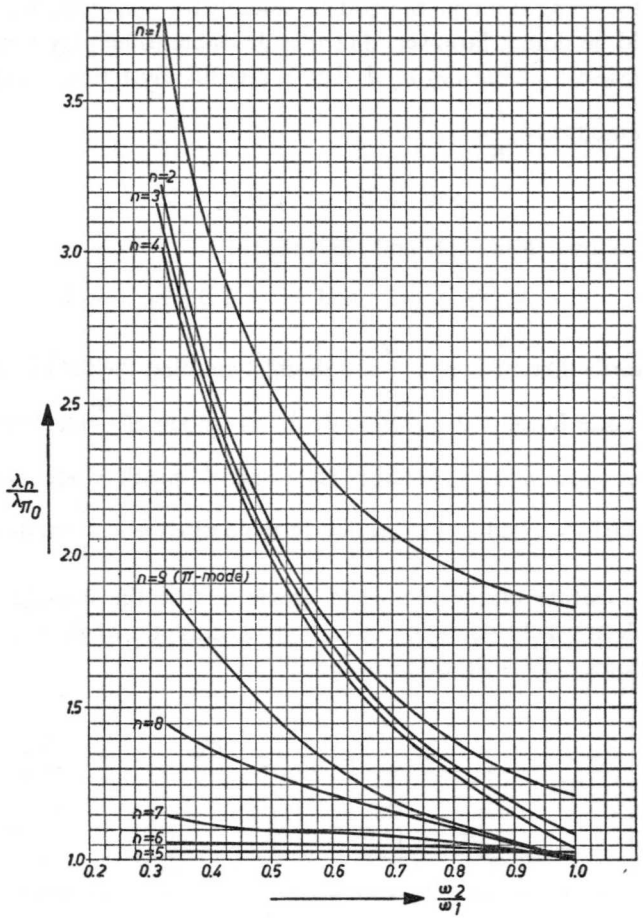

Fig. 34. Mode spectrum of the rising-sun structure with $N = 18$ cavities, plotted against $\frac{\omega_2}{\omega_1}$.

Fig. 34 shows the mode spectrum of a rising-sun anode of $N = 18$ elements, with $\frac{\omega_2}{\omega_1}$ on the horizontal axis and $\frac{\lambda_n}{\lambda\pi_0}$ on the vertical axis. λ_n is the wavelength of the n^{th} mode and $\lambda\pi_0$ that of the π-mode with $\alpha = 1$ (delay line with equal elements). ω_1 is regarded as constant.

It will be noticed that the π-mode ($n = 9$) for $\frac{\omega_2}{\omega_1} = 0.4$ is well separated from the $n = 8$ mode, also that the wavelength of the latter is shorter than that of the π-mode, thus satisfying Equation (122).

Hence the rising sun type of anode is suitable for a magnetron.

It should be noted, however, that it is desirable to employ a value of N that is divisible by 2 but not by 4. If N is divisible by 4, Equation (134) tells us that for mode $n = \frac{N}{4}$:

$$\cos \varphi_1 = 0 \quad \text{or} \quad \cos \varphi_2 = 0$$

It then follows from (131) and (132) that

$$1 + Z_L Y_T = -1 \quad \text{and} \quad 1 + 2 Z_{LL} Y_T = -1$$

in other words that mode $n = \frac{N}{4}$ is a doublet and that the field in both cases will be in accordance with the π-mode for an anode of $\frac{N}{2}$ elements with all the large or small cavity resonators filled in with metal. Modes with $n = \frac{N}{4}$ would be easily excited and operation in the desired $n = \frac{N}{2}$ mode would be difficult.

Another feature of the rising-sun anode is that the 0-mode interferes with the electric field between the cathode and anode when it is operating in the π-mode. This is shown as follows:

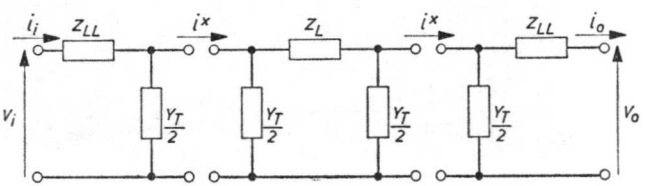

Fig. 35. Equivalent circuit diagram as in Fig. 31, divided into three sections.

Fig. 35 is seen to be the same as Fig. 31 except that Y_T is now divided in halves, one half being added to Z_{LL} and the other to Z_L. The separation in Fig. 35 is identical with that of the delay line by the vanes (see Fig. 30).

For the π-mode: $V_0 = V_i = 0$ and $i_0 = i_i \neq 0$. We now calculate the current i^* passing across the vane between the small and large cavity resonators. With $V_0 = 0$ and $i_0 \neq 0$:

$$i^* = \left(1 + \frac{Z_{LL}Y_T}{2}\right) i_0 \tag{143}$$

Now, with the rising-sun anode operating in the π-mode:

$$\frac{Z_{LL}Y_T}{2} \neq -1, \text{ hence}$$

$$i^* \neq 0. \tag{144}$$

It should be pointed out here that no current passes across the vanes of a delay line in which all the elements are the same.

It appears from (144) that with the π-mode a current i^* flows in all the vanes, in the same direction, which means that the field of the π-mode is interfered with by that of the 0-mode. The greater the difference between the resonant frequency of the large cavity resonators and that of the small ones, the greater the interference.

The fact that a current flows across the vanes can also be seen from a drawing of the distribution of the charge in the π-mode as shown in Fig. 36.

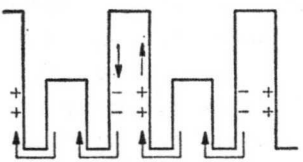

Fig. 36. Occurrence of the 0 mode in the rising sun structure. The arrows indicate the direction of the current.

In this figure the current is shown by means of arrows; it passes all the vanes in the same direction and the consequence of this is that, under certain conditions, the electronic efficiency of the magnetron drops sharply. If the cyclotron frequency of the magnetron corresponds to the frequency of the π-mode, energy is absorbed from the r.f. field and the efficiency accordingly drops. Equation (26) shows the relationship between the magnetic field B and the wavelength λ_c of the cyclotron motion. To ensure a reasonable degree of electronic efficiency for a magnetron design, therefore, a magnetic field must be employed such that $\lambda_\pi \cdot B$ is either much lower or much higher than 11 КГсм. approx.

c. The strapped anode

As we have already seen, the delay line shown in Fig. 17b produces an unsatisfactory mode spectrum.

Supposing that an anode of this type were oscillating in the π-mode,

the r.f. potential would be the same upon alternate vanes. Now, if the vanes of like r.f. potential were to be interconnected by conductors this could be done by means of 4 rings in the manner shown in Fig. 37. At each side of the anode there would then be two such rings or "straps".

It will be appreciated that for the π-mode these straps function as a capacitance for each of the cavity resonators and that the frequency of the π-mode in the strapped system will be lower than without the straps.

For other modes than the π-mode those points which are connected by the straps would be at different r.f. potentials in the unstrapped magnetron. A current therefore flows through the straps and the effect on resonant frequency of these modes will be different.

To ascertain the qualitative effect of the straps it is necessary to consider once more the characteristics of a single element in the delay line, as fitted with straps. But, in order to arrive at a suitable equivalent circuit diagram the unstrapped, closed, delay line must now be regarded in a different light.

Fig. 22 may be regarded as a cross-section of an infinitely long wave-guide. In such a wave-guide various modes can be propagated; each H-mode would have an electric field in the plane of the paper in Fig. 22 and would therefore be identical with one of the modes of the unstrapped magnetron. In common with all wave-guides our wave-guide will have a certain cut-off wavelength for each mode. It is known that the wavelength λ_g in the wave-guide will be infinite if the cut-off frequency is passed into it. It follows from this that the r.f. voltage in the direction of propagation undergoes no variation in amplitude or phase and, hence, that the frequencies of the modes in the unstrapped line must be identical with the cut-off wavelengths of the H-modes for the wave-guide associated with those modes.

The element in the line shown in Fig. 22 can therefore also be regarded as a wave-guide, the characteristic impedance ξ_r of which is:

$$\xi_r = \frac{\xi_0}{\sqrt{1 - \left(\frac{\lambda}{\lambda_c}\right)^2}} \tag{145}$$

ξ_0 is dependent on the $L : C$ ratio of the resonator.

If a wave of wavelength λ travels along this line and the length of the line is h, the phase angle Θ_r between input and output will be:

$$\Theta_r = \frac{2\pi}{\lambda_g} \cdot h = \frac{2\pi h}{\lambda} \cdot \sqrt{1 - \left(\frac{\lambda}{\lambda_c}\right)^2} \tag{146}$$

The single unstrapped element of the delay line can therefore be regarded

as a conductor having a characteristic impedance ξ_e in accordance with Eq. (145) and a length h ("height" of the line). The 4 straps can be regarded as a transmission line above and below each element of the unstrapped line and this gives us the following equivalent circuit (Fig. 38).

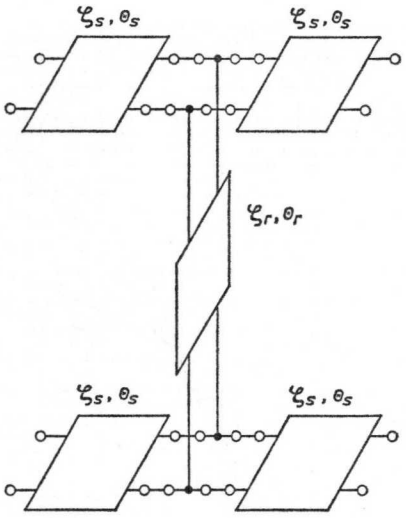

Fig. 38. Equivalent circuit diagram of an element in a delay line strapped on each side with two rings.

The characteristic impedance of this transmission line is denoted by ξ_s and the electrical length Θ_s by:

$$2\,\Theta_s = \frac{2\pi}{\lambda} \cdot s \tag{147}$$

where s is the length of the section of strap per resonator. If we now calculate the phase shift φ as a function of frequency we find that:

$$\cos\varphi = \cos\frac{2\pi s}{\lambda} + \alpha \cdot \sqrt{\left(\frac{\lambda}{\lambda_c}\right)^2 - 1} \cdot \sin\frac{2\pi s}{\lambda} \cdot \tanh\frac{\pi h}{\lambda}\sqrt{\left(\frac{\lambda}{\lambda_c}\right)^2 - 1}$$

$$\text{with } \alpha = \frac{\xi_s}{2\xi_0} \tag{148}$$

When determining the mode frequencies we must bear in mind the fact that for the π-mode the phase shift φ_π along the straps is zero. In general we may write for angle φ_n of the n mode:

$$\varphi_n = \frac{2\pi}{N}\left(\frac{N}{2} - n\right). \tag{149}$$

In Eq. (148) the coefficient α indicates whether the strapping is "heavy" or "light". If a low value is chosen for ξ_s (deep straps, close together), α will be small with constant ξ_0. This represents heavy strapping. A high value of α indicates light strapping.

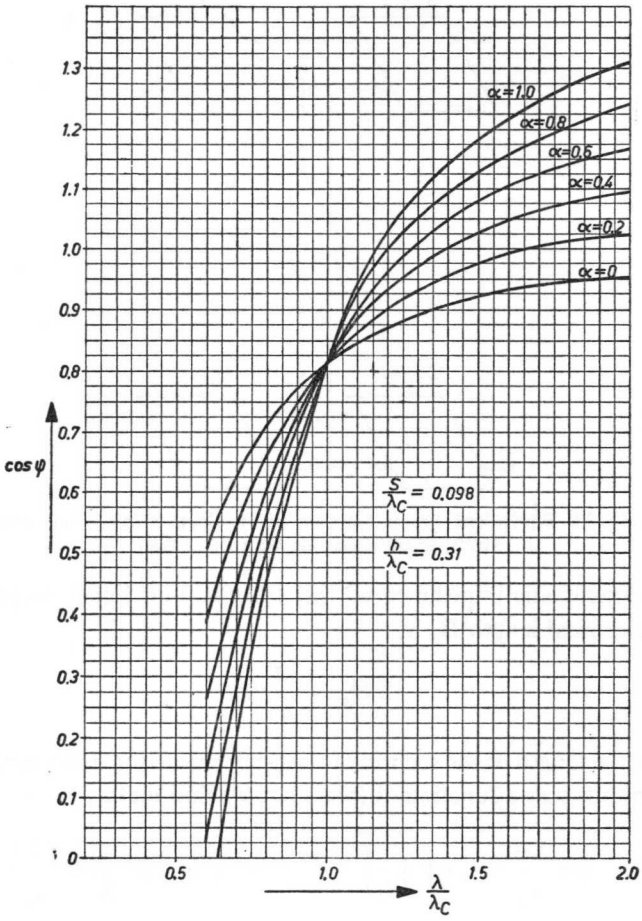

Fig. 39. Phase difference cos φ per element of a strapped delay line as in Fig. 38, plotted against λ/λ_c, with α as parameter.

In Fig. 39 cos φ is shown plotted in accordance with Eq. (148) for various values of α in the region which is of the most interest. It will be seen that where $\lambda = \lambda_c$ (the frequency of the π-mode of the unstrapped line) the curves for every value of α pass through the point $\cos \varphi = \cos \frac{2\pi s}{\lambda_c}$. The

heavier the strapping ($\alpha \to 0$), the greater the wavelength of the π-mode becomes (point of intersection with $\cos \varphi = 1$).

From the point of view of practical operation it is important to know in what manner the mode spectrum changes when the frequency λ_π of the π-mode of the strapped magnetron is kept constant and α is varied. Between α and λ_c the following relationship must exist:

$$1 = \cos \frac{2\pi s}{\lambda_\pi} + \alpha \cdot \sqrt{\left(\frac{\lambda_\pi}{\lambda_c}\right)^2 - 1} \sin \frac{2\pi s}{\lambda_\pi} \cdot \tanh \frac{\pi h}{\lambda_\pi} \sqrt{\left(\frac{\lambda_\pi}{\lambda_c}\right)^2 - 1}$$

or

$$\alpha = \frac{1 - \cos \dfrac{2\pi s}{\lambda_\pi}}{\sqrt{\left(\dfrac{\lambda_\pi}{\lambda_c}\right)^2 - 1} \cdot \sin \dfrac{2\pi s}{\lambda_\pi} \cdot \tanh \dfrac{\pi h}{\lambda_\pi} \sqrt{\left(\dfrac{\lambda_\pi}{\lambda_c}\right)^2 - 1}} \tag{150}$$

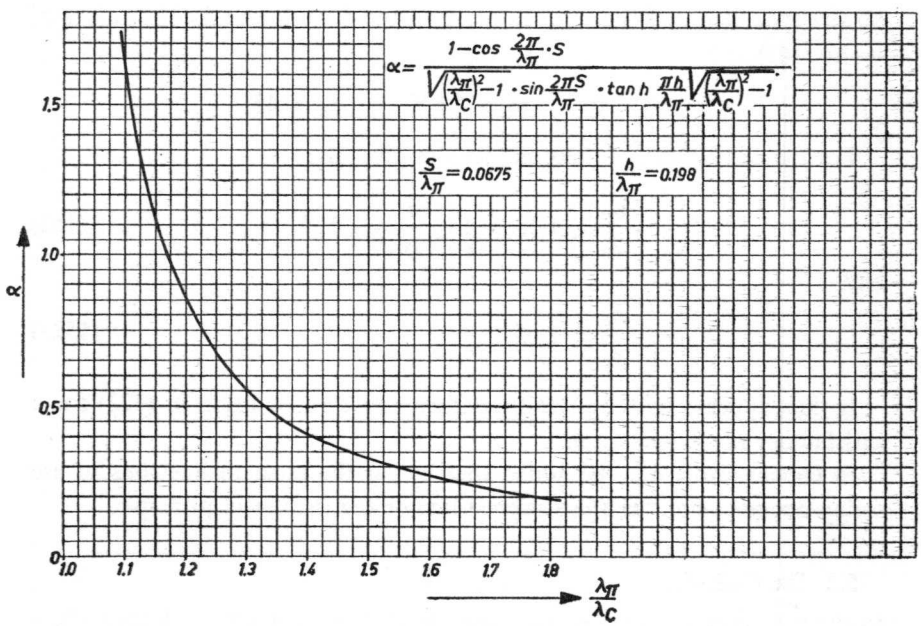

Fig. 40. Relationship between α, λ_c and λ_π with λ_π constant.

The curve of Eq. (150) is shown in Fig. 40 for $\frac{s}{\lambda_\pi} = 0.0675$ and $\frac{h}{\lambda_\pi} = 0.198$. Eq. (148) should then be rewritten in the form:

$$\cos\varphi = \cos\frac{2\pi s}{\lambda_\pi}\cdot\frac{\lambda_\pi}{\lambda} + \\ + \alpha\sqrt{\left(\frac{\lambda}{\lambda_\pi}\right)^2\cdot\left(\frac{\lambda_\pi}{\lambda_c}\right)^2 - 1}\cdot\sin\frac{2\pi s}{\lambda_\pi}\cdot\frac{\lambda_\pi}{\lambda}\tanh\frac{\pi h}{\lambda_\pi}\cdot\frac{\lambda_\pi}{\lambda}\sqrt{\left(\frac{\lambda}{\lambda_\pi}\right)^2\cdot\left(\frac{\lambda_\pi}{\lambda_c}\right)^2 - 1}. \tag{151}$$

If we now insert in Eq. (151) combinations of α and $\frac{\lambda_\pi}{\lambda_c}$ from (150) we shall have the curve of $\cos\varphi$ as a function of $\frac{\lambda_\pi}{\lambda}$ with α as parameter and this is reproduced in Fig. 41. For $\frac{s}{\lambda_\pi}$ and $\frac{h}{\lambda_\pi}$ we have taken:

$$\frac{s}{\lambda_\pi} = 0.0675 \qquad \frac{h}{\lambda_\pi} = 0.198$$

That part of the mode spectrum which is of the greatest interest to us, with $\alpha = 0.5$, can be derived from Fig. 41 for a magnetron with, for example, 16 strapped elements. For the modes 8, 7 and 6 we then take the values of φ (Eq. 149) to be:

$$\varphi_8 = 0 \qquad \varphi_7 = 22.5° \qquad \varphi_6 = 45°$$

For the wavelength of these modes this gives us:

$$\frac{\lambda_\pi}{\lambda_7} = 1.18 > 1 + \frac{2}{N} = 1.125 \tag{152}$$

and

$$\frac{\lambda_\pi}{\lambda_6} = 1.55 \tag{152a}$$

It thus appears that Eq. (152) conforms to the condition in (122) for a satisfactory mode spectrum.

In conclusion it may be added that by far the most magnetrons in use today operate on either the strapped line or the rising-sun principle.

5.2 The Cathode

In the preceding chapters we have seen how the movement of electrons in a delay line produces r.f. energy. At this point we shall examine in greater detail the source of electrons, i.e. the cathode.

First we will consider the requirements to be met by the cathode of a magnetron. These requirements are of course closely related to such parameters as wavelength, average power output, pulsed output, type of delay

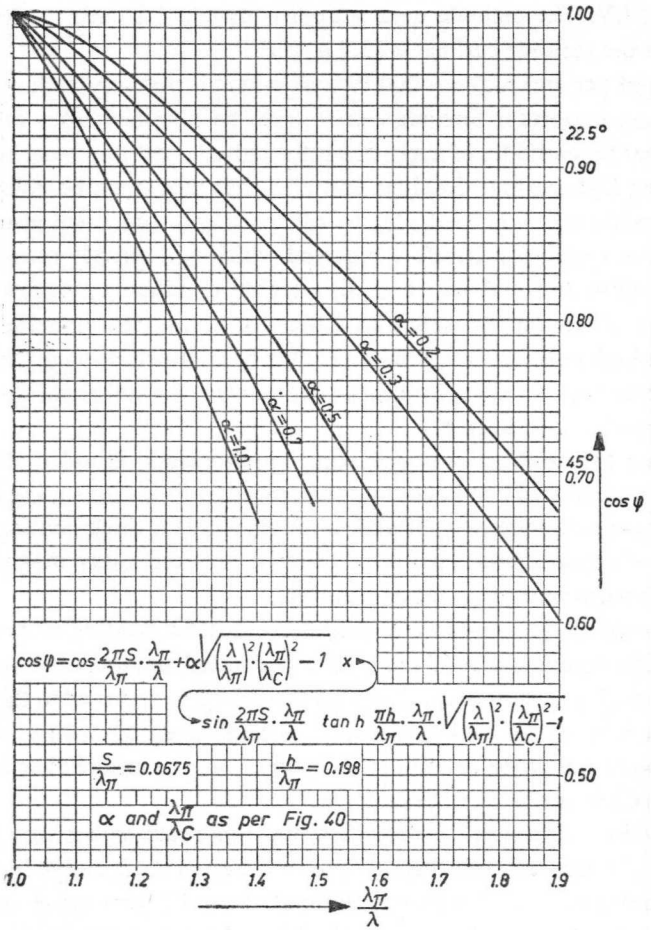

Fig. 41. Phase difference per element of a strapped delay line as a function of $\frac{\lambda_\pi}{\lambda}$ with λ_π constant and α as parameter.

line used and so on. In particular, two quantities define the operating conditions of the cathode, namely, the current density at the surface (in A/cm²) and the input per unit area (W/cm²). The "input" is understood to be the power applied between the anode and cathode; this is a measure of the bombardment of the cathode by returning electrons that the cathode will have to withstand. It can be assumed that some 5 to 10% of the input returns to the cathode in the form of bombardment. Let us take magnetron type 6972 as an example. At a wavelength of 3.2 cm this tube delivers 80 kW pulsed output and an average of 80 W. The pulse current is 15 A and the anode

voltage 15 kV. The cathode area is approximately 1.1 cm^2, so the current density at the cathode surface is 13.5 A/cm^2.

The input per cm^2 is about 200 W/cm^2, which is not very high.

The most important features can at once be obtained from these data, namely that the cathodes of magnetrons for pulsed operation must be capable of carrying high current densities and also that they must be able to withstand considerable bombardment by electrons and sometimes also by ions. An emissive coating is therefore required which will quickly recover in the event of poisoning and which is also highly conductive, electrically and thermally; otherwise the potential difference across the emissive coating, due to the high pulse current, would result in breakdown through the coating. Good thermal conductivity is necessary to prevent the surface of the cathode from becoming overheated.

To some extent these are conflicting requirements. Good thermal conductivity necessitates a thin coating, but recovery from poisoning demands a large reserve of emissive material, in other words a thick coating; special methods of construction have been adopted in present-day magnetrons to meet both requirements as far as possible.

In the case of the magnetrons used for industrial heating purposes very considerable mismatching of the load is permitted as compared with radar magnetrons. This means that relatively more energy is returned to the cathode by bombardment, for which reason a cathode material with a very high melting point has to be used in such magnetrons, to ensure that overloads do not result in melting of the cathode.

The Philips "dispenser" cathode satisfies this requirement very well, the materials for this cathode being porous tungsten and molybdenum; the emissive substance is a barium compound. Two different types are in use, namely the "cavity-type dispenser cathode" and the "impregnated cathode"; Fig. 42 illustrates an example of the cylindrical "cavity" type.

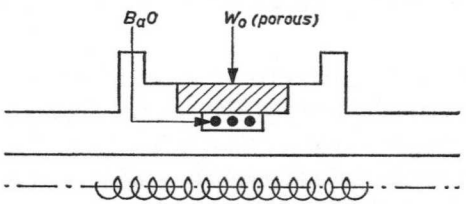

Fig. 42. Schematic diagram of Philips cylindrical cavity type of dispenser cathode.

It will be seen that the cylindrical part, of porous tungsten, and the molybdenum of the cathode support together form a cavity into which pellets of a

suitable barium compound can be introduced. The emissive part is of tungsten.

The two rings, one on each side of the porous tungsten, have a bundling effect on the electrons and prevent electrons from disappearing in the direction of the pole pieces. The cathodes of nearly all types of magnetron are equipped with such rings.

An example of the cylindrical impregnated cathode, the other type of dispenser cathode, is depicted in Fig. 43.

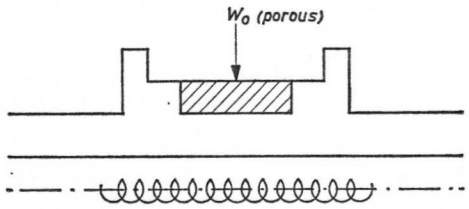

Fig. 43. Schematic diagram of Philips cylindrical dispenser cathode.

In this case there is no separate cavity for the barium emissive material; this is incorporated in the porous tungsten itself. To achieve this the barium compound is melted and drawn into the porous tungsten in the liquid state by capillary action.

Here, too, molybdenum is used to support the porous tungsten. There is some freedom of choice as to the emissive material used; materials are available which yield very little barium and consequently ensure a low rate of evaporation of barium.

Both the above-mentioned types of cathode are used in magnetrons. Where the cathode is of small dimensions (for example in 8 mm magnetrons) the impregnated type is preferred to the cavity type, as the construction of a recess for the barium would present difficulties. Both types of cathode are suitable for magnetrons for a wavelength of 3 cm.

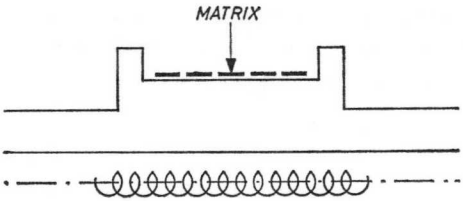

Fig. 44. Schematic diagram of a cylindrical matrix cathode.

Another kind of cathode frequently used is known as the nickel matrix cathode, an example of which is shown in Fig. 44. These cathodes are made

by sintering a large quantity of nickel granules to a nickel or molybdenum support to provide a spongy, highly conductive layer about 200 microns in thickness, in which the emissive material is then incorporated. The area of this type of cathode is not very clearly defined but this is not necessarily always an objection. Because of its simple construction and excellent properties, the nickel matrix cathode is widely employed.

There are also many other kinds of cathode, viz, pressed cathodes, spiral tungsten-thorium cathodes, variations of the matrix cathode and so on, but the use of these is limited to certain special types of magnetron; they are not suitable for universal application.

Mention may be made here of an effect known as end emission. This refers to electrons which reach the anode without taking any part in the interaction with the r.f. electric field. These electrons usually originate from points on the cathode outside the zone in which emission is required, and the phenomenon generally takes place after the magnetron has been in operation for some tens of hours. There may be various reasons for this. For example, migration along the surface or along crystal faces may result in displacement of the emissive material; or again, evaporation or sputtering may cause emissive material to be deposited at points on the cathode where its presence is undesirable. End emission can be kept within acceptable limits by ensuring a suitable design from the point of view of temperature distribution and by using certain materials such as zirconium or carbon which have the effect of suppressing emission.

The modulator in which the magnetron is used may also be a determining factor as to the occurrence of end emission. A voltage pulse with a long "tail" tends to produce more end emission than a short-tail pulse. End emission can also be suppressed by applying between pulses a potential of about + 200 V to the cathode with respect to anode; this can be obtained quite easily from the anode current of the magnetron itself.

In the above remarks the cathode has necessarily been considered only from the aspect of operation of the magnetron, as a more general treatment would be beyond the scope of this book. For further details the reader is referred to the literature on this subject.

VI. THE CHARACTERISTICS OF MAGNETRONS

6.1 The Performance Chart and Rieke Diagram

A number of parameters have to be decided upon in order to fix the working point of a magnetron; at the input side the magnetic field B, the anode current I_A and the anode voltage V_A. As we have already seen, V_A is dependent on B, so the working point for the input side is in effect determined by the independent variables B and I_A. The input power, frequency and efficiency are also important.

A load is of course coupled to the output side and this can be defined by two mutually independent quantities, i.e. $|q|$ (the absolute value of the voltage reflection coefficient of the load) and φ (the phase angle of the reflection coefficient).

The characteristics of the magnetron can be fully delineated by indicating the interdependence of these various parameters and of the many possibilities of so doing, the performance chart and the "Rieke" or load diagram represent the most widely employed practical methods.

The performance chart is a two-dimensional representation of the anode voltage V_A (vertical axis) plotted against the anode current (horizontal axis) with the magnetic field as parameter. As far as the load is concerned, this must be matched to the output waveguide (hence $|q| = 0$). Fig. 45 shows a typical performance chart.

In order to show the dependence of the output power (with matched load)

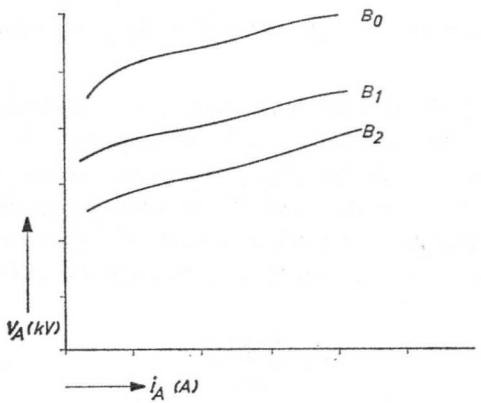

Fig. 45. Performance chart. Graphical form of $V_A = V_A(i_A)$ with magnetic field strength B as parameter.

on the input parameters, lines of constant output power are included in the diagram. Lines of constant efficiency are sometimes also drawn in the diagram.

Hence a performance chart enables us to see, for example, what anode voltage, anode current and magnetic field are required to make available a certain amount of power for a given matched load. To give an actual example, Fig. 46 shows the performance chart of magnetron type 6972.

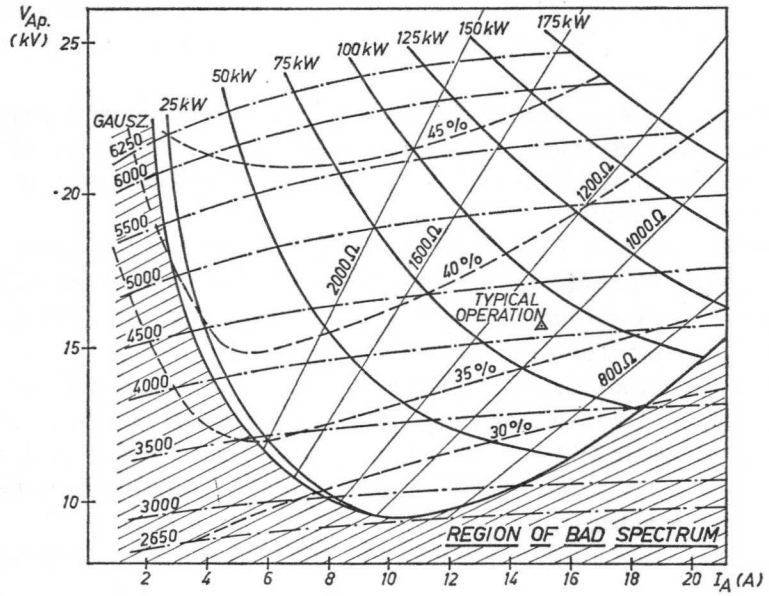

Fig. 46. Performance chart of Philips magnetron type 6972.

If we wish to know the characteristics of a magnetron under different loading conditions we make use of a Rieke diagram. The procedure is as follows. Every load can be defined by the phase and the voltage reflection coefficient; the latter is determined in the following manner. The load is coupled to the end of the waveguide and the standing wave ratio σ and phase angle φ of the line are measured with the aid of a probe and signal generator.

Now,

$$\sigma = \frac{V_{max}}{V_{min}} \geqslant 1 \tag{153}$$

$$\varphi = 4\pi \frac{\Delta L}{\lambda_g} \text{ in radians} \tag{154}$$

$$\varphi = 720 \cdot \frac{\Delta L}{\lambda_g} \text{ in degrees}$$

Here, ΔL is the distance from the first standing wave minimum to the reference plane, usually taken as the coupling flange of the magnetron, but in any case always clearly indicated in the published data.

The angle φ according to Eq. (154) is identical with the phase angle of the reflection coefficient of the load.

The absolute value $|q|$ of the reflection coefficient is related to the standing wave ratio σ under test as follows:

$$|q| = \frac{\sigma - 1}{\sigma + 1} \tag{155}$$

If we now consider a system of polar co-ordinates in which the radius r is equal to the absolute value $|q|$ of the reflection coefficient, the angle will be equal to that of the phase angle of the load (Fig. 47).

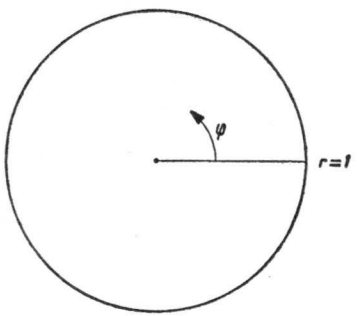

Fig. 47a. Rieke diagram: reflection coefficient $q = |q| e^{i\varphi}$ plotted on polar co-ordinates.

In this manner any given load can be represented by a point within the circle of radius 1. For example, the matched load lies at the centre of the circle; a short circuit would be $r = 1$, $\varphi = 180°$.

All the parameters for the input are now fixed (these are indicated in the Rieke diagram) and the phase angle and reflection coefficient are varied, with the result that the output power and frequency will also vary. Lines of constant frequency and power are drawn in the polar system of coordinates referred to above. A diagram of this kind relating to the magnetron type 6972 is reproduced in Fig. 48.

It will be seen from this figure that with a reflective load both frequency and output power are very dependent on the phase angle. For practical purposes it is important to fix the relationship between the frequency drift

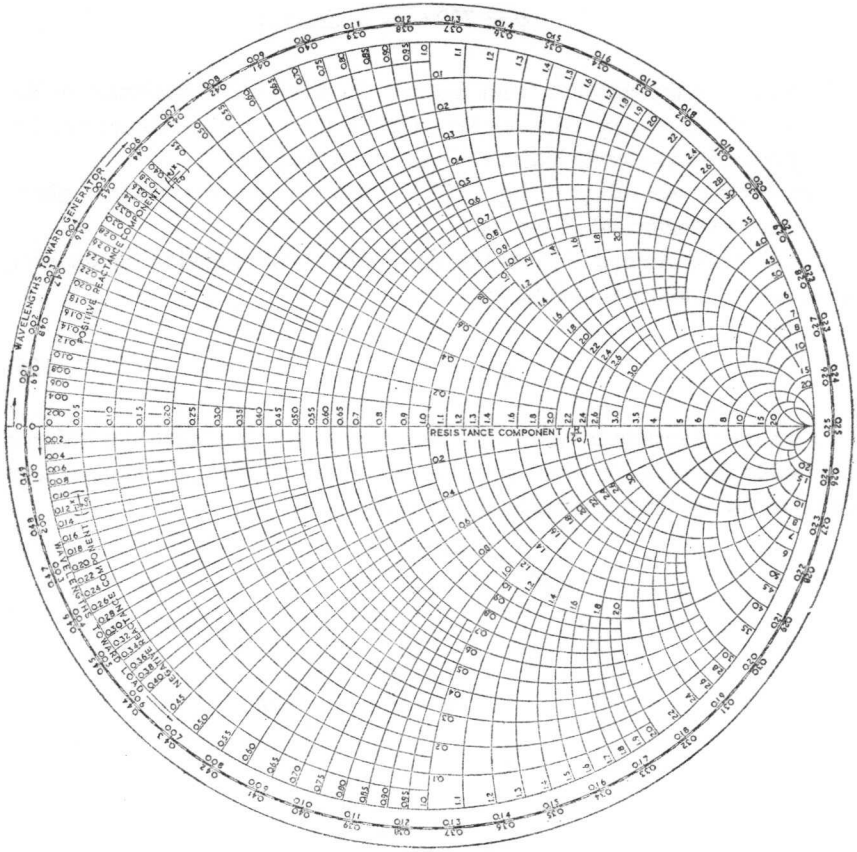

Fig. 47b. Impedance diagram (Smith chart) based on Fig. 47a. Every point in the diagram represents a certain reflection coefficient q as given in Fig. 47a.

and mismatching in the form of a single value; accordingly the maximum frequency variation that can occur with a reflection coefficient of 0.2 and phase rotation of 360° is known as the pulling figure of the magnetron. This figure can be easily obtained from the load diagram. A load diagram may also include the indication "minimum towards load", by which is meant that ΔL in Eq. (154), which determines the phase angle, is measured as the distance from the reference plane to the next successive minimum in the direction of the load.

The performance chart and Rieke diagram are indispensable for assessing the suitability of a magnetron for a given task. Certain zones will often be

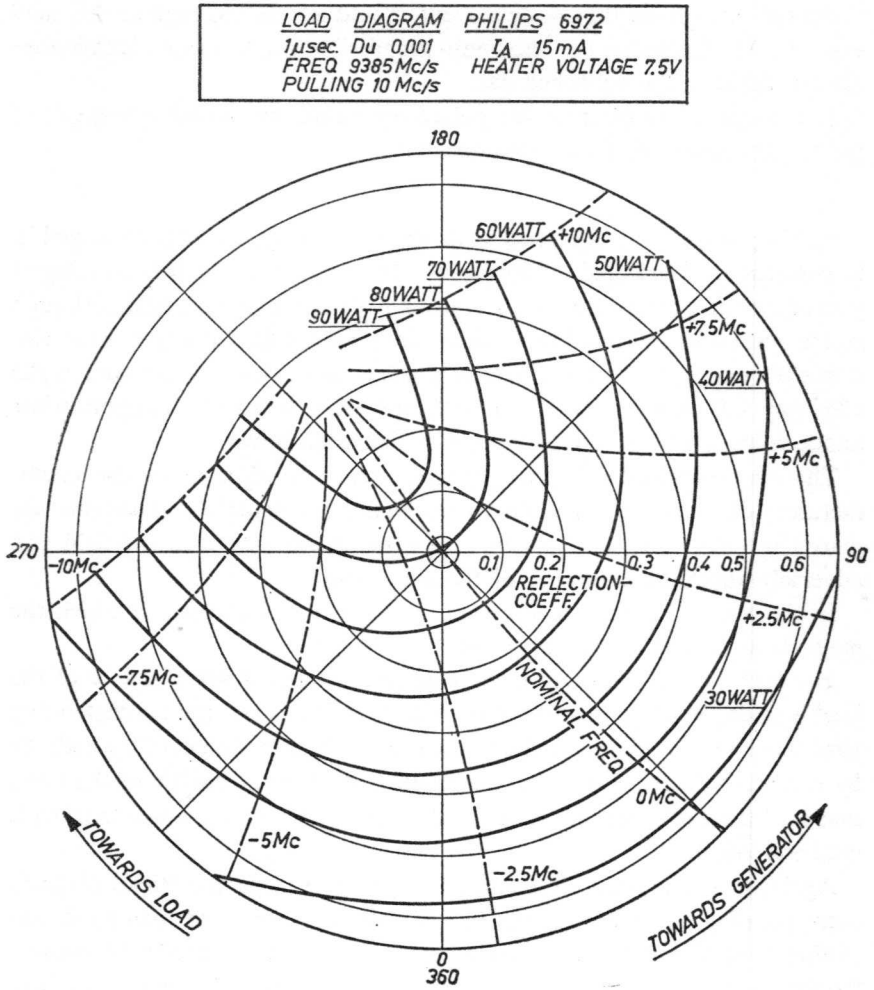

Fig. 48. Rieke diagram for Philips magnetron type 6972.

found in the diagram in which the magnetron should not be operated as the performance would be poor or the life too short.

In the following, those zones in the performance chart in which the magnetron should not be operated are discussed.

a. In general, magnetrons do not operate well in the π-mode at very low anode currents. As rule this applies at a current of from 0 to approximately 0.3 times the nominal current rating, although magnetrons for c.w. will usually continue to oscillate at lower values.

On the other hand the anode current should not be too high as this may easily lead to flashover; the maximum permissible anode current is therefore always stated in the published data.

In the case of magnetrons for pulsed operation we accordingly speak of the "stable range" of the anode current.

b. Magnetrons not equipped with their own magnets ("unpackaged"), in contrast to "packaged" magnetrons, the magnet of which is an integral part of the tube, can be used with almost any desired magnetic field, although stable operation is ensured only within limits; if the field strength is too low either the magnetron will oscillate in another mode than the π-mode, or the efficiency will be very low. If the field strength is too high the appropriate anode voltage will also be too high, with risk of flashover.

The magnetic field of packaged magnetrons is adjusted by the manufacturer; care should be taken to see that no magnetic components are placed too close to the magnetron as these might attenuate the field and adversely affect the operation of the magnetron.

In the Rieke diagram, too, certain zones can be indicated in which the magnetron cannot operate properly.

For each type of magnetron the maximum standing wave ratio σ of the load is given, at which the tube may be operated; beyond the corresponding zone there will be a considerable increase in the bombardment of the cathode by returning electrons, with a consequent reduction in the life of the tube, that is, if the working point is such that the output power is lower than with matched loading.

Again, if a magnetron is operated within a zone in the Rieke diagram corresponding to higher output power than with matched loading it will readily tend to oscillate in some other mode than the π-mode. Moreover, the frequency (owing to the pronounced convergence of the lines of constant frequency in that area) will vary appreciably with slight changes in the load; in the case of pulsed magnetrons there is then a marked degeneration of the pulse spectrum: In tunable magnetrons frequency transients may also occur

6.2 The "Q" value

In Chapter III it was pointed out that the geometrical dimensions of the delay line determine the frequency at which the magnetron will operate. We have also seen that under conditions of oscillation electromagnetic waves travel along the line; in other words that electromagnetic energy is distributed along the line. The delay line thus functions as a means of

storing electromagnetic energy. Let us denote the quantity of energy so stored by E_0

It is also known that the oscillating magnetron delivers power to the load (effective power) and that losses occur in the line (heating of the line). The amount of energy delivered to the load during one cycle of the r.f. oscillation is E_b and the energy absorbed by the circuit in the form of losses is E_c.

Three quantities can now be defined:

$$Q_u = 2\pi \cdot \frac{E_0}{E_c} \quad (Q \text{ unloaded}) \tag{156}$$

$$Q_e = 2\pi \cdot \frac{E_0}{E_b} \quad (Q \text{ external}) \tag{157}$$

$$Q_L = 2\pi \cdot \frac{E_0}{E_b + E_c} \quad (Q \text{ loaded}) \tag{158}$$

These Q-values accordingly give 2π times the ratio of the field energy in the delay line to the energy dissipated per cycle of the oscillation.

A high value of Q therefore means that the line is lightly damped; conversely a low value of Q indicates heavy damping.

From Eqs. (156) to (158) we can at once write:

$$\frac{1}{Q_L} = \frac{1}{Q_e} + \frac{1}{Q_u} \tag{159}$$

Thus two known values of Q enable us to calculate a third. Further, it will be seen that the circuit efficiency (see also Eq. (1)) can be expressed in terms of Q, viz.

$$\eta_c = \frac{E_b}{E_b + E_c} = \frac{Q_L}{Q_e} \tag{160}$$

The stability of the frequency of a magnetron against variations in the load or in the space charge will be greater, the higher the values of Q. The reason for this is that the field energy E_0, to give a mechanical example, plays the same part as the kinetic energy in the flywheel of an engine.

Eqs. (156) to (158) can be converted by introducing the power W_b and W_c in place of E_b and E_c, for

$$W_b = f \cdot E_b \tag{161}$$

$$W_c = f \cdot E_c \tag{162}$$

f denotes the frequency of the r.f. oscillations.

which gives us the following values of Q_0

$$Q_u = \omega \cdot \frac{E_0}{W_c} \tag{163}$$

$$Q_e = \omega \cdot \frac{E_0}{W_b} \tag{164}$$

$$Q_L = \omega \cdot \frac{E_0}{W_0 + W_b} \tag{165}$$

The values of Q can also be expressed in another form on the basis of the following:

The magnetron is represented by L with C in parallel (Fig. 49), with R as the internal circuit losses and a resistance ξ as load.

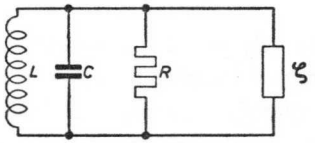

Fig. 49. Equivalent circuit of the cold magnetron for frequencies in the region of the π-mode. L and C represent the delay line, R the losses in the magnetron and ξ the load resistance.

Now, if the L–C circuit oscillates at a voltage $V = V_0 \sin \omega t$, the electromagnetic field energy will be:

$$E_0 = \frac{V_0^2}{2} \cdot C \tag{166}$$

the circuit losses:

$$W_c = \frac{V_0^2}{2R} \tag{167}$$

and the effective power:

$$W_b = \frac{V_0^2}{2\xi} \tag{168}$$

According to Eqs. (163) to (165) the values of Q will thus be:

$$Q_u = R \cdot C \cdot \omega \tag{169}$$

$$Q_e = \xi \cdot C \cdot \omega \tag{170}$$

$$Q_L = \frac{R \cdot \xi}{R + \xi} \cdot C \cdot \omega \tag{171}$$

All these Q values are characteristics of the circuit only and can therefore be measured with the magnetron in the cold, i.e. static condition. Methods of measurement will be given later.

6.3 The "cold" pulling

As we have seen, the delay line is the factor which determines the frequency at which magnetrons operate. Now the line is coupled to the load by means of a transformer, so variations in the load interact with the line and tend to affect the frequency of the oscillation.

Suppose that a load is coupled to a magnetron with a reflection coefficient of:

$$q = |q| \cdot e^{i\varphi} \tag{172}$$

and φ is varied from 0 to 360°; the magnetron frequency will then vary between two limits. The difference between these limits ΔF depends on the absolute value $|q|$ of the reflection coefficient as well as on the characteristics of the magnetron. This relationship is calculated in the following manner.

Taking first the conditions in a wave-guide terminated with a load whose reflection coefficient is q, with a wave

$$V_i = V_0 \cos \omega t \tag{173}$$

at the input of the line, the load reflects a wave

$$V_2 = V_0 \cdot |q| \cdot e^{i\varphi} \cdot \cos \omega t \tag{174}$$

A current wave is also propagated along the line in the direction of the load:

$$i_1 = \frac{V_0}{\xi} \cdot \cos \omega t \tag{175}$$

and reflected as:

$$i_2 = \frac{V_0}{\xi} \cdot |q| \cdot e^{i\varphi} \cdot \cos \omega t \tag{176}$$

Hence the admittance A at the input depends on $|q|$ and φ in the following manner:

$$A = \frac{i_1 + i_2}{V_1 + V_2} = \frac{1}{\xi} \cdot \frac{1 - |q| e^{i\varphi}}{1 + |q| e^{i\varphi}} = X + \mathrm{j}Y \tag{177}$$

Substituting:

$$e^{i\varphi} = \cos\varphi + \mathrm{j}\sin\varphi \tag{178}$$

the imaginary part of A gives us:

$$Y = \frac{1}{\xi} \cdot \frac{2\,|\,q\,|\sin\varphi}{1 + |\,q\,|^2 + 2\,|\,q\,|\cos\varphi} \tag{179}$$

If we now vary φ from 0 to 360° the maximum value of Y will be:

$$Y_{\max} = \pm\frac{1}{\xi} \cdot \frac{2\,|\,q\,|}{1 - |\,q\,|^2} \tag{180}$$

In the previous chapter it was shown that the magnetron can be represented as a parallel circuit, particularly in the neighbourhood of the resonant frequency.

If a load having a reflection coefficient q is now connected and the phase rotated, the maximum downward variation Δf in the frequency can be expected when $Y_{\max}$ is connected to the magnetron.

Now,

$$Y_{\max} = \frac{1}{\xi} \cdot \frac{2\,|\,q\,|}{1 - |\,q\,|^2} = \omega \cdot \Delta C \text{ and} \tag{181}$$

$$-\frac{\Delta f}{f_0} = \frac{\Delta C}{2\Delta} = \frac{|\,q\,|}{\xi \cdot C \cdot \omega\,(1 - |\,q\,|^2)} \tag{182}$$

With the phase angle φ of the reflection coefficient such that $-Y_{\max}$ is presented to the magnetron, the frequency will be f_0 plus Δf, thus making the total difference in frequency:

$$\Delta F = 2\Delta f = \frac{2\,|\,q\,| \cdot f_0}{Q_e\,(1 - |\,q\,|^2)} \tag{183}$$

This expression shows the extent of the maximum frequency swing when a load with a reflection coefficient q is connected to a magnetron with a Q value of Q_e, and the phase is rotated 360°.

If we take $|\,q\,| = 0.2$, the value of ΔF, per definition, is the "cold"pulling figure of the magnetron. Hence, from Eq. (183):

$$\Delta F_{0.2} = 0.417 \cdot \frac{f_0}{Q_e} \tag{184}$$

In calculating ΔF we have taken into account only the circuit characteristics of the magnetron, disregarding possible variations in the space charge. Thus Eq. (184) must represent the "cold" pulling figure.

The "hot" pulling figure, as measured with the magnetron in oscillation may accordingly differ from the "cold" value, but experience has shown that the difference is not more than 10% as a rule.

6.4 Effect of a long transmission line

We shall now examine the effect of the distance between the reflecting load and the magnetron when this distince is large compared with the wavelength. The phenomenon arising from this is called "long line effect".

When a voltage wave is applied to the input of the line:

$$\vec{V} = V_0 \cdot \sin\left(\omega t - \frac{2\pi}{\lambda} \cdot x\right) \tag{185}$$

a load of reflection coefficient q will reflect a voltage wave:

$$\overleftarrow{V} = V_0 \cdot q \cdot \sin\left(\omega t + \frac{2\pi}{\lambda} \cdot x\right) \tag{186}$$

There will be the sum of the two on the line, viz.

$$V = \vec{V} + \overleftarrow{V} = V_0 \cdot q\left[\sin\left(\omega t + \frac{2\pi}{\lambda} x\right) + \sin\left(\omega t - \frac{2\pi}{\lambda} x\right)\right] + \\ + V_0(1 - q) \cdot \sin\left(\omega t - \frac{2\pi}{\lambda} x\right) \tag{187}$$

which can be converted to:

$$V = 2V_0 \cdot q \cdot \sin \omega t \cos \frac{2\pi}{\lambda} x + V_0(1 - q) \cdot \sin\left(\omega t - \frac{2\pi}{\lambda} x\right) \tag{188}$$

Here the second term on the right-hand side represents a wave of amplitude $V_0(1 - q)$ travelling in the direction from the input to the load.

The first term of Eq. (188) shows that there is also a standing wave on the line, the maximum amplitude of which is $2V \cdot q$. Owing to the presence of this standing wave a quantity of electric field energy is stored in the transmission line and does not reach the load. A line of this kind thus behaves in the same way as an oscillatory circuit with load, as this also stores energy in the L and C, whilst energy is dissipated in the load.

Let us now evaluate the stored energy E.

If the characteristic impedance of the line is denoted by ξ the capacitance of the line per unit of length will be:

$$C = \frac{10^{-10}}{3} \cdot \frac{1}{\xi} \tag{189}$$

The energy E is now computed from the distribution of voltage along the line, in accordance with Eq. (188):

$$E = \frac{10^{-10}}{6 \cdot \xi} \cdot \int 4V_0^2 q^2 \cos^2 \frac{2\pi}{\lambda} x \, dx \tag{190}$$

The integral with respect to limits $x = 0$ and $x = \frac{\lambda}{2}$ will now give us the energy E_0 stored per (average) unit length of the line.

$$E_0 = \tfrac{2}{3} \cdot 10^{-10} \cdot \frac{V_0^2 \cdot q^2}{\xi} \tag{191}$$

A line of length L will thus store:

$$E = \tfrac{2}{3} \cdot 10^{-10} \cdot \frac{V_0^2 \cdot q^2}{\xi} \cdot L \tag{192}$$

The power W dissipated in the load R is given by:

$$W = \frac{V_0^2 (1 - q^2)}{2\xi} \tag{193}$$

In other words, in accordance with Eq. (163) the line behaves as an oscillatory circuit with Q_u

$$Q_u = \tfrac{4}{3} \cdot 10^{-10} \cdot \omega \cdot \frac{q^2}{1 - q^2} \cdot L \tag{194}$$

To obtain some idea of practical values of Q_u we shall assume that $L = 100$ cm, $q = 0.2$, $\omega = 6.28 \times 10^{10}$, and hence $\lambda = 3$ cm. Eq. (194) then gives us $Q_u = 35$.

Even a fairly short line, therefore, has quite marked resonant characteristics, and in the following we shall show the effects of this on the operation of the magnetron.

Take the case of a magnetron to which a reflecting load is connected by a long transmission line (Fig. 50).

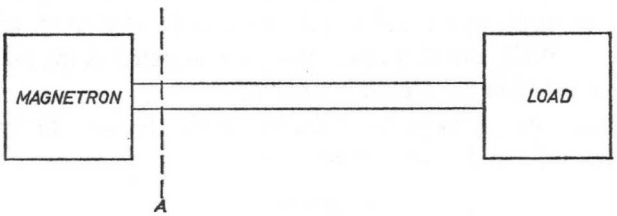

Fig. 50. Long-line effect. In the plane A, the oscillating magnetron must conform to $-\overleftarrow{A} = \overrightarrow{A}$.

The system will oscillate only when in plane A the following holds:

$$\vec{A} + \overleftarrow{A} = 0 \tag{195}$$

where $\overleftarrow{A}$ is the admittance as seen at the plane A looking towards the magnetron; $\vec{A}$ is the admittance at that plane when looking towards the load. With the aid of Eq. (195) the resonant frequency of the system can be ascertained.

To simplify calculation we shall assume the plane A to be at a point as close to the magnetron as possible, where the plane will function as a parrallel resonator. The admittance $\overleftarrow{A}$ as a function of the frequency is then:

$$\overleftarrow{A} = \mathrm{j}\left(\omega C - \frac{1}{\omega L}\right) + \frac{1}{R} = \mathrm{j} \cdot \frac{2Q_e}{\xi} \cdot \frac{\Delta f}{f_0} + \frac{1}{R} \tag{196}$$

where Q_e is the external Q of the magnetron, f_0 its resonant frequency and Δf the departure from the resonant frequency.

We now calculate the admittance $\vec{A}$ with respect to the load, at plane A, also as a function of the frequency.

It is known that the wavelength is dependent on the frequency:

$$\lambda_g = \frac{\lambda_0}{\sqrt{1 - \left(\frac{\lambda_0}{\lambda_c}\right)^2}} \tag{197}$$

where λ_g is the wavelength of the waveguide, λ_c its cut-off wavelength and λ_0 the wavelength in space. Differentiation then gives us:

$$\mathrm{d}\lambda_g = -\frac{\lambda_g^3}{\lambda_0^2} \cdot \frac{\mathrm{d}f}{f} = -\frac{\lambda_g^3}{c^2} \cdot f \cdot \mathrm{d}f \tag{198}$$

where c is the speed of light.

According to Eq. (198) the wavelength varies to the extent of $\mathrm{d}\lambda_g$ when the frequency is varied by an amount $\mathrm{d}f$. If the length of our transmission line is N wavelengths, then, a point where the phase is the same is displaced by $N \cdot \mathrm{d}\lambda_g$ with a variation in frequency of $\mathrm{d}f$. So:

$$\frac{\mathrm{d}\lambda_g}{\lambda_g} = -N \cdot \left(\frac{\lambda_g}{\lambda_0}\right)^2 \cdot \frac{\mathrm{d}f}{f} \tag{199}$$

The phase shift is accordingly:

$$\varphi = -4\pi \cdot N \cdot \left(\frac{\lambda_g}{\lambda_0}\right)^2 \cdot \frac{\mathrm{d}f}{f} \text{ (radians)} \tag{200}$$

or:

$$\varphi = -720 \cdot N \cdot \left(\frac{\lambda_g}{\lambda_0}\right)^2 \cdot \frac{df}{f} \text{ (degrees)} \tag{201}$$

According to Eq. (179):

$$\vec{A} \cdot \xi = -\frac{2\,|q| \cdot \sin 4\pi \cdot N \cdot \left(\frac{\lambda_g}{\lambda_0}\right)^2 \frac{df}{f}}{1 + |q|^2 + 2\,|q| \cdot \cos 4\pi \cdot N \cdot \left(\frac{\lambda_g}{\lambda_0}\right)^2 \cdot \frac{df}{f}} \cdot \tag{202}$$

From Equations (202), (196) and (195) the possible resonant frequencies can accordingly be obtained. In Eq. (195) only the imaginary part of (196) is included and the solution of this equation is best found by graphical means. We have assumed the following in Fig. 51:

$$Q_e = 100,\ N = 20,\ \frac{\lambda_g}{\lambda_0} = 1.4,\ |q| = 0.2.$$

It is seen from the diagram that the resonator line and the load line intersect, and under such conditions the system will have only one resonant frequency. However, if the magnetron be detuned (by displacing the magne-

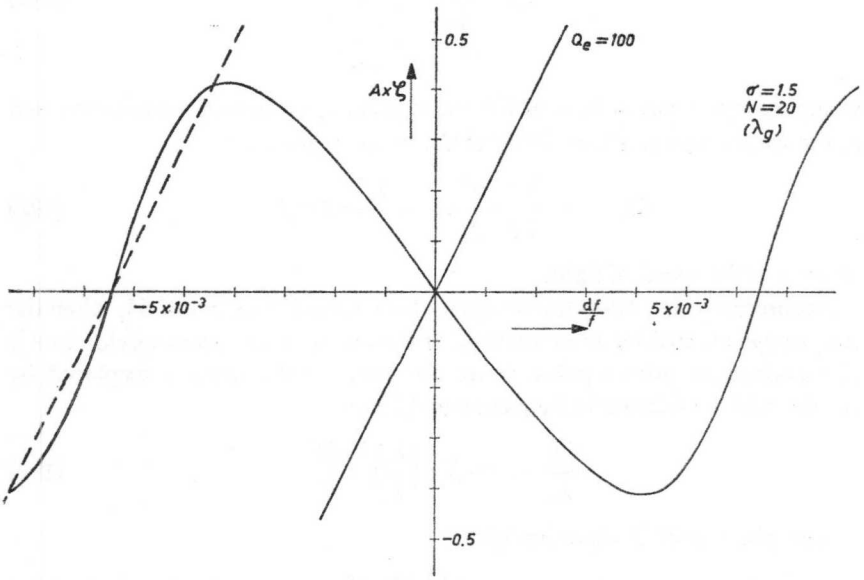

Fig. 51. Long-line effect. The point of intersection of the straight magnetron line with the load line shows the possible conditions of oscillation.

tron line along the f-axis), or if we change the phase of the load (by displacing the load line along the f-axis) the magnetron line may be found to intersect the load line at two or three places. The frequency of the magnetron will then jump from the one extreme to the other; the centre point is a point of instability, at which the magnetron can never operate (dotted line in Fig. 51).

This frequency jumping is one of the possible forms of long line effect and it may be encountered when a tuned magnetron is detuned for measurement of the pulling figure.

It will be noticed from Fig. 51 that such frequency jumping may be expected when the load line is steeper than the line of the magnetron.

Differentation of Eq. (202) shows that the greatest possible slope of the load line is:

$$\left(\frac{\mathrm{d}\,(\vec{A}\cdot\xi)}{\mathrm{d}\left(\frac{\mathrm{d}f}{f}\right)}\right)_{\max} = \frac{2q}{(1-q)^2}\cdot 4\pi\cdot N\cdot\left(\frac{\lambda_g}{\lambda_0}\right)^2 \tag{203}$$

whilst Eq. (196) gives the slope of the magnetron line as:

$$\frac{\mathrm{d}\,(\overleftarrow{A}\xi)}{\mathrm{d}\left(\frac{\mathrm{d}f}{f}\right)} = 2\,Q_e \tag{204}$$

Both will run parallel as in:

$$Q_e = 4\pi\cdot\frac{q}{(1-q)^2}\cdot N\cdot\left(\frac{\lambda_g}{\lambda_0}\right)^2 \tag{205}$$

If N is greater than is compatible with Eq. (205) frequency jumping may be expected.

In practice, however, it is more usual to work with the standing wave ratio σ in place of the reflection coefficient q:

$$|q| = \frac{\sigma-1}{\sigma+1} \tag{206}$$

and, with Eq. (205):

$$Q_e = \pi\cdot(\sigma^2-1)\cdot N\cdot\left(\frac{\lambda_g}{\lambda_0}\right)^2 \tag{207}$$

In Fig. 52, N is shown plotted as a function of Q_e for various values of

$(\sigma^2 - 1)$. $\left(\frac{\lambda_g}{\lambda_0}\right)^2$; if the transmission line is any longer than as given by Fig. 52 frequency jumping will take place.

With a line only slightly shorter than would be in accordance with Eq. (207), once the unfavourable phase angle has been passed, the spectrum will tend to widen, owing to the fact that the stability of the frequency of the whole system is then only low.

6.5 Measurement of Q values

We have shown in the foregoing that certain important circuit characteristics of a magnetron are revealed by the Q values. We shall now concern ourselves with the experimental measurement of these values.

It should be said at once that a large number of methods of measurement have been evolved and published. The greater the accuracy of measurement, the longer the time needed for the work; we shall here describe a method which is particularly suitable for routine measurements and which accordingly saves time. The attainable accuracy of measurement is within 10%.

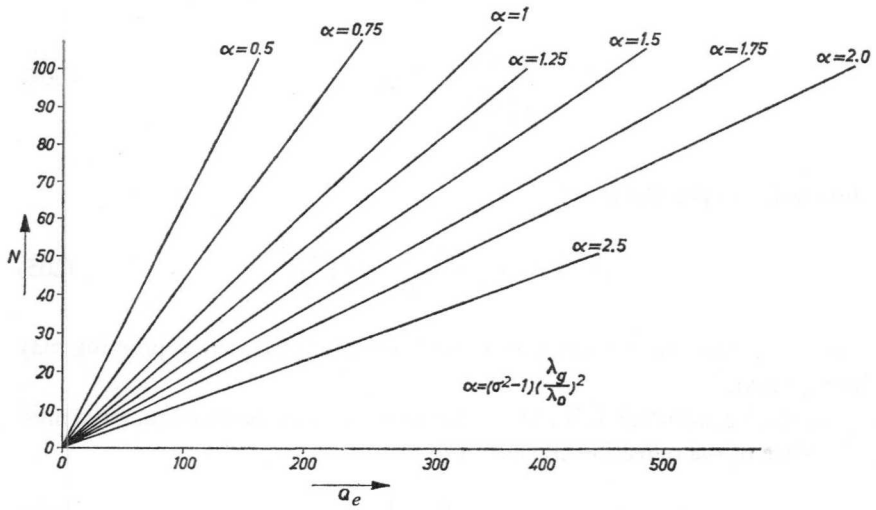

Fig. 52. Long-line effect. Curve used for determining the theoretical maximum permissible distance between magnetron and reflection.

The measuring equipment, which is shown schematically in Fig. 53, consists of an oscillator klystron *KL* the frequency of which is modulated at 50 c/s over the whole range of oscillation by applying the horizontal deflection voltage of a cathode ray oscilloscope *O* to the reflector.

The signal thus obtained is taken via an attenuator to a standing wave detector which is terminated by the "cold" magnetron M. A wavemeter W is included in the circuit to measure the frequency. The signal picked up by the probe is detected by means of a crystal and is then applied to the vertical deflection plates of the oscilloscope.

Now, before describing the practical method of measurement, let us consider the theory.

In a given plane in the test line the magnetron functions as a parallel resonator, so in that plane the admittance A is:

$$A = \mathrm{j}\left(\omega C - \frac{1}{\omega L}\right) + \frac{1}{R} \tag{208}$$

We may also write:

$$A = \frac{1}{\xi} \cdot \left(\mathrm{j} \cdot 2\, Q_e \cdot \frac{\Delta f}{f_0} + \xi \cdot G\right) \tag{209}$$

where

$$f = f_0 + \Delta f, \tag{210}$$

ξ is the characteristic impecdane of the measuring line and $G = \frac{1}{R}$ the real admittance produced by the losses in the magnetron; f_0 is the resonant frequency of the magnetron.

According to definition the reflection coefficient q of the termination of a transmission line is dependent on the admittance in accordance with:

$$q = \frac{1 - A\xi}{1 + A\xi} = |\, q \,| \cdot e^{i\varphi} \tag{211}$$

If we now combine Eq. (211) with (209) for the solution of the phase angle φ:

$$\tan\varphi = -\frac{4\, Q_e \cdot \dfrac{\Delta f}{f_0}}{1 - 4\, Q_e^{\,2} \left(\dfrac{\Delta f}{f_0}\right)^2 - (\xi G)^2} \tag{212}$$

The solution for Q_e is then:

$$Q_e = \frac{f_0}{2\Delta f} \cdot \left[+ \sqrt{\frac{1}{\tan^2\varphi} + 1 - (\xi G)^2} \quad - \frac{1}{\tan\varphi} \right] \tag{213}$$

If $R > \xi$, then $\eta_c > 0.5$, and

$$\xi G = \frac{1}{\sigma} \tag{214}$$

where σ is the standing wave ratio at the resonant frequency f_0.

In this case:

$$Q_e = \frac{f_0}{2\Delta f} \cdot \left[+ \sqrt{\frac{1}{\tan^2 \varphi} + 1 - \frac{1}{\sigma^2}} \; - \frac{1}{\tan \varphi} \right] \tag{215}$$

For the less common case where $R < \xi$ and $\eta_c < 0.5$:

$$Q_e = \frac{f_0}{2\Delta f} \cdot \left[\pm \sqrt{\frac{1}{\tan^2 \varphi} + 1 - \sigma^2} \; - \frac{1}{\tan \varphi} \right] \tag{216}$$

From Eq. (215) the following methods of measurement of Q_e can be derived. The relationship $\varphi = \varphi(f)$ in the region of the resonant frequency is determined experimentally by means of the test layout shown in Fig. 53.

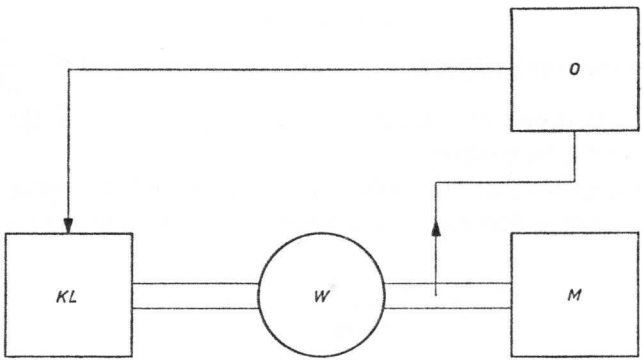

Fig. 53. Block diagram of circuit for measurements on a cold magnetron.

Then, if we locate the points $\varphi = \pm 90°$ from the curve $\varphi = \varphi(f)$ and read off the values $\left(\frac{f_0}{\Delta f}\right)_{\varphi = 90°}$ Eq. (215) gives:

$$Q_e = \tfrac{1}{2} \cdot \left(\frac{f_0}{\Delta f}\right)_{\varphi = 90°} \cdot \sqrt{1 - \frac{1}{\sigma^2}} \tag{217}$$

To compute Q_e therefore, we must also determine σ (the standing wave ratio of the magnetron at the resonant frequency).

In order to use more points on the curve $\varphi = \varphi(f)$ for the determination of Q_e the points for $\varphi = \pm 110°$ and $\varphi = \pm 130°$ can also be located. Eq. (216) then gives us:

$$Q_e = \tfrac{1}{2} \cdot \left(\frac{f_0}{\Delta f}\right)_{\varphi = 110°} \cdot \left(0.364 + \sqrt{1.132 - \frac{1}{\sigma^2}}\right) \tag{218}$$

$$Q_e = \tfrac{1}{2} \cdot \left(\frac{f_0}{\Delta f}\right)_{\varphi = 130°} \cdot \left(0.840 + \sqrt{1.705 - \frac{1}{\sigma^2}}\right) \tag{219}$$

To facilitate the calculation of Q_e in accordance with Eqs. (217) to (219) the factors $\sqrt{1 - \frac{1}{\sigma^2}}$, $\left(0.364 + \sqrt{1.132 - \frac{1}{\sigma^2}}\right)$ and $\left(0.840 + \sqrt{1.705 - \frac{1}{\sigma^2}}\right)$ are shown plotted as a function of σ in Fig. 54.

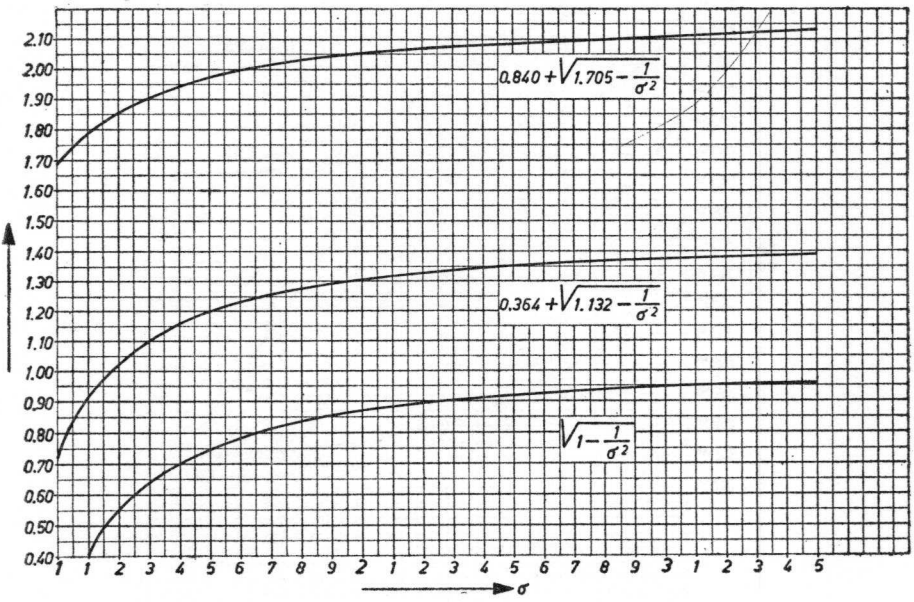

Fig. 54. Table for use in calculating Q_e and Q_u in accordance with Eqs. (217, (218) and (219).

If sufficient accuracy is observed, the three values of Q_E will be found to differ only very slightly and the results may be regarded as reliable.

However, a quicker method can be derived from Eq. (215).

A certain value for Δf is chosen such that:

$$\frac{f_0}{\Delta f} = \pm \vartheta \tag{220}$$

and the accompanying value of φ_ϑ is determined.
Thus:

$$Q_e = \tfrac{1}{2} \cdot \vartheta \cdot \left[\sqrt{\frac{1}{\tan^2 \varphi_\vartheta} + 1 - \frac{1}{\sigma^2}} - \frac{1}{\tan \varphi_\vartheta} \right] \tag{221}$$

If σ can be measured, Q_e can be obtained from (221) and, in order to sim-

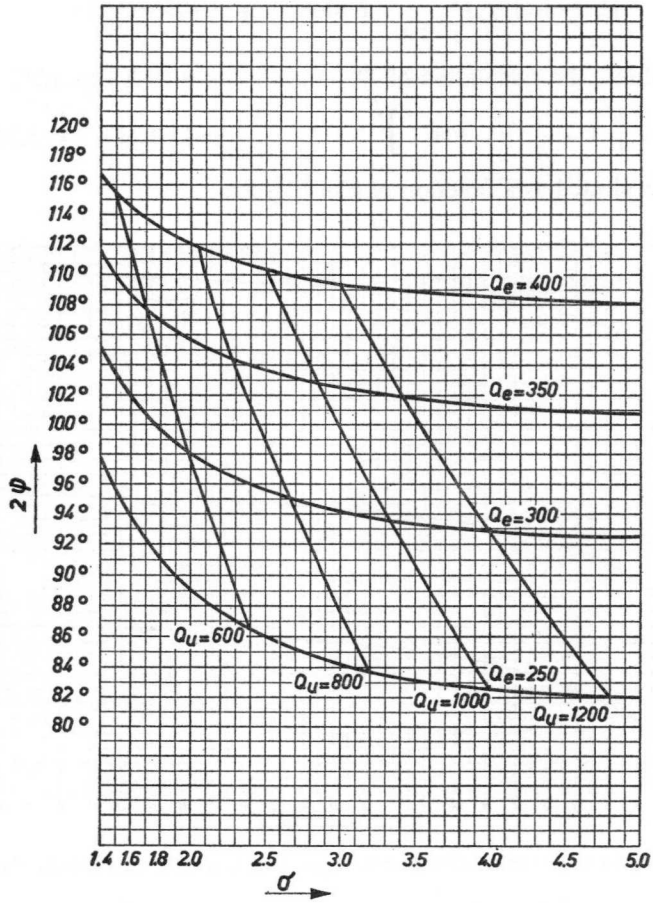

Fig. 55. Chart based on Eq. (222), used for the quick calculation of Q_e and Q_u in the manufacture of magnetrons.

$$\vartheta = 1.7 \cdot 10^{-3}$$

plify the calculation, it is helpful to plot $\varphi = \varphi(\sigma)$ with Q_e and Q_u as parameter (Fig. 55). For this purpose use is made of Eq. (212):

$$\tan \varphi_\vartheta = \pm \frac{4Q_e \cdot \frac{1}{\vartheta}}{1 - \frac{4Q_e^2}{\vartheta^2} - \frac{1}{\sigma^2}} \tag{222}$$

By inserting the particular value of ϑ, with certain values of Q_e as parameter (100, 200, 300 etc.), we then evaluate $\varphi_\vartheta = \varphi(\sigma)$ and plot the curve.

The method of measurement is as follows. Ascertain the resonant frequency, measure σ (standing wave ratio at $\Delta f = 0$), measure φ at $\frac{\Delta f}{f} = \pm \frac{1}{\vartheta}$; for the last-mentioned the measuring accuracy is greatest when ϑ is so chosen that $\varphi \simeq 110°$.

Q_e and Q_u are then read from the chart for the values obtained. This method is particularly suitable for measuring large numbers of magnetrons which do not differ greatly from one another.

It should be noted when determining the angle φ, however, that the wavelength is dependent on the frequency; owing to the finite distance between the test probe and the magnetron the plane where φ = constant does not remain in the same place in the test circuit when the frequency is varied.

LITERATURE

H. G. BRUIJNING: *Impulsvorming en voeding van het magnetron*, Tijdschrift van het Nederl. Radiogenootschap, deel **19**, No. 1, januari 1954.

P. H. J. A. KLEIJNEN: *Magnetron*, Tijdschrift van het Nederl. Radiogenootschap, deel **18**, No. 5/6, november 1953.

J. M. G. SEPPENS and J. VERSTRATEN: *An 8 mm. High-definition Radar set*, Philips Telecommunication Review, vol. **20**, No. 1, sept. 1958.

J. VERWEEL: *Magnetrons*, Philips Tech. Rev. vol. **14**, No. 2.

J. B. FISK, H. D. HAGSTRUM, and P. L. HARTMAN: *The magnetron as a generator of centimeter waves*, The Bell System Technical Journal, vol. **25**, No. 2, april 1946.

J. VERWEEL and G. H. PLANTINGA: *A range of pulsed magnetrons for centimetre and millimetre waves*, Philips Tech. Rev., vol. **21**, No. 1.

LATHAM, KING and RUSHORTER: *The magnetron*, Chapman and Hall Ltd., London 1952.

SLATER: *Microwave Electronics*, D. van Nostrand Company, New York 1950.

G. B. COLLINS: *Microwave Magnetrons*, Mc. Graw-Hill Book Company Inc., New York 1948.

W. J. KLEEN: *Microwave Tubes*, Academic Press, London 1958.

S. FLÜGGE: *Handbuch der Physik*, Band **XXI.**, Speiziger Verlag, Berlin 1956.

S. FLÜGGE: *Handbuch der Physik*, Band **XVI.**, Speiziger Verlag, Berlin 1956.

CLEMENS SCHAEFER: *Einführung in die Theoretische Physik*, Walter de Gruyter und Co., Berlin 1950.

E. G. DORGELO: *Über die Technologie von Magnetrons und Klystrons I*, Vakuumtechnik **4.** Jahrgang, heft 8.

E. G. DORGELO: *Technologie von Magnetrons und Klystron II*, Vakuumtechnik, **5.** Jahrgang, Heft 8.

W. KLEEN: *Einführung in die Mikrowellen-Elektronik*, Hirzel Verlag, Zürich 1952.

W. SCHMIDT: *Die Anwendung von Mikrowellenenergie in der Industrie*, NTZ, **12.** Jahrgang, Heft 2, 1959.

G. A. ESPERSEN: *Dispenser cathode magnetrons*, I.R.E. Trans. Electron Divices, vol. **6**, No. 1, 1959.

W. SCHMIDT: *Güte-Kaltmessverfahren für Magnetrons*, Elektronische Rundschau, Band **11** 1957.